AFWAL-TR-82-4040

STATISTICS OF CRACK GROWTH IN ENGINE MATERIALS - VOLUME 1: CONSTANT AMPLITUDE FATIGUE CRACK GROWTH AT ELEVATED TEMPERATURES

J. N. Yang
The George Washington University
Washington, D. C. 20052

G. C. Salivar
C. G. Annis, Jr.
Pratt & Whitney Aircraft
West Palm Beach, Florida 33402

July 1982

Interim Report for Period 15 January 1981 - 15 January 1982

Materials Laboratory
Air Force Wright Aeronautical Laboratories
Air Force Systems Command
Wright-Patterson Air Force Base, Ohio 45433

NOTICE

When Government drawings, specifications, or other data are used for any purpose other than in connection with a definitely related Government procurement operation, the United States Government thereby incurs no responsibility nor any obligation whatsoever; and the fact that the government may have formulated, furnished, or in any way supplied the said drawings, specifications, or other data, is not to be regarded by implication or otherwise as in any manner licensing the holder or any other person or corporation, or conveying any rights or permission to manufacture use, or sell any patented invention that may in any way be related thereto.

This report has been reviewed by the Office of Public Affairs (ASD/PA) and is releasable to the National Technical Information Service (NTIS). At NTIS, it will be available to the general public, including foreign nations.

This technical report has been reviewed and is approved for publication.

Robert C. Donath

ROBERT C. DONATH
Metals Behavior Branch
Metals and Ceramics Division

FOR THE COMMANDER

John P. Henderson

JOHN P. HENDERSON
Metals Behavior Branch
Metals and Ceramics Division

"If your address has changed, if you wish to be removed from our mailing list, or if the addressee is no longer employed by your organization please notify AFWAL/MLLN *, W-PAFB, OH 45433 to help us maintain a current mailing list".*

Copies of this report should not be returned unless return is required by security considerations, contractual obligations, or notice on a specific document.

REPORT DOCUMENTATION PAGE		READ INSTRUCTIONS BEFORE COMPLETING FORM
1. Report Number AFWAL-TR-82-4040	2. Govt Accession No.	3. Recipient's Catalog Number
4. Title *(and Subtitle)* STATISTICS OF CRACK GROWTH IN ENGINE MATERIALS-VOLUME 1: CONSTANT AMPLITUDE FATIGUE CRACK GROWTH AT ELEVATED TEMPERATURES		5. Type of Report & Period Covered 15 Jan 1981 — 15 Jan 1982 Interim Report 6. Performing Org. Report Number PWA/GPD/FR-16444
7. Author(s) J. N. Yang G. C. Salivar C. G. Annis, Jr.		8. Contract or Grant Number(s) F33615-80-C-5189
9. Performing Organization Name and Address Mechanics of Materials Structures Pratt & Whitney Aircraft Group Government Products Division West Palm Beach, FL 33402		10. Program Element, Project, Task Area & Work Unit Numbers 2420-01-28
11. Controlling Office Name and Address Materials Laboratories (AFWAL/MLLN) Air Force Wright Aeronautical Laboratories (AFSC) Wright-Patterson Air Force Base, Ohio 45433		12. Report Date July 1982 13. Number of Pages 90
14. Monitoring Agency Name & Address *(if different from Controlling Office)*		15. Security Class. *(of this report)* Unclassified 15a. Declassification/Downgrading Schedule

16. Distribution Statement *(of this Report)*
Approved for public release; distribution unlimited.

17. Distribution Statement *(of the abstract entered in Block 20, if different from Report)*

18. Supplementary Notes

19. Key Words *(Continue on reverse side if necessary and identify by block number)*
Statistical Fatigue Crack Growth; Engine Materials; Elevated Temperature; and Fracture Mechanics

20. Abstract *(Continue on reverse side if necessary and identify by block number)*
Classically crack propagation analyses for engine components employed in residual life predictions are deterministically based. They typically account for materials scatter by the incorporation of a safety factor. A statistical treatment of materials scatter is necessary to permit a maximum utilization of component life. Two fracture mechanics-based statistical models for the fatigue crack growth damage accumulation in engine materials are proposed and investigated. These statistical models are based on the synergistic fracture mechanics models, i.e., hyperbolic sine crack growth rate function, developed by Pratt & Whitney. Test results of IN-100, a superalloy used in the F-100-

20. Abstract *(Continued)*
engine, at various elevated temperatures, loading frequencies, stress ratios, etc., have been compiled and analyzed statistically. The statistical distributions of (1) the crack growth rate; (2) the propagation life to reach any given crack size; and (3) the crack size at any service life, have been derived. It is demonstrated that the correlation between the test results and two statistical models is very good.

PREFACE

This work was performed under Materials Laboratory Contract F33615-80-C-5189, "Statistics of Crack Growth in Engine Materials." The program is being conducted by the Mechanics of Materials and Structures section of Pratt & Whitney Aircraft, Government Products Division under the cognizance of Dr. R. C. Donath, AFWAL/MLLN. Professor J. N. Yang is the principal investigator, Dr. G. C. Salivar is the responsible engineer and C. G. Annis, Jr., is the program manager reporting to M. C. Van Wanderham, Manager, Mechanics of Materials and Structures. This interim report summarizes the work performed during the period 15 January 1981 to 15 January 1982.

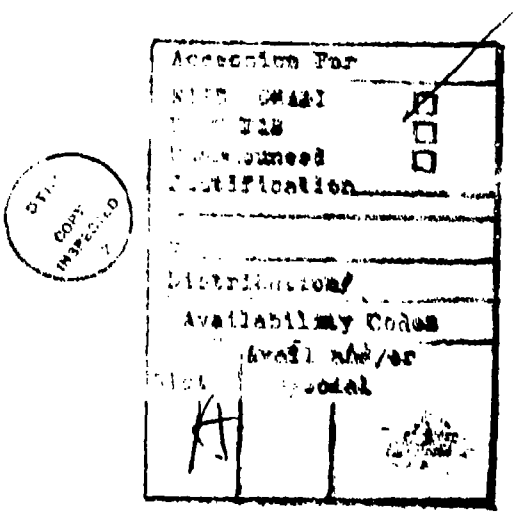

TABLE OF CONTENTS

LIST OF ILLUSTRATIONS

LIST OF ILLUSTRATIONS (Continued)

LIST OF ILLUSTRATIONS (Continued)

LIST OF ILLUSTRATIONS (Continued)

LIST OF TABLES

SECTION I

INTRODUCTION

Engine components have traditionally been designed using a crack initiation criterion. This approach has been very successful from a safety standpoint, but the conservatism inherent in this method has resulted in poor utilization of the intrinsic life of the component. The development of high temperature fracture mechanics has permitted basing residual life analyses on a crack propagation criterion. Using this approach, lives from a specified defect size can be calculated and combined with periodic inspection to determine component retirement.

Propagation analyses classically employed in residual life predictions are deterministically based. They typically account for materials scatter by the incorporation of a safety factor. A more rigorous treatment of materials scatter is necessary to permit maximum utilization of component life.

The objective of this program is to develop a methodology capable of incorporating the scatter observed in crack growth data into component residual life analyses. Such a methodology is desired for use in damage-tolerant and/or Retirement for Cause (RFC) concepts. This objective includes: identifying the distribution functions which best describe crack growth rate (da/dn) behavior; characterizing fatigue-crack propagation (FCP) controlling parameters as to their effects on crack growth rate variability; studying correlations between this variability and propagation life distributions; and developing a generic methodology applicable to all engine materials, although particular program emphasis is placed on IN100, Waspaloy, and Ti 6-2-4-6.

When the critical components of gas turbine engines, such as disks, must be used beyond the fatigue crack initiation stage, an accurate prediction of crack growth damage accumulation for these components under service loading spectra becomes very important. Test results under laboratory conditions of the crack growth rates for engine materials such as IN100 and Waspaloy, exhibit considerable statistical variability [e.g., Refs. 1-7]. Typical test results of the crack growth rate da/dN versus the stress intensity range ΔK are shown in Figures 1 and 2 for IN100 under two different test conditions. As a result, for a rational prediction of the fatigue crack growth damage accumulation of engine components, it is essential to take into account its inherent statistical variability. Unfortunately, a statistical model and analysis procedure for the crack growth damage behavior of engine materials have not been established to date.

Numerous studies have been carried out in the past decade on the crack growth behavior of aluminum alloys, steels, and titaniums (e.g., Ref. 8). These studies are essentially for airframe materials.

In general, literature dealing with the statistical analysis of fatigue crack growth damage accumulation can be classified into three categories. Papers in the first category consider the random crack propagation resulting from random fatigue loading spectra or random service loads, such as narrow-banded or wide-banded Gaussian random processes. Typical literature is given in Ref. 9-18. Within this category, another effort has also been made to convert random service loads into simplified deterministic loading spectra that will result in an equivalent fatigue crack growth behavior, e.g., Ref. 19-23, thus saving a significant amount of computational effort. A conversion of cycle-by-cycle integration for the crack growth into a flight-by-flight integration is a typical example (Ref. 19-23).

Papers in the second category deal with statistical crack propagation in the small crack size region using fractographical results in order to establish the so-called equivalent initial flaw size,

e.g., References 24-33. Literature in the third category deals with statistical crack growth behavior under deterministic laboratory loading spectra, e.g., Ref. 33-45, thus reflecting the inherent crack growth variability due to the material itself.

Unlike airframe structures, the loading environments of engine components are rather predictable. Hence literature in the third category is relevant to the present project and has been examined carefully. While the statistical characterization of the crack growth rate presented in Ref. 34 and 35 is very reasonable, the methodology is not applicable to the present problem because our sample size is too small under each test condition. Likewise, the statistical distributions of the crack size in service have not been solved satisfactorily in Ref. 34 and 35. The statistical models and analysis methodologies presented in Ref. 33 were developed essentially for aluminum alloys in which a simple crack growth rate equation can be used. The statistical model presented in Ref. 38-41 appears to be superior to that of Ref. 36-37. However, a considerable amount of effort in further research and development is needed before it can be applied to engine components due to the complex loading environments.

The following problems are unique to engine materials and environments: (1) the statistical distribution of the crack growth damage accumulation is influenced by many parameters such as temperature T, loading frequency ν, stress ratio R, holding time T_h, etc., (2) the number of specimens tested under a single environmental condition mentioned in (1) is very small, and (3) the homogeneous data base does not exist, since each specimen was usually tested using different specimen geometry, maximum load, initial crack size, and final crack size. Thus, it is necessary to develop new and simple statistical models capable of dealing with the unique features associated with engine environments on the basis of the fracture mechanics approach.

Two fracture mechanics-based statistical models for the fatigue crack growth damage accumulation in engine materials are proposed and investigated. These statistical models are based on the synergistic fracture mechanics models, i.e., hyperbolic sine crack growth rate function, developed by Pratt & Whitney [Ref 1]. Test results of IN-100, a superalloy used in the F100 engine, at various elevated temperatures, loading frequencies, stress ratios, etc., have been compiled and analyzed statistically. The statistical distributions of (1) the crack growth rate; (2) the propagation life to reach any given crack size; and (3) the crack size at any service life, have been derived. It is demonstrated that the correlation between the test results and two statistical models is very good.

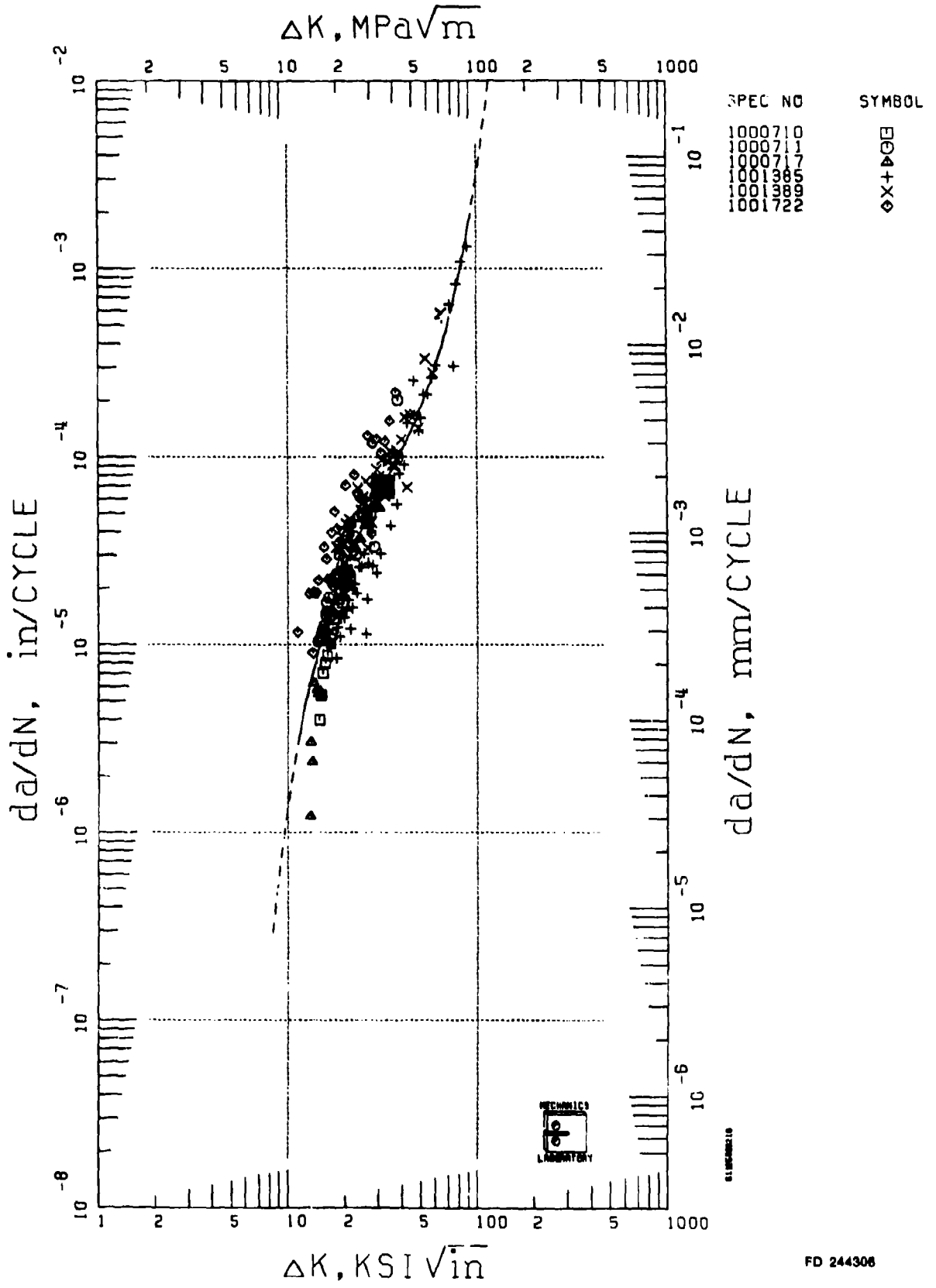

Figure 1. Crack Growth Rate vs Stress Intensity Range for IN100 Under Test Condition No. 4

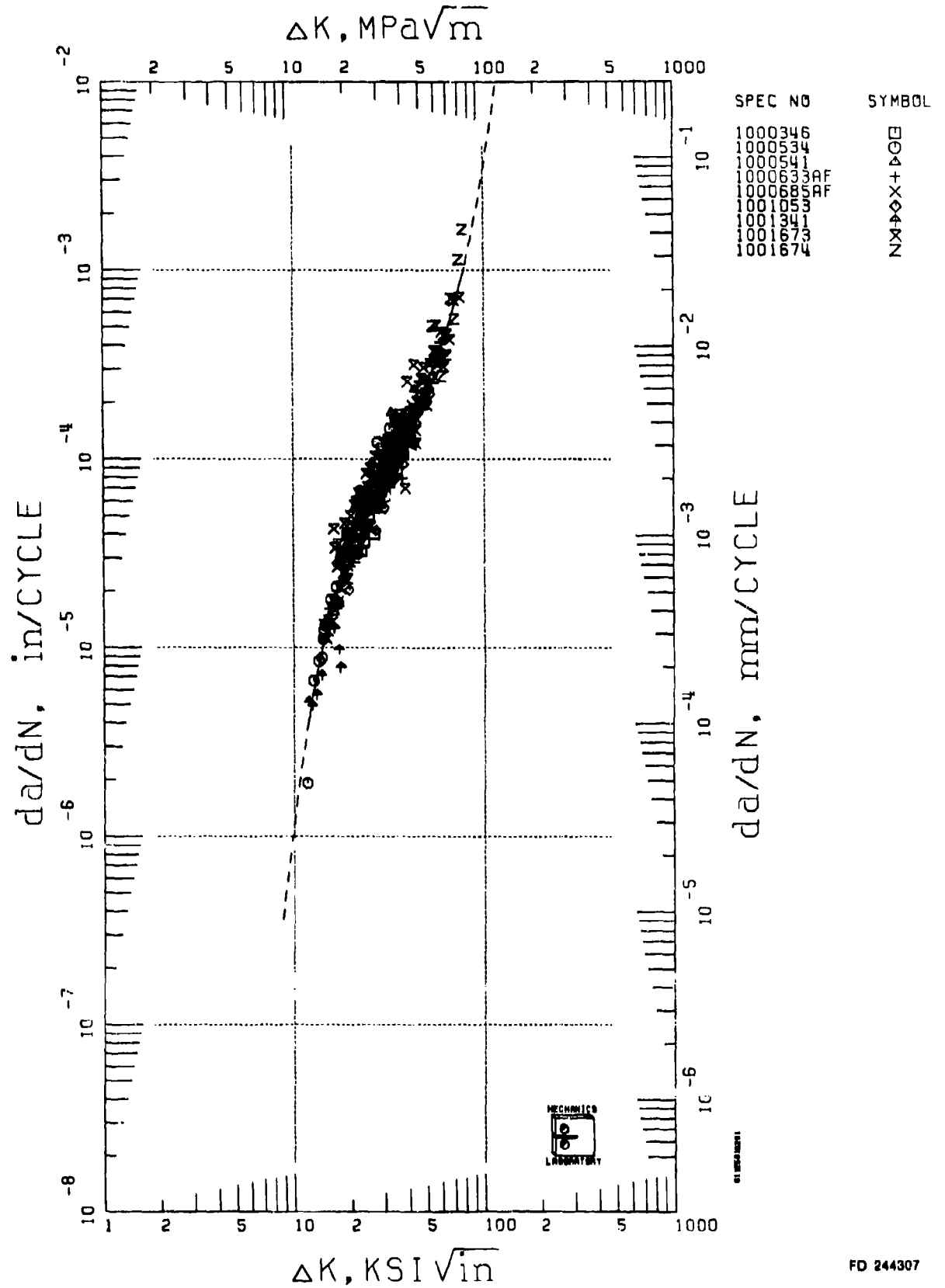

Figure 2. Crack Growth Rate vs Stress Intensity Range for IN100 Under Test Condition No. 5

SECTION II

LOGNORMAL CRACK GROWTH RATE MODEL

The crack growth rate equation proposed by Pratt & Whitney Aircraft (Ref. 1) is given by

$$Y = C_1 \sinh [C_2(X + C_3)] + C_4 \tag{1}$$

in which

$$Y = \log \frac{da}{dn}, \quad X = \log \Delta K \tag{2}$$

where ΔK = stress intensity range, C_1 is a material constant, and C_2, C_3 and C_4 are functions of temperature T, loading frequency ν, stress ratio R and others.

The first statistical model assumes that the crack growth rate Y is a homogeneous Gaussian random process

$$Y = C_1 \sinh [C_2(X + C_3)] + C_4 + Z(X) \tag{3}$$

in which Z(X) is a homogenous Gaussian random process with zero mean and a power spectral density $S_{ZZ}(\omega)$.

The statistical model described by Eq. 3 is very general and versatile. Two extreme cases of the Gaussian random process Z(X) are described briefly in the following:

On one extreme, Z(X) is a Gaussian white noise. For a Gaussian white noise, the correlation between $Z(X_1)$ and $Z(X_2)$ is zero as long as $X_1 \neq X_2$, and the autocorrelation function is a Dirac delta function of X. Physically, the Gaussian white noise resembles the random walk model. Sample functions of Z(X) and Y(X) are schematically shown in Figure 3.

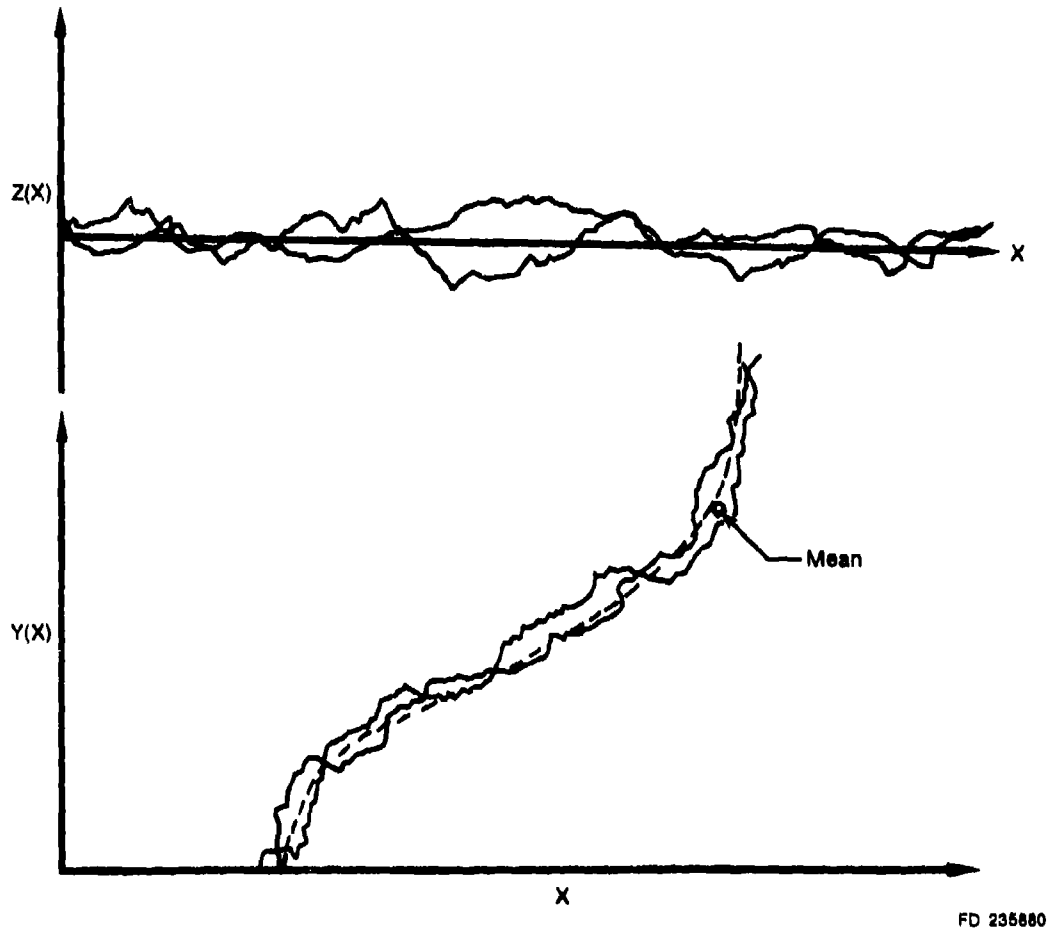

Figure 3. Sketch of Sample Functions of Stationary Gaussian White Noise Z(X) and Log Crack Growth Rate Y(X)

Based on the white noise model, the statistical dispersion of the number of load cycles, N(a), to reach a given crack size "a" or the crack size, a(n), at any number of cycles, n is the smallest in the category of the general Gaussian random process. Hence, the Gaussian white noise model results in an unconservative prediction for either N(a) or a(n). Consequently, such an extreme case is not appropriate for the engineering analysis and design because of its unconservative nature. Likewise the mathematical solution for such a problem is quite involved.

On the other extreme, Z(X) is completely correlated for all X values, i.e., Z(X)=Z is a Gaussian random variable. Physically, the random variable model indicates that a specimen starting with a faster (or slower) crack growth rate will always preserve the faster (or slower) crack growth rate throughout its crack propagation life. Sample functions are schematically shown in Figure 4 to illustrate the behavior of Z(X) and Y(X).

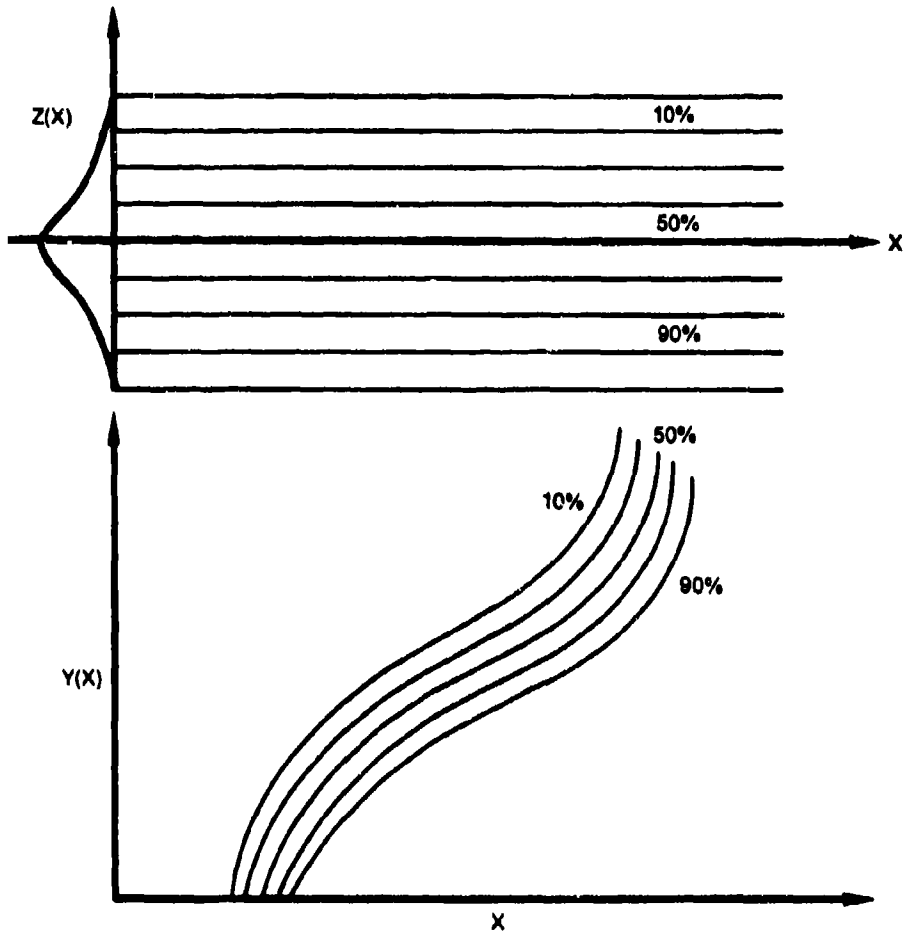

Figure 4. Sketch of Sample Functions of Gaussian Random Variable Z(X) and Log Crack Growth Rate Y(X)

Based on the random variable model, the statistical dispersion of N(a) or a(n) is the largest in the general class of Gaussian random processes. Thus, the statistical prediction for the crack growth damage accumulation using such a model is conservative. From the mathematical standpoint the random variable model is the simplest model. As a result, the random variable model appears to be useful and appropriate for the engineering analysis and design purpose, and it will be presented in this report.

In reality, sample functions of the crack growth rate may lie between these two extreme cases as schematically shown in Figure 5. Investigation of the general case is currently underway and the results will be presented in the next report.

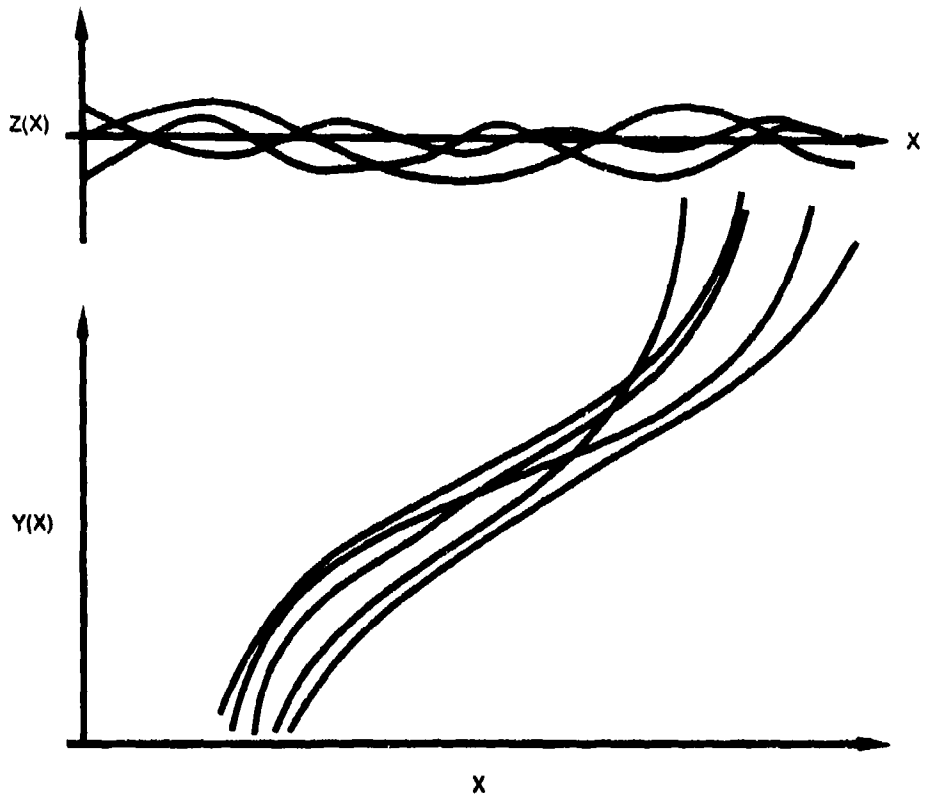

Figure 5. Sketch of Sample Functions of Stationary Gaussian Random Process Z(X) and Log Crack Growth Rate Y(X)

Based on the random variable model, Eq. 3 can be written as

$$Y = C_1 \sinh[C_2(X+C_3)] + C_4 + Z \tag{4}$$

where Z is a normal random variable with zero mean and a standard deviation σ_z.

It follows from Eqs. 4 and 2 that the log crack growth rate Y is a normal random variable and the crack growth rate da/dn is a lognormal random variable defined in the positive domain. The mean value, μ_y, and the standard deviation, σ_y, of Y can be obtained from Eq. 4 as

$$\mu_y = C_1 \sinh[C_2(X+C_3)] + C_4 \tag{5}$$

$$\sigma_y = \sigma_z \tag{6}$$

Hence, the probability density function of the log crack growth rate Y is given by

$$f_Y(y) = \frac{1}{\sqrt{2\pi}\,\sigma_y} \exp\left\{-\frac{1}{2}\left(\frac{y-\mu_y}{\sigma_y}\right)^2\right\} \tag{7}$$

in which μ_y and σ_y are given by Eqs. 5 and 6.

It is observed from Eqs. 5-7 that the probability density function of Y involves four parameters, i.e., C_2, C_3, C_4 and σ_y. These parameters will be estimated from test results using the method of maximum likelihood.

Let (x_i,y_i) for $i = 1,2,\ldots,n$ be a set of observations of X and Y under a particular test condition (ν,R,T) where ν = loading frequency, R = stress ratio and T = temperature. The likelihood function $L(y_1,y_2,\ldots,y_n; C_2,C_3,C_4,\sigma_y)$ is given by

$$L(y_1,\ldots,y_n;C_2,C_3,C_4,\sigma_y) = \prod_{i=1}^{n} \frac{1}{\sqrt{2\pi}\,\sigma_y} \exp\left\{-\frac{1}{2}\left(\frac{y_i-\mu_{y_i}}{\sigma_y}\right)^2\right\} \tag{8}$$

in which it follows from Eq. 5 that

$$\mu_{y_i} = C_1\sinh[C_2(x_i+C_3)] + C_4 \tag{9}$$

Taking the natural logarithm of both sides of Eq. 8, one obtains

$$\ell nL(y_1,\ldots,y_n;C_2,C_3,C_4,\sigma_y) = -n\ell n(\sqrt{2\pi}\,\sigma_y) - (2\sigma_y^2)^{-1} \sum_{i=1}^{n} (y_i - \mu_{y_i})^2 \tag{10}$$

The maximum likelihood estimates of C_2, C_3, and C_4 and σ_y are determined by maximizing Eq. 10 as follows:

$$\frac{\partial \ell nL(y_1,\ldots,y_n;C_2,C_3,C_4,\sigma_y)}{\partial C_2} = 0 \tag{11}$$

$$\frac{\partial \ell nL(y_1,\ldots,y_n;C_2,C_3,C_4,\sigma_y)}{\partial C_3} = 0 \tag{12}$$

$$\frac{\partial \ell nL(y_1,\ldots,y_n;C_2,C_3,C_4,\sigma_y)}{\partial C_4} = 0 \tag{13}$$

$$\frac{\partial \ell nL(y_1,\ldots,y_n;C_2,C_3,C_4,\sigma_y)}{\partial \sigma_y} = 0 \tag{14}$$

Substituting Eq. 10 into Eqs. 11-14, one obtains the following nonlinear coupled equations

$$\sum_{i=1}^{n} (x_i+C_3)(y_i-\mu_{y_i})\cosh[C_2(x_i+C_3)] = 0 \tag{15}$$

$$\sum_{i=1}^{n} (y_i-\mu_{y_i})\cosh[C_2(x_i+C_3)] = 0 \tag{16}$$

$$\sum_{i=1}^{n} (y_i-\mu_{y_i}) = 0 \tag{17}$$

$$\sigma^2_y = \frac{1}{n} \sum_{i=1}^{n} (y_i-\mu_{y_i})^2 \tag{18}$$

in which μ_{y_i} is a function of C_2, C_3, C_4 and x_i (Eq. 9).

Equations 15-17 do not involve σ_y and hence they can be used to solve for C_2, C_3 and C_4 simultaneously. After C_2, C_3 and C_4 are determined from Eqs. 15-17, the standard deviation σ_y can easily be computed from Eq. 18.

It should be mentioned that Eqs. 15-17 are identical to those equations derived by using the method of least squares as described in Ref. 1. Therefore, the least square estimates of C_2, C_3 and C_4 are identical to those obtained using the method of maximum likelihood described above. Thus the computer program developed in Ref. 1 for the numerical solution of Eqs. 15-17 can be used.

Since Y is a normal random variable, the crack growth rate G = da/dn follows the lognormal distribution. The coefficient of variation of the crack growth rate G, denoted by V, is related to the standard deviation σ_y of Y through

$$V = [e^{(\sigma_y \ell n 10)^2} - 1]^{1/2} \tag{19}$$

The distribution function $F_G(\eta)$ and the probability density function $f_G(\eta)$ of the crack growth rate G = da/dn are given by

$$F_G(\eta) = P[G \le \eta] = P\left[\frac{da}{dn} \le \eta\right] = \Phi\left(\frac{\log \eta - \mu_y}{\sigma_y}\right) \tag{20}$$

$$f_G(\eta) = \frac{\log e}{\sqrt{2\pi}\eta\sigma_y} \exp\left\{-\frac{1}{2}\left(\frac{\log \eta - \mu_y}{\sigma_y}\right)^2\right\} \tag{21}$$

in which $\Phi(\xi)$ is the standardized normal distribution function

$$\Phi(\xi) = \int_{-\infty}^{\xi} e^{-t^2/2}\, dt \tag{22}$$

and μ_y is given by Eq. 5

$$\mu_y = C_1 \sinh[C_2(X+C_3)] + C_4 \tag{23}$$

whereas C_2, C_3, C_4 and σ_y are estimated from Eqs. 15-18.

Test results for the log crack growth rate Y = log (da/dn) versus the log stress intensity range X = log ΔK are presented in Figure 6 as discrete points for five specimens in the test condition No. 1 (T = 1000°F, ν = 10 cpm, R = 0.1). All the crack growth rate data shown in Figure 6 have been used to estimate C_2, C_3, C_4 and σ_y using the method of maximum likelihood. The results are presented in the first row of Table 1 and plotted in Figure 6 as a solid curve. The maximum likelihood estimates of C_2, C_3, C_4 and σ_y are shown in Table 1 for different test conditions (ν, R, T). Also presented in Table 1 are the corresponding coefficients of variation V, Eq. 19, of the crack growth rate G = da/dn.

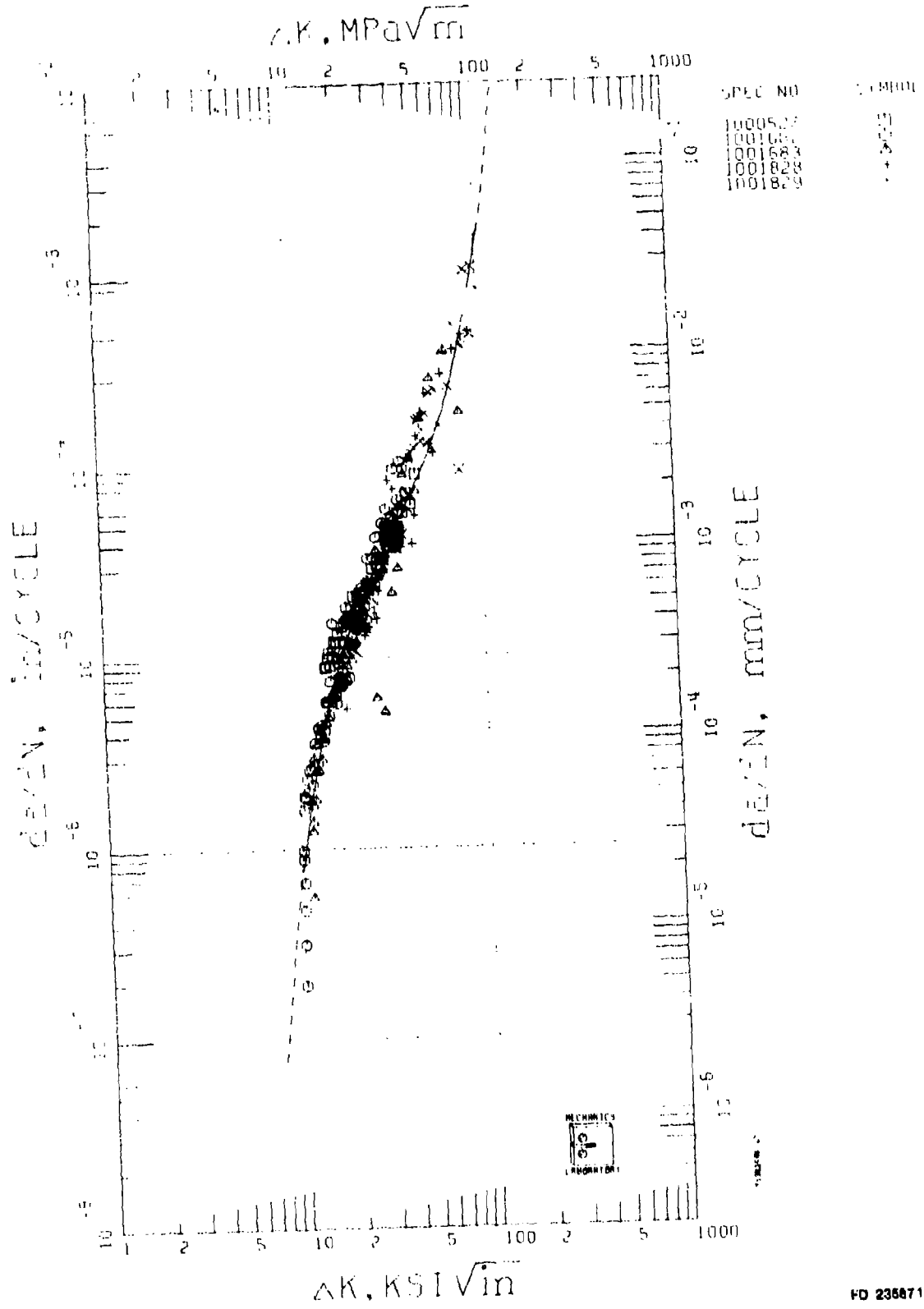

Figure 6. Data Analyses for Crack Growth Rate Based on Model No. 1

TABLE 1. MAXIMUM LIKELIHOOD ESTIMATE OF C_2, C_3, C_4, STANDARD DEVIATION σ_y AND THE COEFFICIENT OF VARIATION V OF Da/Dn

*Test Condition**	C_2	C_3	C_4	σ_y	*Coef. of Variation*	*No. of Data Points*
1	3.8033	−1.5239	−4.3563	0.1673	40.00%	258
2	4.9323	−1.4073	−3.9895	0.1692	40.49%	150
3	4.3093	−1.3032	−4.4450	0.1240	29.14%	130
4	3.8524	−1.5054	−4.1594	0.2078	50.72%	188
5	3.8982	−1.5376	−3.9341	0.1026	23.96%	342
Average					36.86%	

*Test Conditions

1. T = 1000°F, ν = 10 cpm, R = 0.1
2. T = 1350°F, ν = 10 cpm, R = 0.1
3. T = 1200°F, ν = 10 cpm, R = 0.5
4. T = 1200°F, ν = 20 cpm, R = 0.05
5. T = 1200°F, ν = 10 cpm, R = 0.1

To show the validity of the assumption that Z follows the normal distribution with zero mean, sample values of Z corresponding to test results (x_i,y_i), denoted by z_i, are computed from Eq. 4 as

$$z_i = y_i - C_1\sinh[C_2(x_i+C_3)] - C_4; \text{ for } i = 1,2.....,n \tag{24}$$

Sample values of z_i (i = 1,2,....,n) for each test condition (υ, R, T) are plotted on the normal probability paper in Figures 7-11 as circles. The normal probability paper is constructed using linear scales for both the ordinate Q and the abscissa Z. Sample values of Z are ranked in an ascending order and the plotting position for the jth data point z_j is $Q_j = \Phi^{-1}(j/n+1)$. Also shown in these figures are the straight lines representing the normal distribution of Z with zero mean and $\sigma_z = \sigma_y$ given in Table 1. It is observed in each figure that the test results z_i are scattered around the respective straight line, indicating that the normal distribution is reasonable for Z.

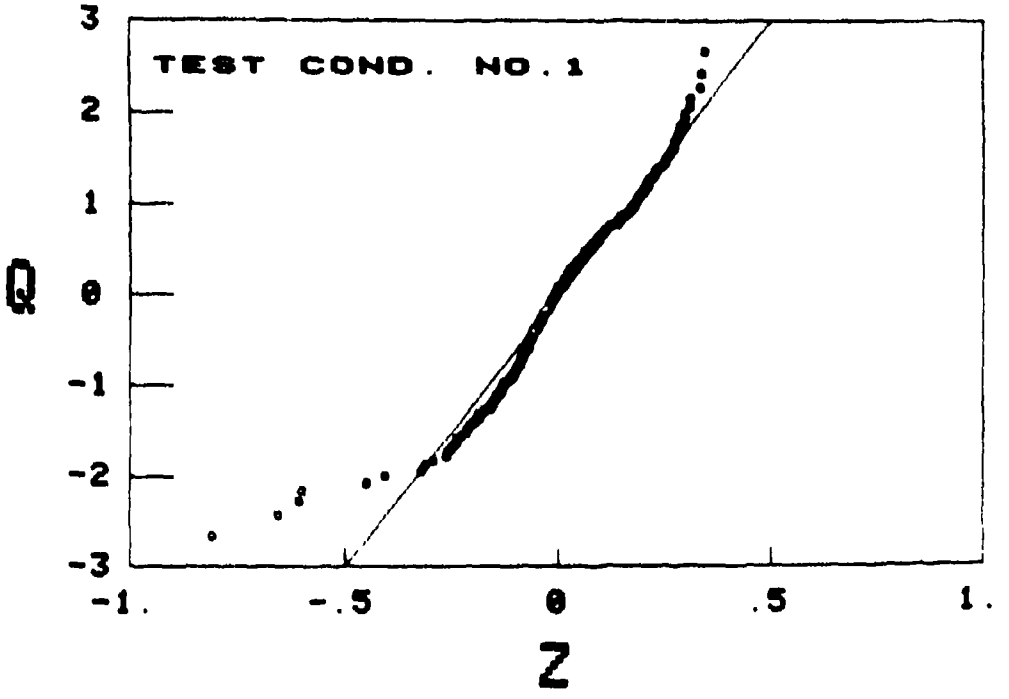

Figure 7. Normal Probability Plot for Z (Test Condition 1)

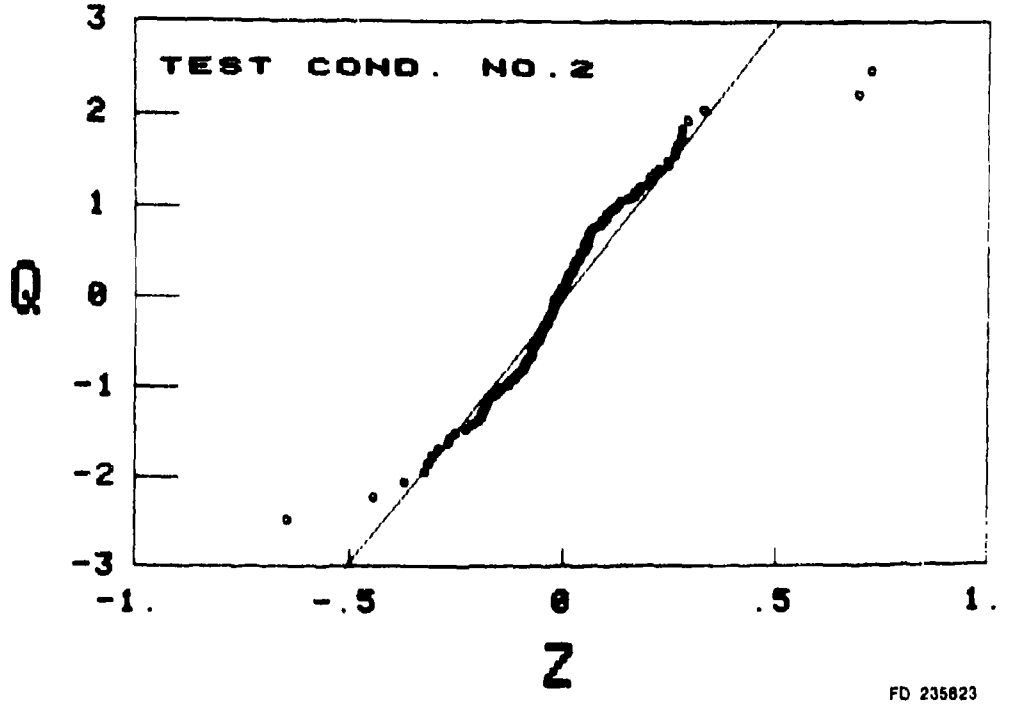

Figure 8. Normal Probability Plot for Z (Test Condition 2)

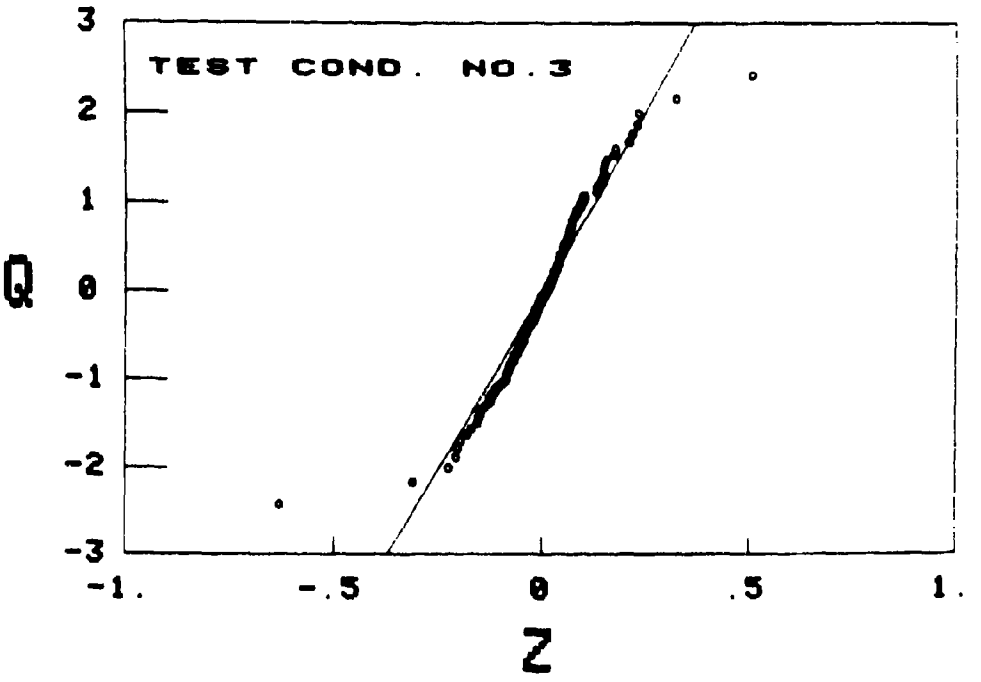

FD 235824

Figure 9. Normal Probability Plot for Z (Test Condition 3)

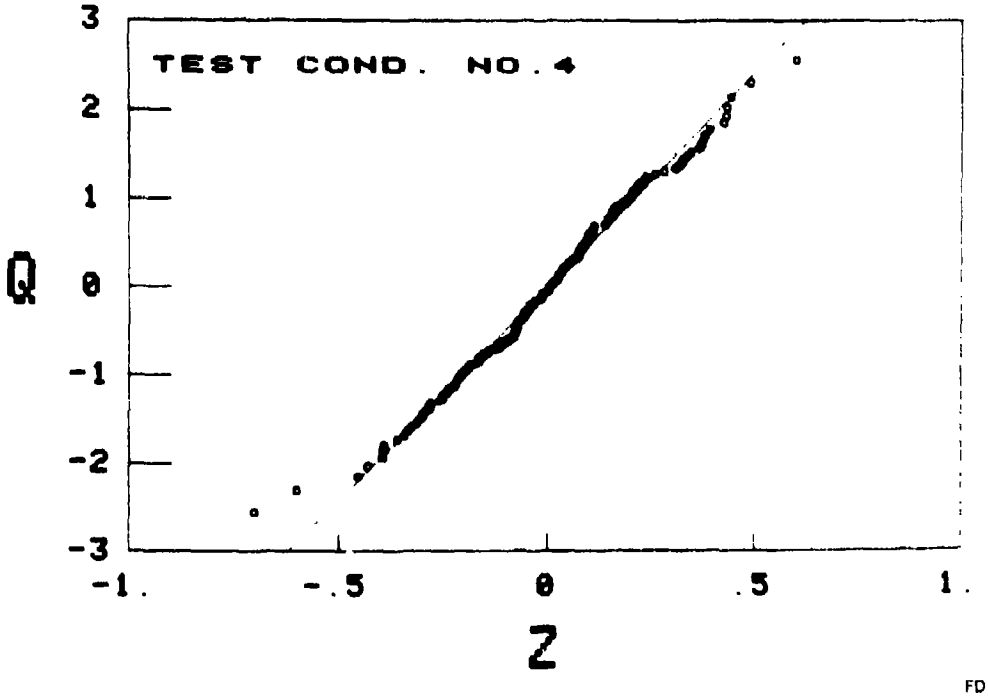

FD 235825

Figure 10. Normal Probability Plot for Z (Test Condition 4)

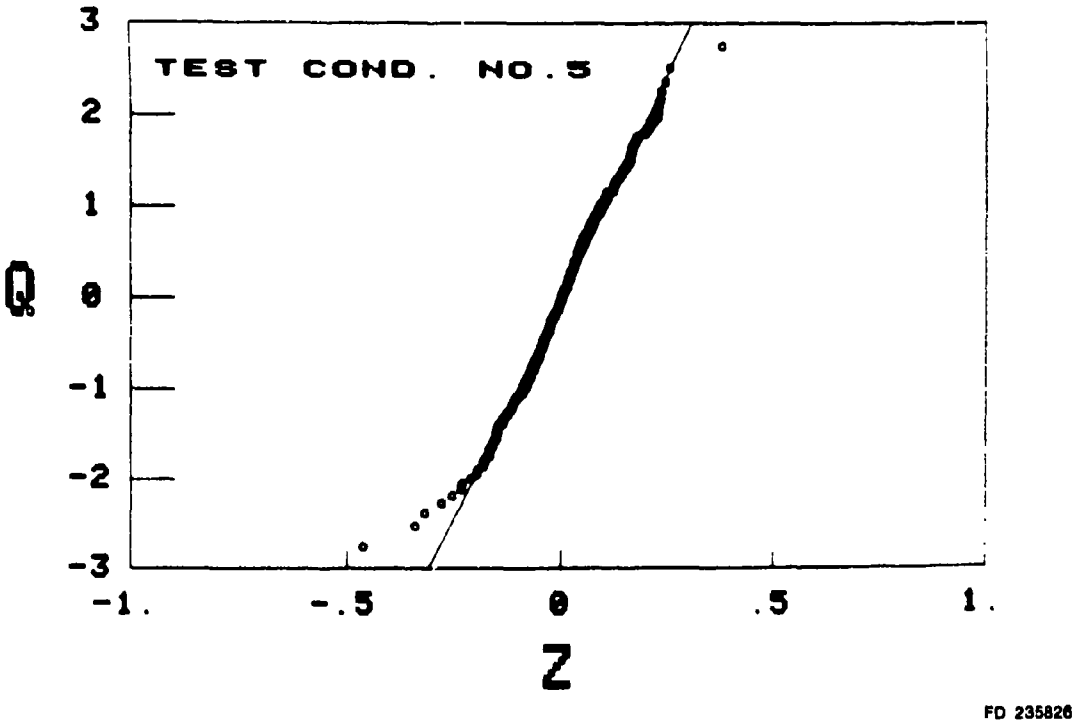

Figure 11. Normal Probability Plot for Z (Test Condition 5)

Tests for goodness-of-fit using the Kolmogorov-Smirnov (K-S) test have been carried out. The observed K-S statistics D_n along with the critical value D_n'' associated with α level of significance are presented in Table 2 for each test condition (υ, R, T). From Table 2 the normal distribution is acceptable for Z at a 20% level of significance for test conditions 3-5, whereas the level of significance is 5% for test conditions 1 and 2.

TABLE 2. COMPARISON OF OBSERVED D_n AND CRITICAL VALUES OF D_n'' IN THE KOLMOGOROV-SMIRNOV TEST FOR Z

Test Condition	*Sample Size, n*	*Observed D_n*	*Critical Values of D_n''*			
			$\alpha = 0.2$	$\alpha = 0.1$	$\alpha = 0.05$	$\alpha = 0.01$
1	258	0.081	0.067	0.076	0.085	0.102
2	150	0.114	0.088	0.100	0.111	0.133
3	130	0.091	0.094	0.107	0.119	0.143
4	188	0.064	0.078	0.089	0.099	0.119
5	342	0.050	0.058	0.066	0.735	0.088

α = level of significance

It is important to emphasize that the present statistical model (random variable model in Eq. 4), referred to as the first statistical model, has a significant advantage in that the statistical distribution of the crack growth damage accumulation can be obtained analytically.

Statistical Distribution of Crack Growth Rate

After C_2, C_3, C_4 and σ_y have been estimated from Eqs. 15-18 for each test condition given in Table 1, the distributions of the crack growth rates of $Y(\Delta K,C_i) = \log da/dn$ and $G(\Delta K,C_i) = da/dn$, for i = 2,3,4 are, respectively, normal and lognormal as given by Eqs. 7, 20-21.

To theoretically demonstrate the behavior of the distributions of Y and da/dn, let z_γ be the γ percentile of Z, i.e.,

$$\gamma\% = P[Z>z_\gamma] = 1 - \Phi\left(\frac{z_\gamma}{\sigma_z}\right) \tag{25}$$

where Z follows the normal distribution with zero mean and the standard deviation $\sigma_z = \sigma_y$ (see Eq. 6). Inversely Eq. 25 can be written as

$$z_\gamma = \sigma_z \Phi^{-1}(1-\gamma\%) \tag{26}$$

in which $\sigma_z = \sigma_y$ and $\Phi^{-1}(\ )$ is the inversed function of $\Phi(\ )$.

The γ percentile of the log crack growth rate $y_\gamma(\Delta K,C_i)$, (i = 2,3,4), follows from Eq. 4 as

$$y_\gamma(\Delta K,C_i) = C_1 \sinh[C_2(X + C_3)] + C_4 + z_\gamma \tag{27}$$

and the γ percentile of the crack growth rate

$$\left(\frac{da}{dn}\right)_\gamma = G_\gamma(\Delta K,C_i) \tag{28}$$

becomes

$$G_\gamma(\Delta K,C_i) = (10)^{y_\gamma(\Delta K,C_i)} \tag{29}$$

in which $y_\gamma(\Delta K,C_i)$ is given by Eqs. 26 and 27.

Note that $G_\gamma(\Delta K,C_i)$ and $y_\gamma(\Delta K,C_i)$ are functions of the stress intensity range ΔK and C_i (i = 2, 3, 4) that depend on test conditions (v, R, T).

The γ percentile log crack growth rate path $y_\gamma(\Delta K, C_i)$ are computed from Eqs. 26 and 27 and plotted in Figure 12 for the test condition No. 1 (v = 10 cpm, R = 0.1 and T = 1000°F) for γ = 5, 25, 50, 75, 95. Curves in Figure 12 also represent possible sample paths of the crack growth rate. For instance, the crack growth rate path associated with γ = 5% indicates that 5% of the specimens will have a crack growth rate path higher (or faster) than that shown by the curve. It is observed from Figure 12 that sample paths of the crack growth rate do not intermingle, and that a specimen with a higher crack growth rate always preserves it over the entire range of ΔK.

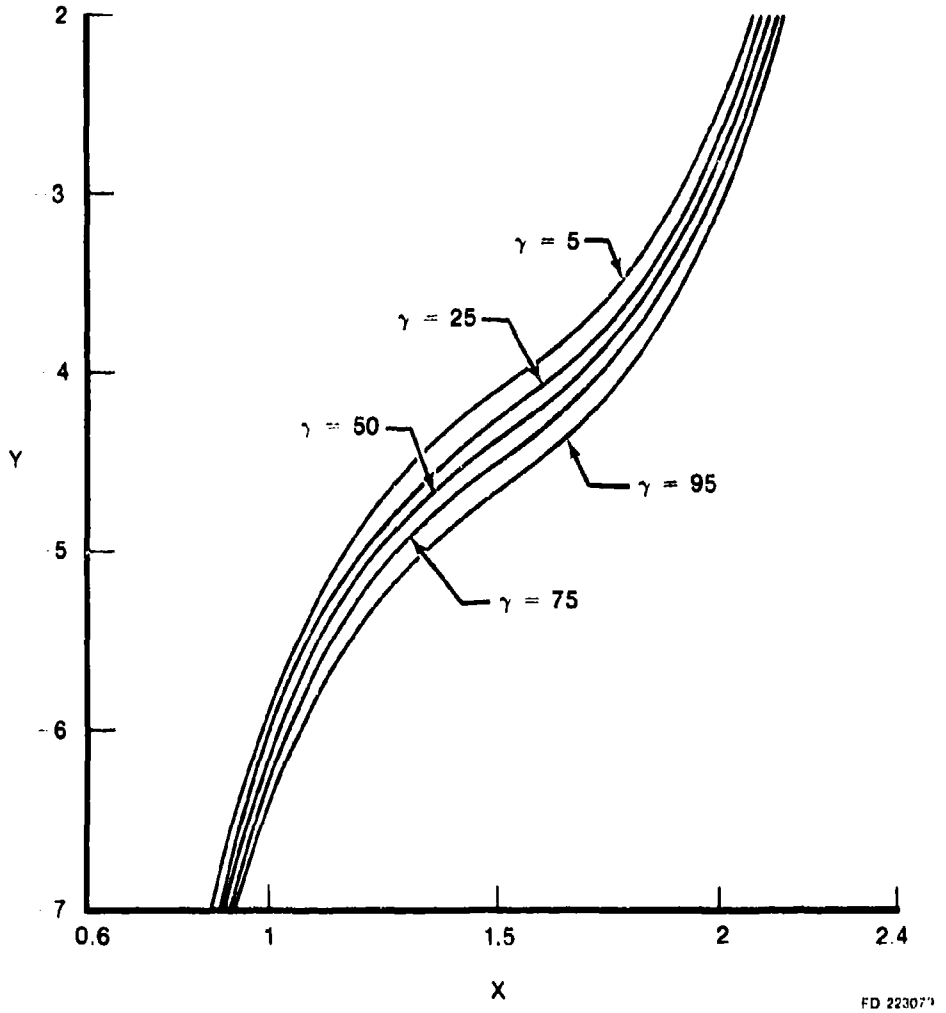

Figure 12. Percentiles of Log Crack Growth Rate Y as Function of Log Stress Intensity Range X for Model 1 and Test Condition No. 1

Statistical Distribution of Crack Size and Time to Reach Given Crack Size

The γ percentile crack size after n load cycles, denoted by $a_\gamma(n)$, can be computed using the γ percentile crack growth rate $G_\gamma(\Delta K, C_i)$ as follows:

$$\left(\frac{da}{dn}\right)_\gamma = G_\gamma(\Delta K, C_i) \tag{30}$$

$$\Delta a_j(\gamma) = G_\gamma(\Delta K, C_i)\Delta n_j \tag{31}$$

$$a_\gamma(n) = a_0 + \sum_{j=1}^{m} \Delta a_j(\gamma) \tag{32}$$

in which a_0 is the initial crack size and

$$n = \sum_{j=1}^{m} \Delta n_j \tag{33}$$

The cycle-by-cycle numerical integration given by Eqs. 30-33 is deterministic and straightforward. Hence, by varying the value of the γ percentile, one obtains from a cycle-by-cycle integration a set of crack growth curves $a_\gamma(n)$, i.e., the crack size versus the number of cycles for each γ value. The γ percentiles of the crack growth damage accumulation $a_\gamma(n)$ are plotted in Figure 13 for the test condition No. 1 (ν = 10 cpm, R = 0.1 and T = 1000°F) with the following specimen geometry and loading condition: ASTM CT specimen, thickness = 0.25 in., width = 2.502 in., maximum load = 1.4 ksi, initial crack size = 0.5 in., final crack size 2.0 in., C_1 = 0.5 and C_i, i=2,3,4 given in Table 1. For instance, the crack growth curve $a_\gamma(n)$ corresponding to γ=10 in Figure 13 indicates that there are 10% of the specimens having a crack size larger than those indicated by this curve at any number of load cycles n.

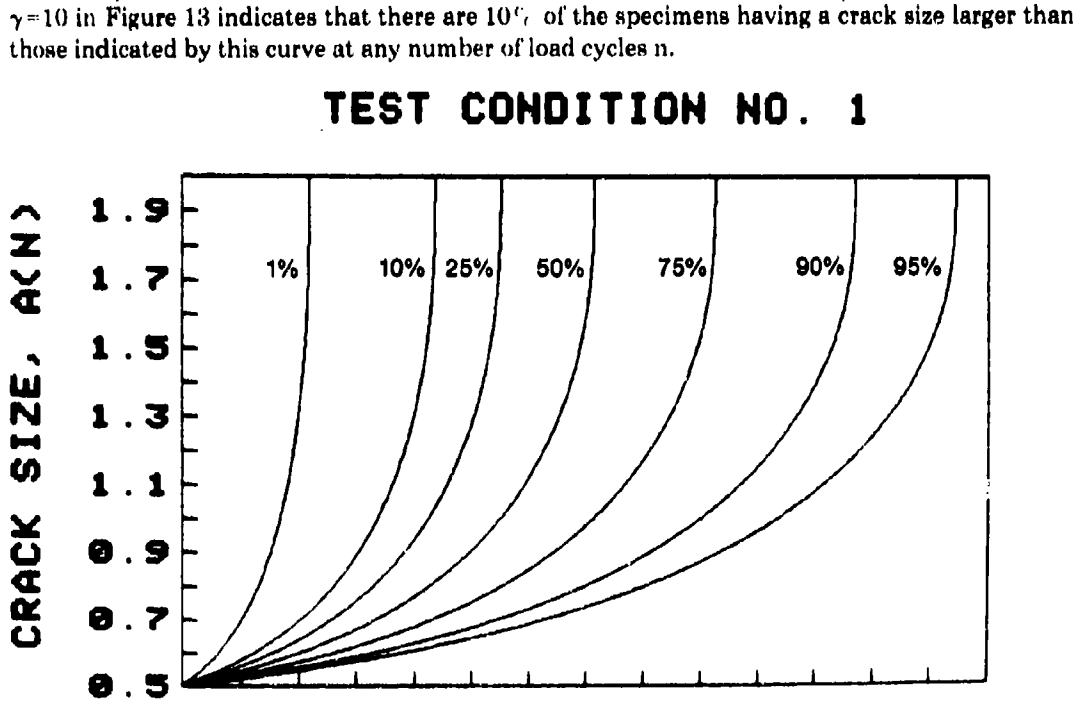

Figure 13. Distribution for Crack Growth Damage Accumulation a(n) for Model 1 and Test Condition No. 1

After constructing a series of crack growth damage accumulation curves $a_\gamma(n)$ for many values of γ as shown in Figure 13, one can establish (i) the distribution function $F_{N(a)}(n)$ of the number of load cycles N(a) to reach any crack size "a" by drawing a horizontal line through "a" and (ii) the distribution function $F_{a(n)}(x)$ of the crack size a(n) at any number of load cycles n by drawing a vertical line through n.

For instance, the distribution $F_{N(a)}(n)$ for the number of load cycles to reach the crack sizes a = 1.0 in. and 2.0 in. are shown in Figure 14(a) and 14(b), respectively, as solid curves. The complement of the distribution function of the crack size a(n) at n = 25,000 load cycles, i.e.,

$F^*_{a(n)}(x) = 1 - F_{a(n)}(x)$, is presented in Figure 15 as a solid curve. In Figure 15 the ordinate $F^*_{a(n)}$ is the probability that the crack size will exceed the corresponding value indicated by the abscissa. For instance, the probability is 0.41 that the crack size at n = 25,000 cycles will exceed 0.65 in. as shown by a square on the solid curve in Figure 15. Figure 15 is referred to as the crack exceedance curve. In conclusion, on the basis of the present statistical model, the distribution of the crack growth damage accumulation presented in Figure 13 contains all the information needed for the analysis of retirement for cause of engine materials.

Correlation With Test Results

One of the difficult problems encountered in the present program is that the number of test specimens under each environmental condition (υ, R, T) is very small. Even with such a small sample size, each specimen is usually tested using different specimen geometry, initial crack size, final crack size and maximum load. A summary of specimen geometries and loading conditions for all the test specimens is presented in Table 3. It is obvious from Table 3 that the experimental results of the crack growth damage accumulation are not homogeneous, making the correlation study difficult. A qualitative correlation study is carried out in the following.

In order to correlate the test results with the predictions based on the statistical model proposed previously, homogeneous test environments have been assumed for each test condition as shown in Table 4. The maximum loads P_{max} given in Table 4 are chosen in order to avoid excessive extrapolation far into the region of ΔK in which actual test results do not exist. Test results of the crack growth rate for each specimen are best-fitted by Eq. 1 using the method of least squares to estimate values of C_2, C_3 and C_4. The least squares best fit procedures have been described in Ref. 1. Sample values of C_i (i=2,3,4) thus obtained for each specimen are presented in Table 5 for various test conditions. As an example, the best-fitted crack growth rate for the five specimens in the test condition No. 1 are plotted in Figure 16 using Eq. 1 and C_i (i=2,3,4) values given in Table 5. The regions of Y and X shown by solid curves are the regions in which test data exist, whereas the dotted curves represent the extrapolation into the regions where test data are nonexistent.

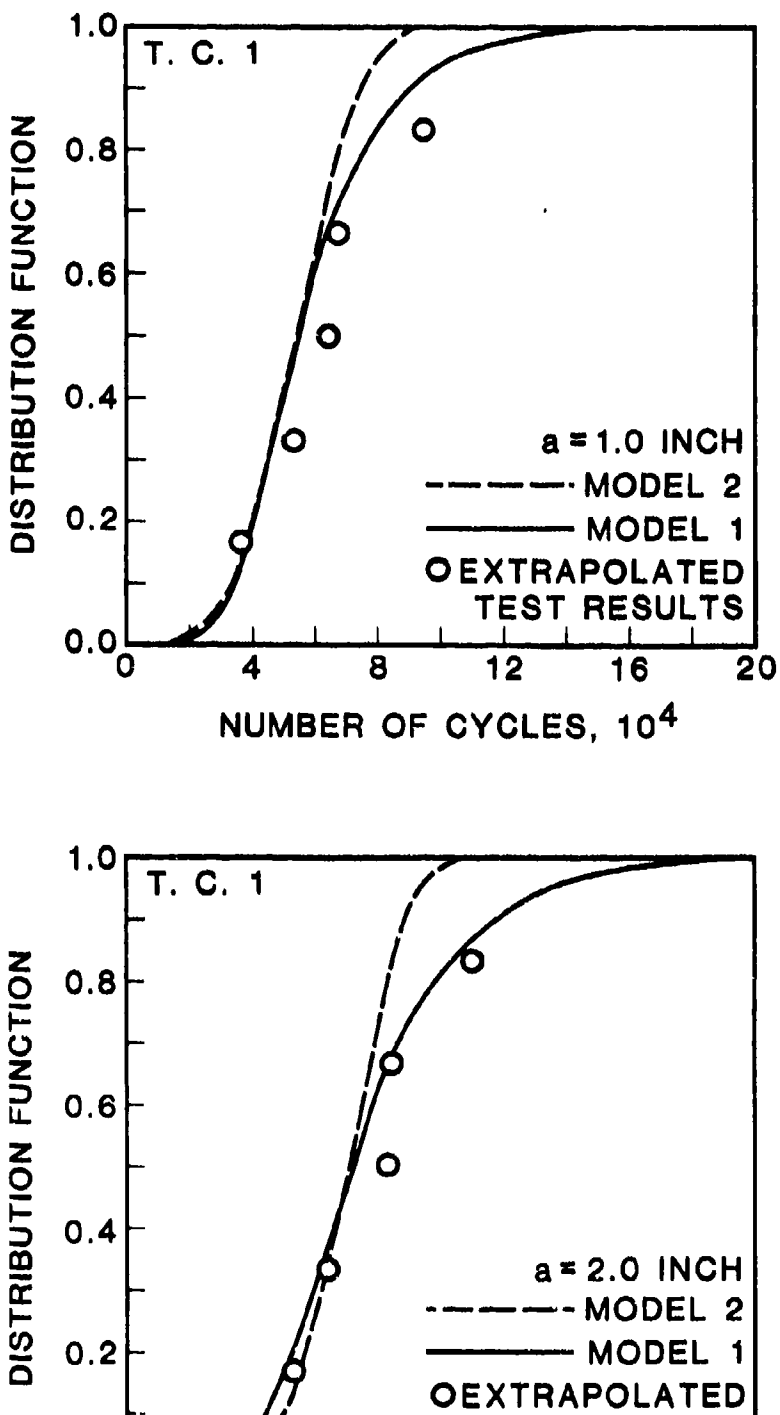

Figure 14. Distributions of Cycles to Reach a Given Crack Size for Test Condition No. 1

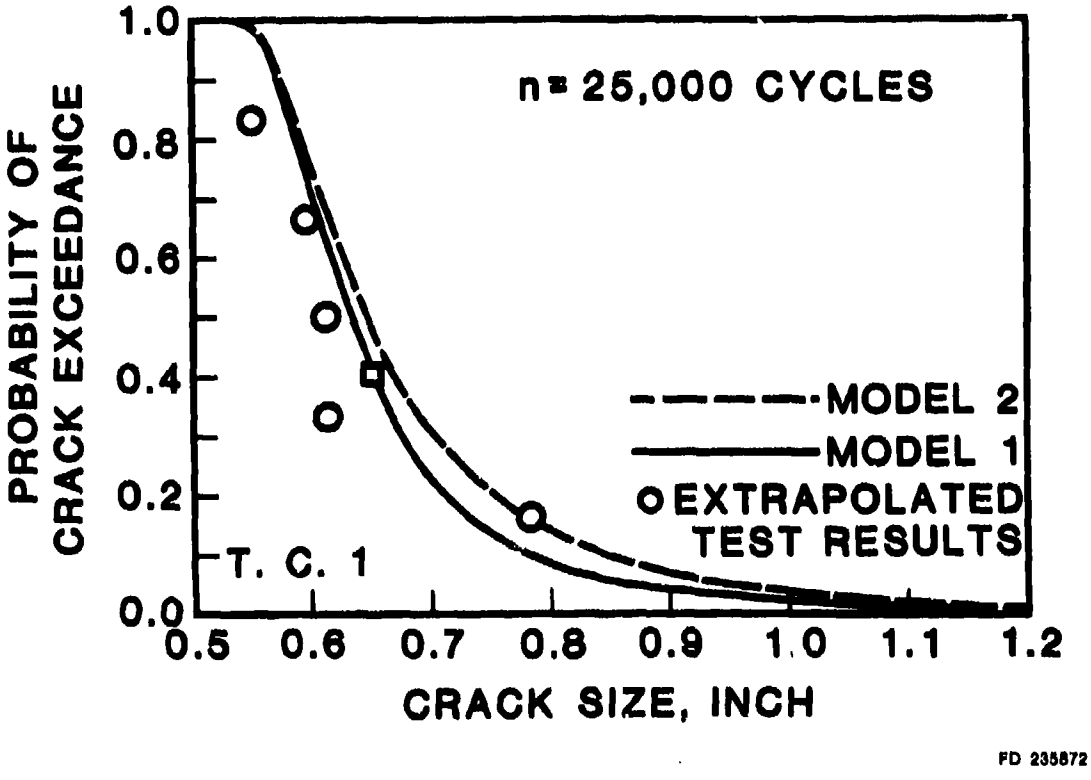

Figure 15. Probability of Crack Exceedance at 25,000 Load Cycles for Model 1 and Test Condition No. 1

TABLE 3. SPECIMEN GEOMETRY AND MAXIMUM LOAD FOR EACH TEST SPECIMEN

Specimen No.	*a (0) (in.)*	*a_f (in.)*	*W (in.)*	*B (in.)*	*P_{max} (kips)*
		Test Condition No. 1			
0582	0.812	1.788	2.502	0.250	1.008
1682	0.759	1.819	2.599	0.499	1.643
1683	0.742	2.021	2.538	0.501	1.823
1828	0.724	1.598	2.004	0.497	1.845
1829	0.370	1.427	2.008	0.499	3.564
		Test Condition No. 2			
0318	0.8188	1.373	2.497	0.479	1.705
0371	0.838	1.797	2.499	0.502	2.027
0543	0.804	1.757	2.498	0.452	1.754
1765	0.517	1.640	2.503	0.501	2.573
		Test Condition No. 3			
0334	0.836	1.936	2.496	0.501	2.018
0393	0.928	1.927	2.505	0.500	2.037
1826	0.620	1.467	2.00	0.500	2.20
1827	0.980	1.518	2.001	0.500	1.528
		Test Condition No. 4			
0710	0.859	1.251	2.499	0.826	3.145
0711	0.975	1.710	2.513	0.499	1.675
0717	1.168	1.911	2.509	0.364	0.916
1385	0.926	1.948	2.507	0.498	2.219
1389	0.818	1.805	2.506	0.500	2.426
1722	0.162	0.545	1.251	0.138	2.438
		Test Condition No. 5			
0634	0.895	2.012	2.505	0.501	1.501
0641	0.808	1.717	2.496	0.499	2.693
0633AF	1.005	1.733	2.512	0.250	0.906
0685AF	0.826	1.768	2.507	0.870	3.520
1053	0.852	1.760	2.493	0.299	1.480
1341	0.088	0.353	0.986	0.296	7.168
0346	1.491	2.009	2.503	0.501	1.356
1673	0.451	1.691	2.497	0.501	3.533
1674	0.475	1.669	2.503	0.499	3.811

TABLE 4. ASSUMED HOMOGENOUS TEST ENVIRONMENTS FOR TEST SPECIMENS

Test Condition	*a (0) (in.)*	*a_f (in.)*	*W (in.)*	*B (in.)*	*P_{max} (kips)*
1	0.5	2.0	2.502	0.25	1.4
2	0.5	2.0	2.503	0.501	2.6
3	0.5	1.8	2.00	0.50	2.60
4	0.5	2.0	2.506	0.50	3.0
5	0.5	2.0	2.497	0.501	3.533

a(0) = initial crack size
a_f = final crack size
W = specimen width
B = specimen thickness
P_{max} = maximum load

TABLE 5. TEST RESULTS OF C_2, C_3 AND C_4 FOR EACH SPECIMEN UNDER VARIOUS TEST CONDITIONS

	Specimen No.	C_2	C_3	C_4
(a)	Test Condition No. 1 T = 1000°F, ν = 10 cpm, R = 0.1			
	0582	3.3620	−1.345	−4.690
	1682	5.051	−1.358	−4.676
	1683	3.989	−1.490	−4.490
	1828	3.962	−1.537	−4.346
	1829	4.041	−1.605	−4.148
(b)	Test Cordition No. 2 T = 1350°F, ν = 10 cpm, R = 0.1			
	0318	5.349	−1.097	−4.836
	0371	4.827	−1.388	−4.085
	0643	3.823	−1.538	−3.743
	1765	5.556	−1.407	−3.938
(c)	Test Condition No. 3 T = 1200°F, ν = 10 cpm, R = 0.5			
	0334	4.806	−1.158	−4.879
	0393	5.234	−1.202	−4.681
	1826	4.036	−1.347	−4.310
	1827	4.794	−1.280	−4.531
(d)	Test Condition No. 4 T = 1200°F, ν = 20 cpm, R = 0.05			
	0710	5.554	−1.433	−4.276
	0711	4.470	−1.397	−4.336
	0717	4.201	−1.561	−3.994
	1386	4.484	−1.566	−4.149
	1389	3.733	−1.490	−4.144
	1722	4.139	−1.307	−4.390
(e)	Test Condition No. 5 T = 1200°F, ν = 10 cpm, R = 0.1			
	0534	4.272	−1.528	−3.825
	0541	3.780	−1.566	−3.858
	0633AF	3.322	−1.649	−3.731
	0685AF	3.799	−1.566	−3.877
	1053	3.804	−1.539	−3.971
	1341	4.047	−1.533	−3.972
	0346	3.674	−1.369	−4.402
	1673	3.391	−1.497	−3.960
	1674	4.126	−1.510	−4.045

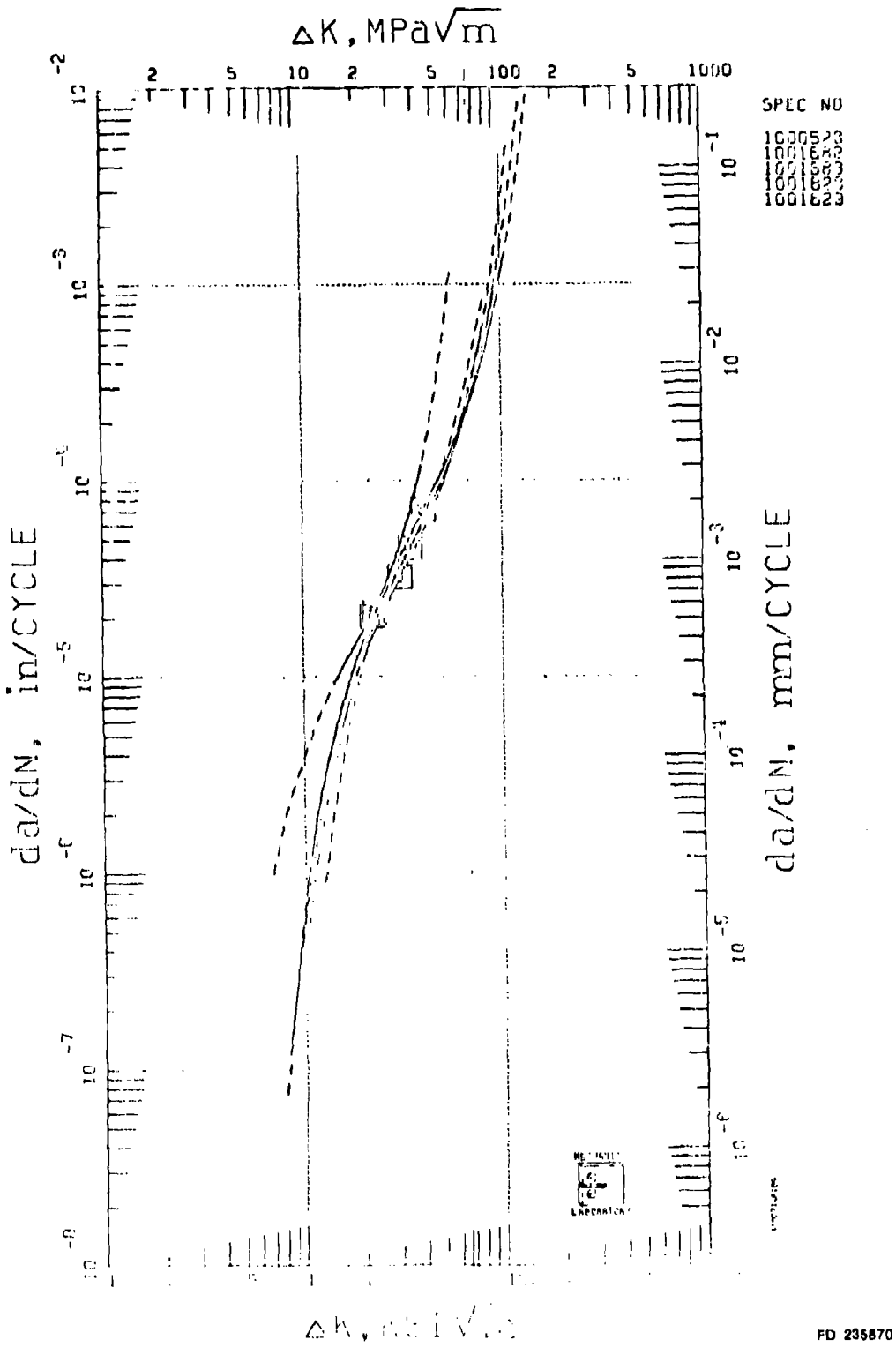

Figure 16. Best-Fitted Crack Growth Rate for each Specimen in Test Condition No. 1

The best-fitted C_2, C_3 and C_4 values for each test specimen presented in Table 5 are used to grow the crack under assumed homogeneous test environments shown in Table 4. The crack growth damage accumulation thus obtained is referred to as the "extrapolated test results" in the sense that they are not the actual test results.

Let us consider the test condition No. 1. Based on the theoretical model, the maximum likelihood estimates of C_2, C_3, C_4 and σ_y obtained in Table 1 are used to construct various percentiles of the log crack growth rate Y = log (da/dn) versus the log stress intensity range X = log ΔK. The results are presented in Figure 17(a). The least square estimates of C_2, C_3 and C_4 for each specimen obtained in Table 5 are used along with Eq. 1 to construct Y versus X as shown in Figure 17(b). Figure 17(b) is referred to as the "extrapolated test results" since the actual test data do not exist in the entire region of ΔK.

With the assumed homogeneous test conditions given in Table 4, the log crack growth rates displayed in Figure 17 have been integrated to yield the crack growth damage accumulation. The corresponding crack size, a(n), versus the number of load cycles, n, is shown in Figure 18. A comparison between Figures 18(a) and 18(b) indicates that the correlation between the extrapolated test results and the statistical model is reasonable.

In the same manner, the log crack growth rate, Y, versus the log stress intensity range, X, and the crack size, a(n), versus the number of load cycles, n, have been computed and presented in Figures 19-26 for test conditions No. 2 to 5. It is observed from these figures that the correlation between the extrapolated test results and the statistical model is reasonable.

The distributions $F_{N(a)}(n)$ for the number of load cycles N(a) to reach any crack size based on the statistical model is plotted in Figures 27-31 as solid curves for all the test conditions and two particular crack sizes. The corresponding distribution functions for the extrapolated test results are determined from Figures 18(b), 21(b)-24(b) and shown in Figures 27-31 as circles. In constructing the distribution function (circles) of the extrapolated test results in Figure 27, for instance, one obtains five data points from Figure 18(b) by drawing a horizontal line through a = 1.0 in. These five data points are ranked in an ascending order and the ordinate of the ith data point is i/(m+1) where m=5 is the total number of data points. Figures 27-31 demonstrate a good correlation between the statistical model (solid curves) and the extrapolated test results (circles).

The procedures for determining the distribution of the crack size a(n) at any number of load cycles, n, have been described previously. The complement of the distribution function $F^*_{a(n)}(x)$ of a(n), referred to as the crack exceedance curve, is plotted in Figures 32-36 as solid curves. For instance, the square shown in Figure 32 indicates that at n=25,000 load cycles the probability that the crack size will exceed 0.65 in. (abscissa) is 0.41 (ordinate) for the test condition No. 1. It is observed that the exceedance probability reduces as the crack size increases. The extrapolated test results for a(n) are obtained from Figures 18(b), 23(b)-26(b) by drawing a vertical line through the number of load cycles, n, of interest. They are plotted in Figures 32-36 as circles for all test conditions. Figures 32-36 demonstrate that the correlation for the crack size distribution between the statistical model and the extrapolated test results is very reasonable.

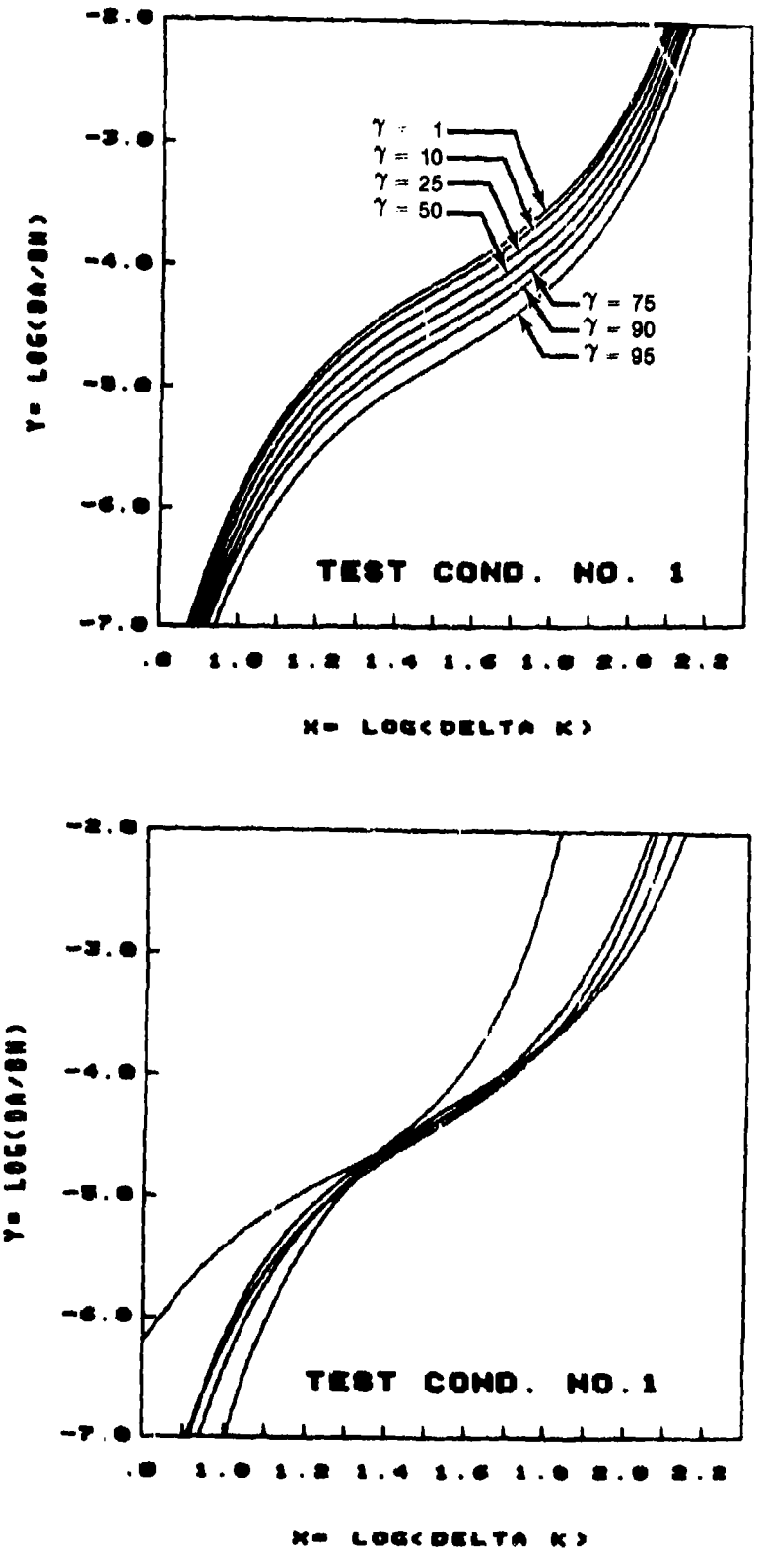

Figure 17. Log Crack Growth Rate Y(X) vs Log Stress Intensity Range X for Test Condition No. 1; (a) Statistical Model No. 1 and (b) Extrapolated Test Results

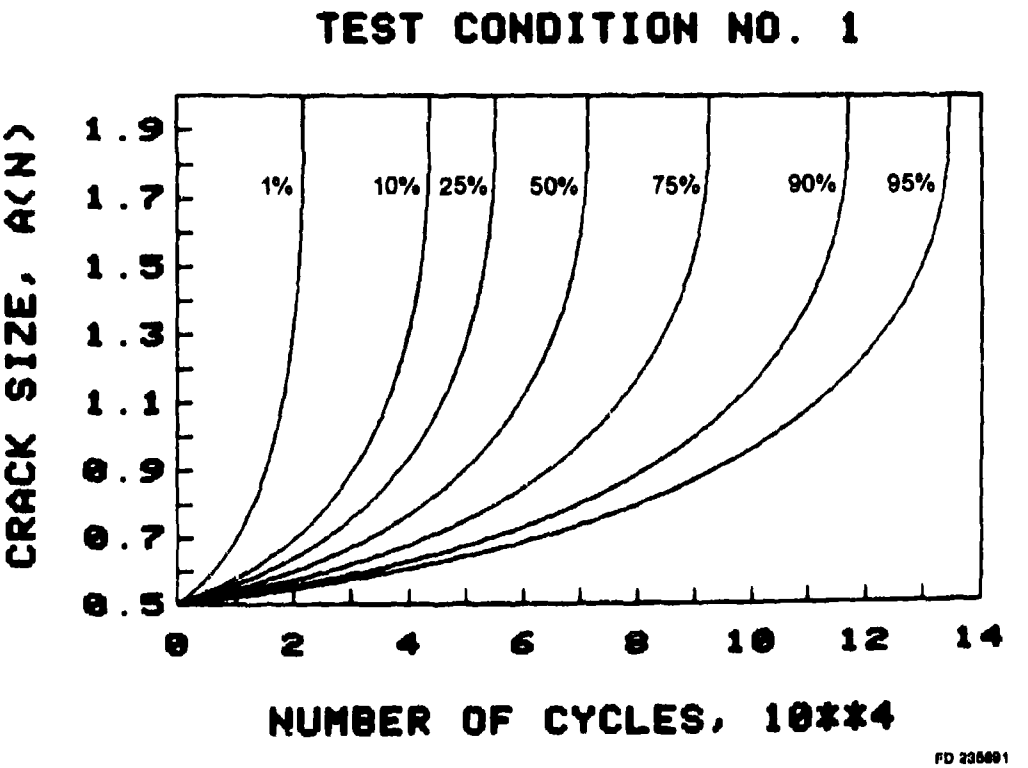

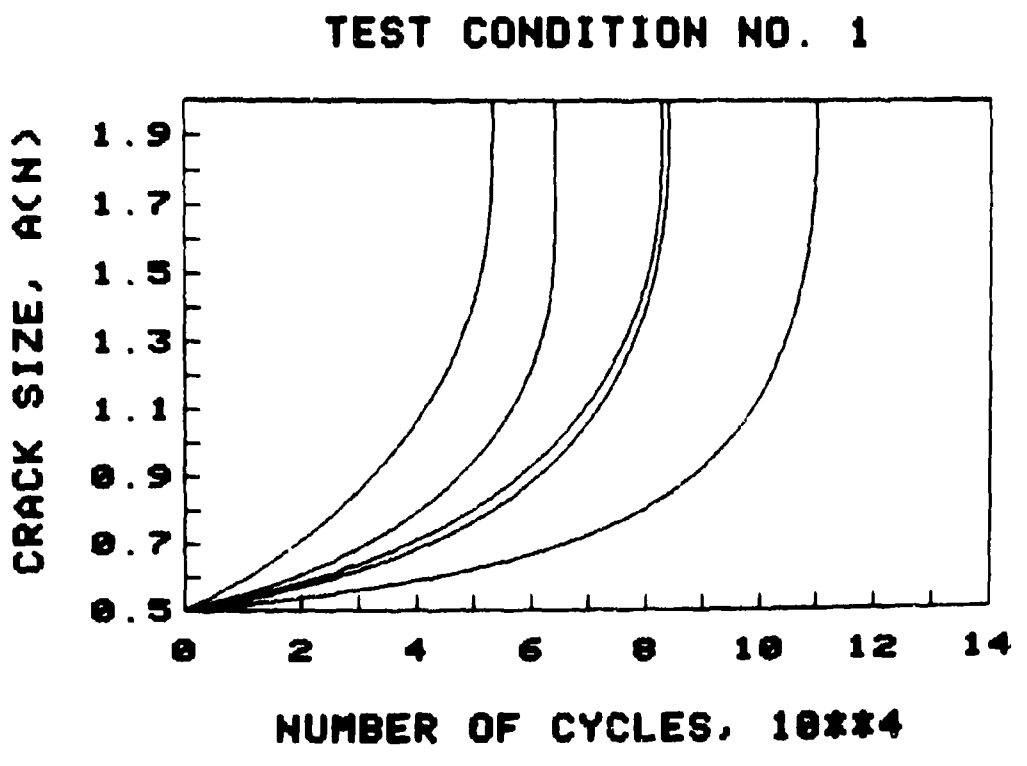

Figure 18. Crack Growth Damage Accumulation for Test Condition No. 1; (a) Statistical Model and (b) Extrapolated Test Results

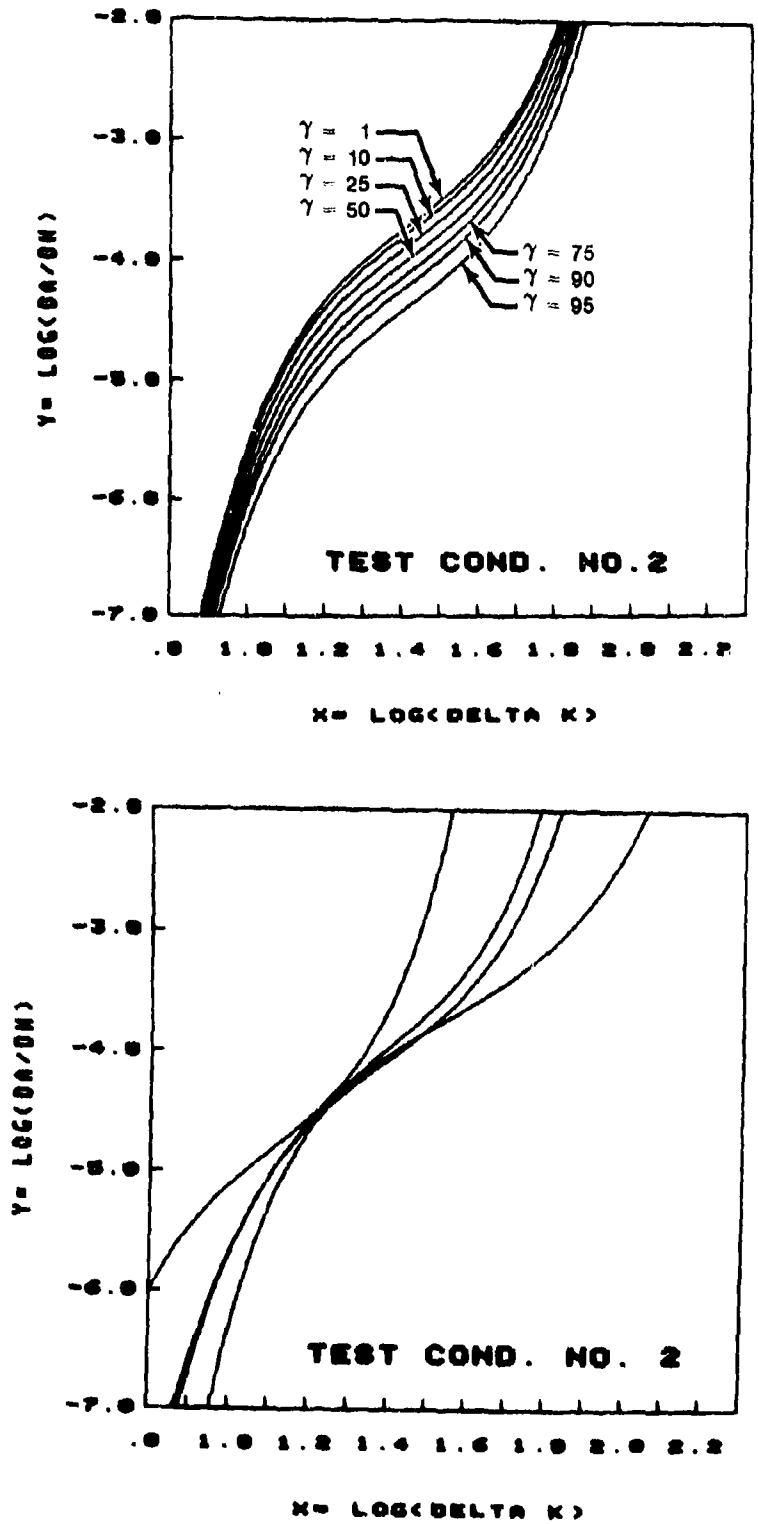

Figure 19. Log Crack Growth Rate Y(X) vs Log Stress Intensity Range X for Test Condition 2; (a) Statistical Model No. 1 and (b) Extrapolated Test Results

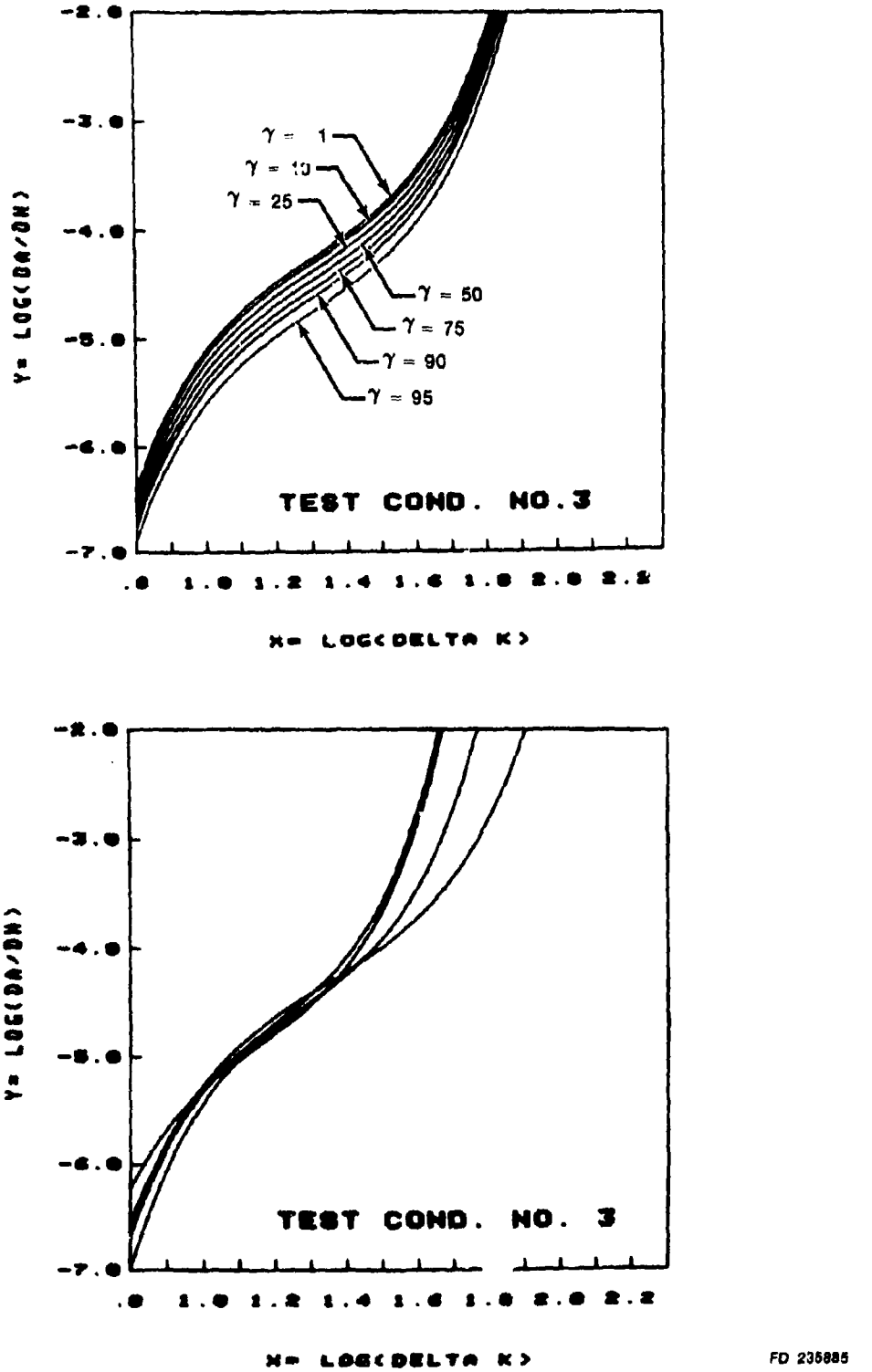

Figure 20. Log Crack Growth Rate Y(X) vs Log Stress Intensity Range X for Test Condition No. 3; (a) Statistical Model No. 1 and (b) Extrapolated Test Results

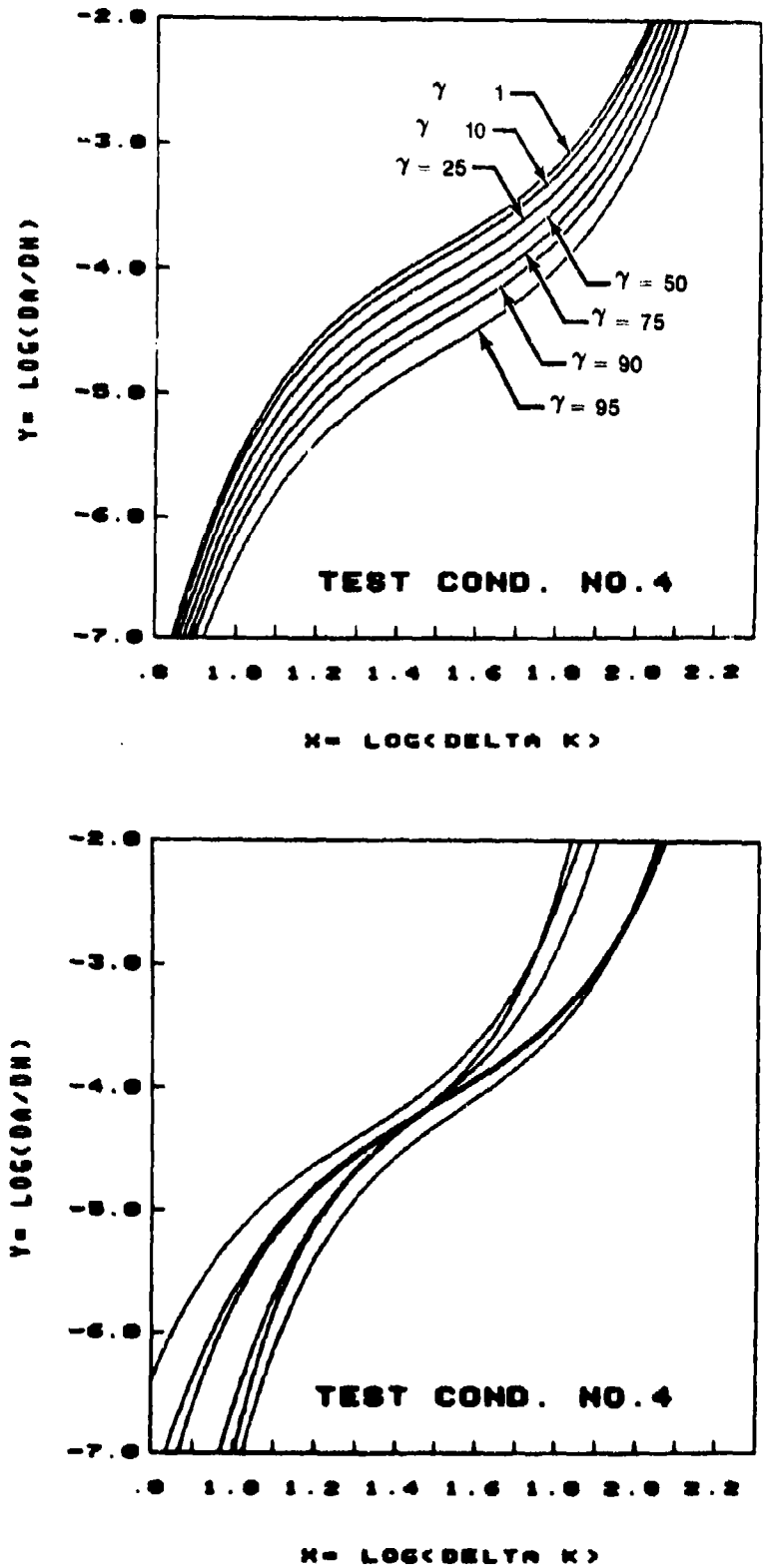

Figure 21. Log Crack Growth Rate Y(X) vs Log Stress Intensity Range X for Test Condition No. 4; (a) Statistical Model No. 1 and (b) Extrapolated Test Results

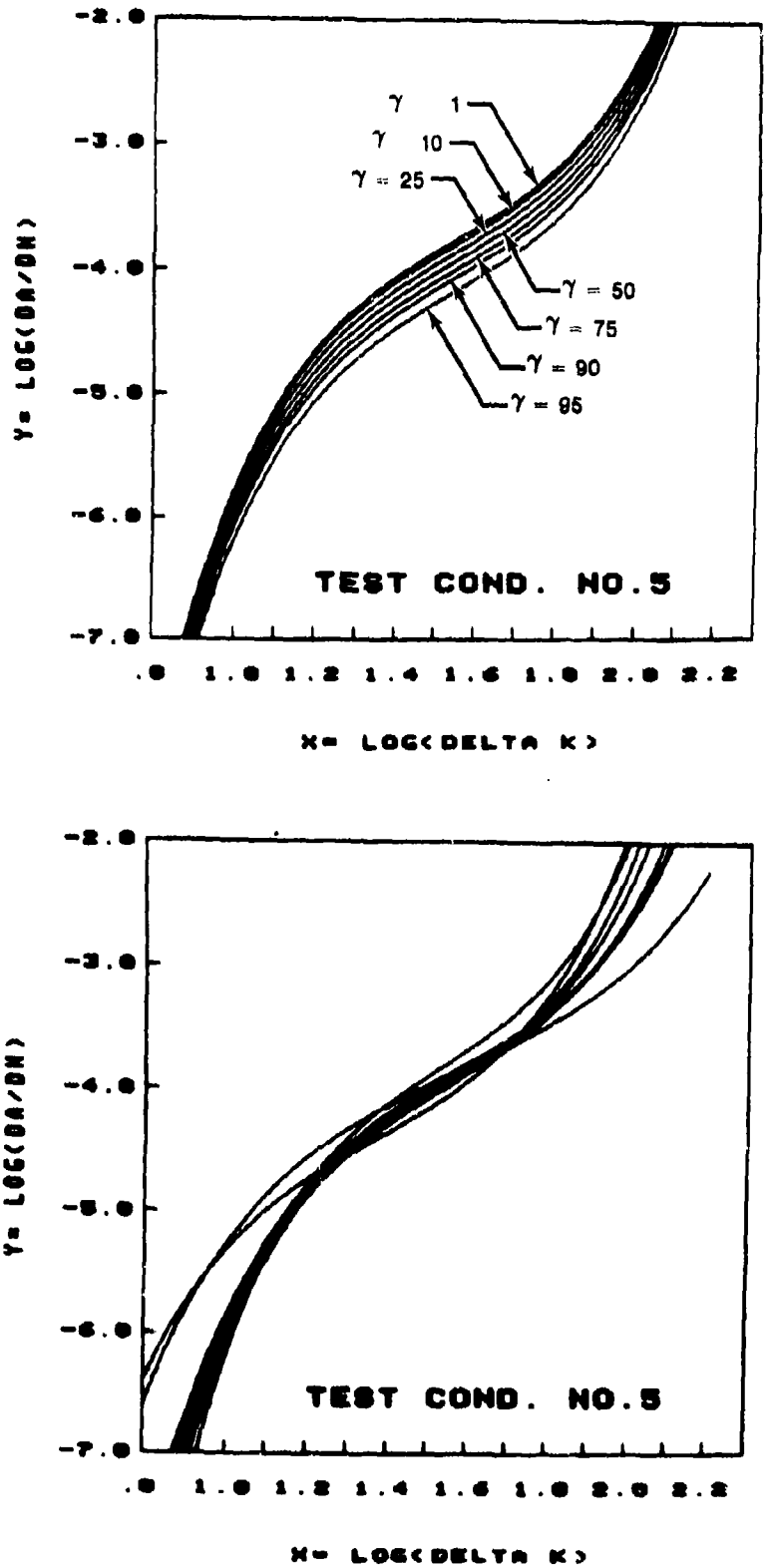

Figure 22. Log Crack Growth Rate Y(X) vs Log Stress Intensity Range X for Test Condition No. 5; (a) Statistical Model No. 1 and (b) Extrapolated Test Results

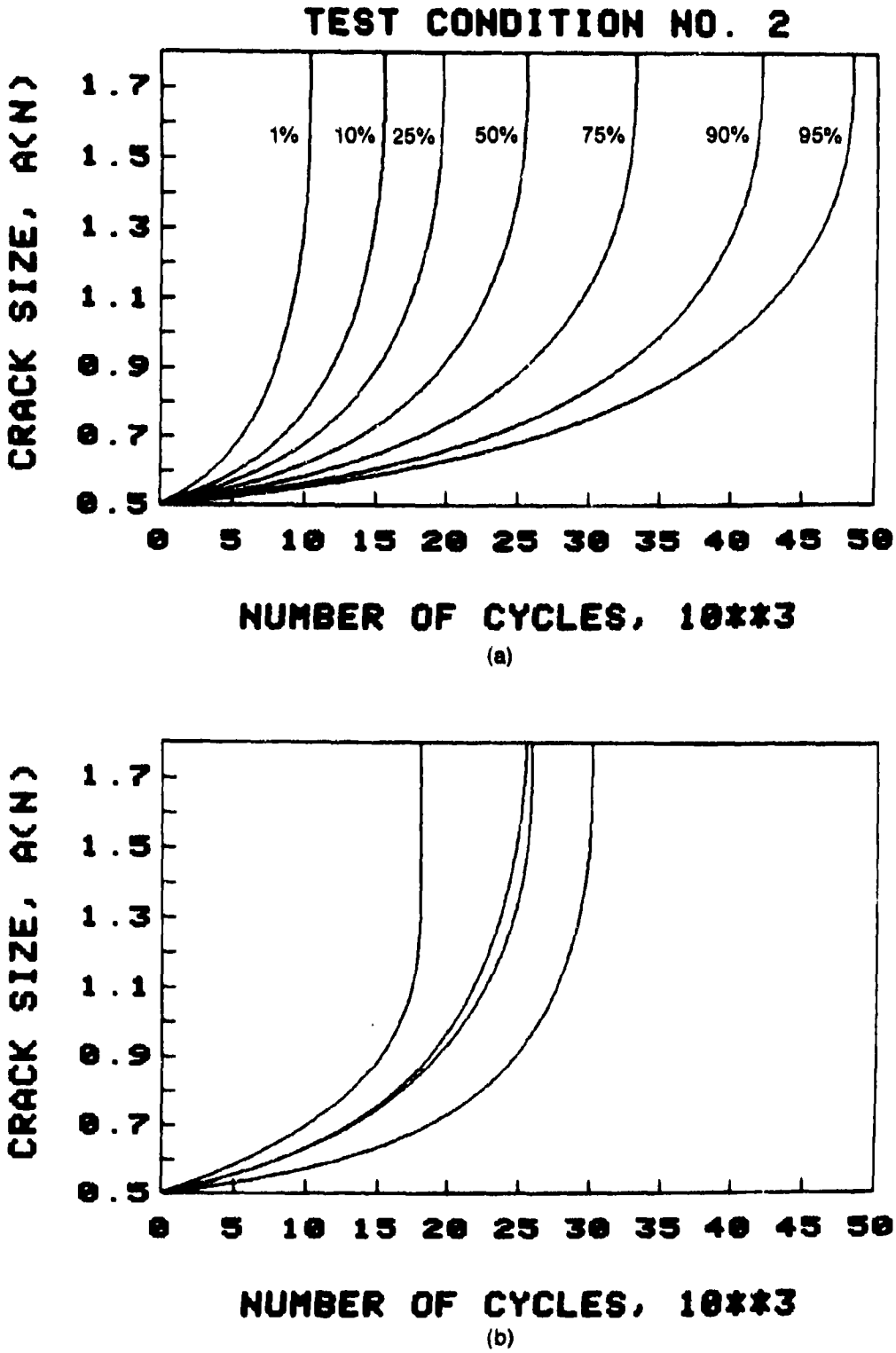

Figure 23. Crack Growth Damage Accumulation for Test Condition No. 2; (a) Statistical Model No. 1 and (b) Extrapolated Test Results

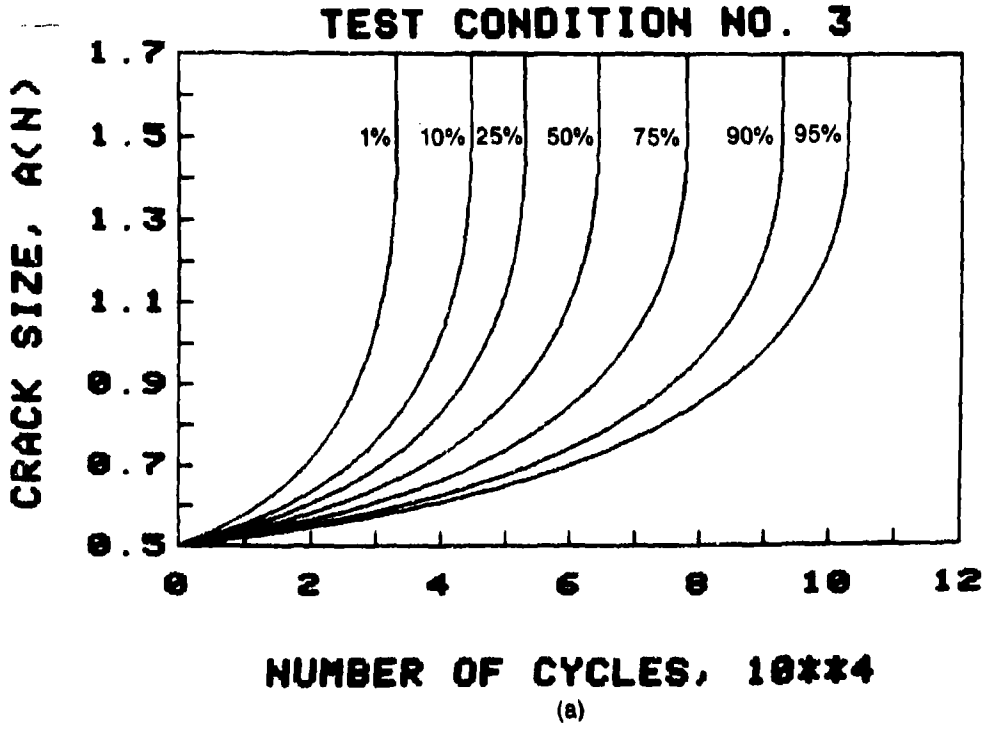

(a)

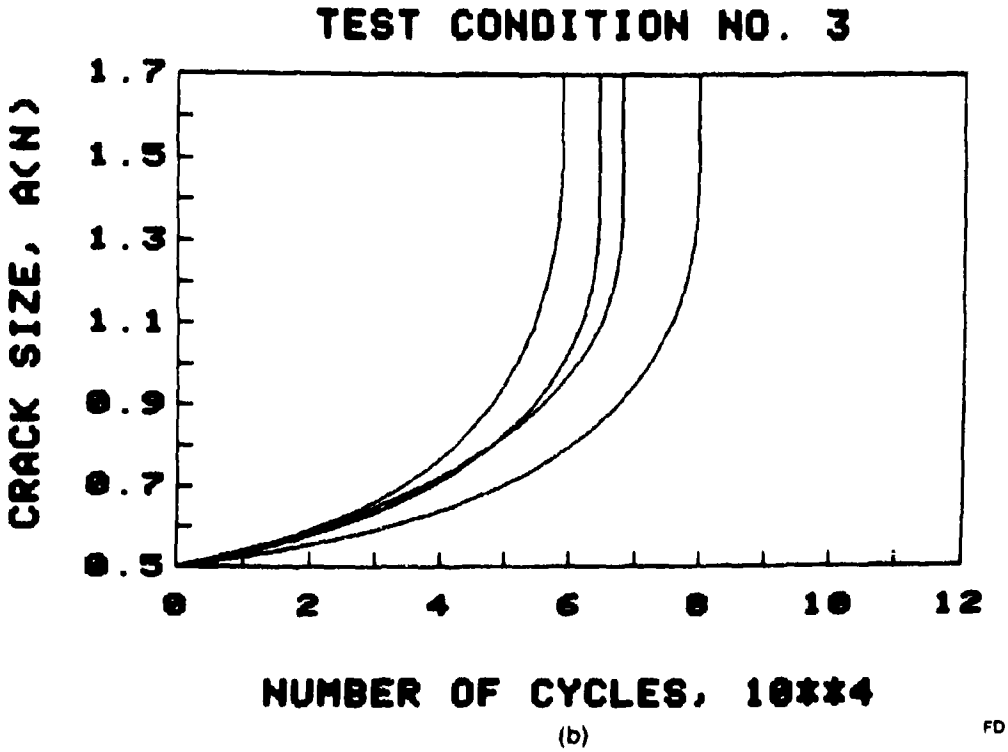

(b)

FD 235893

Figure 24. Crack Growth Damage Accumulation for Test Condition No. 3; (a) Statistical Model No. 1 and (b) Extrapolated Test Results

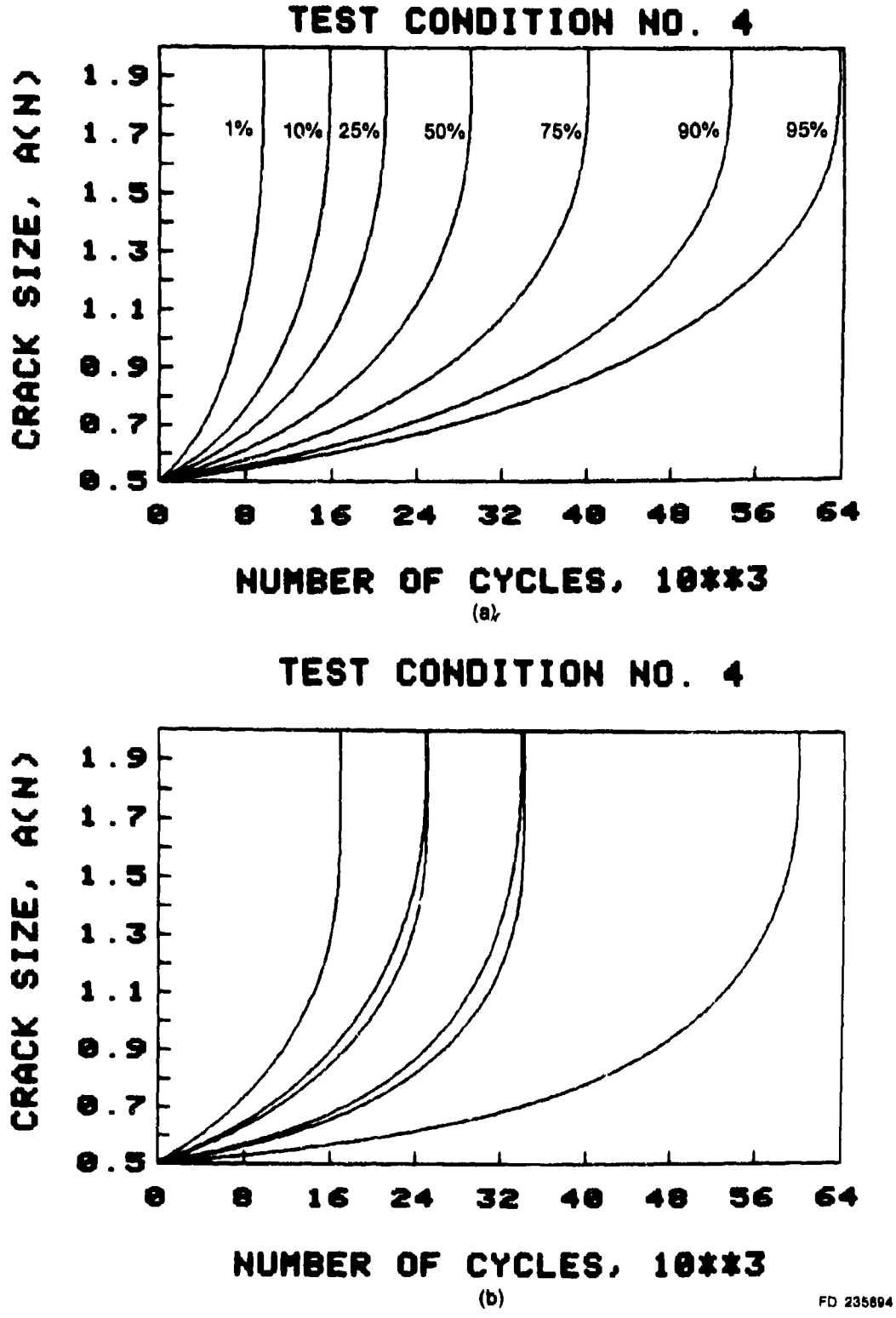

Figure 25. Crack Growth Damage Accumulation for Test Condition No. 4; (a) Statistical Model No. 1 and (b) Extrapolated Test Results

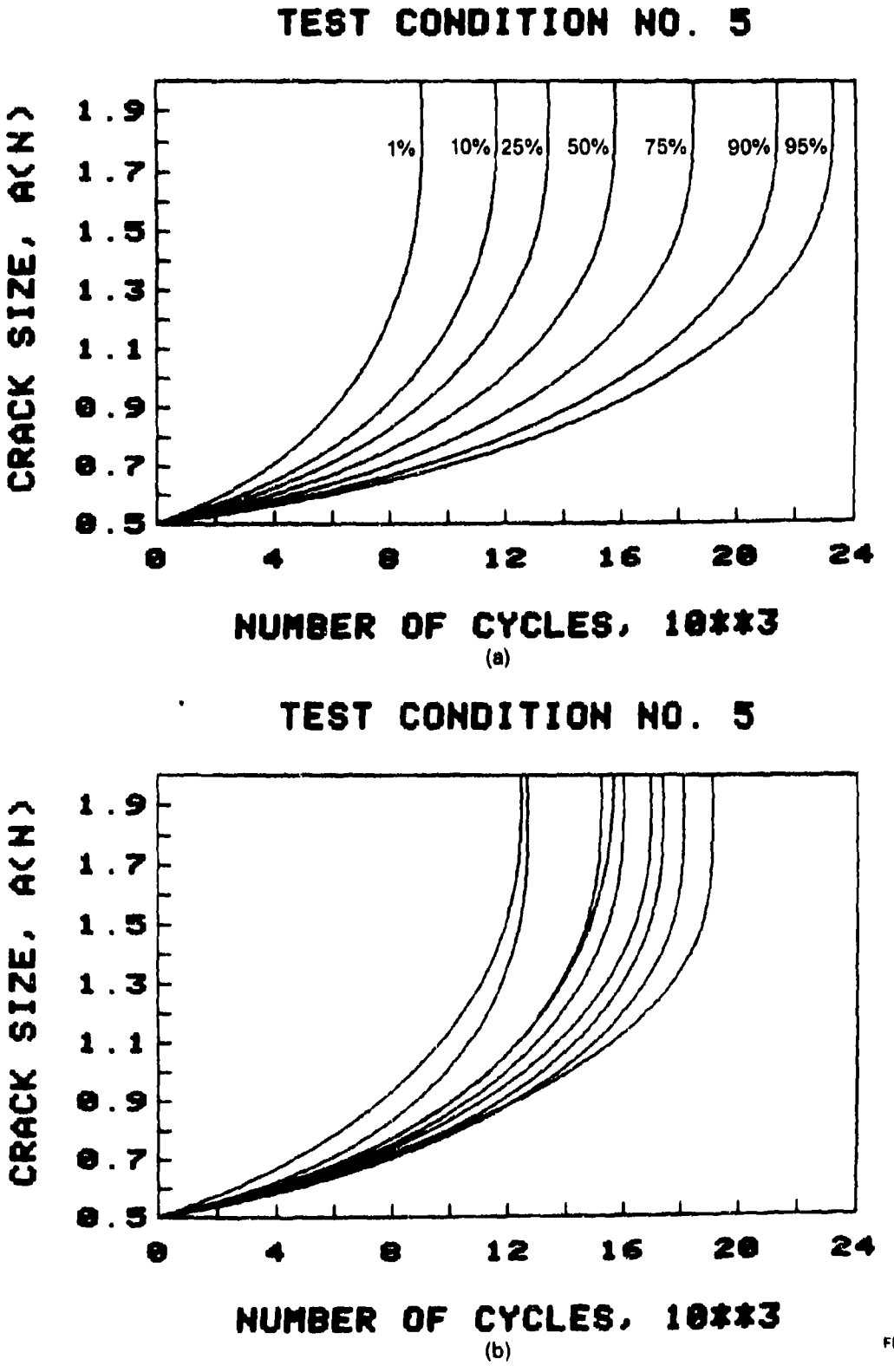

Figure 26. Crack Growth Damage Accumulation for Test Condition No. 5; (a) Statistical Model No. 1 and (b) Extrapolated Test Results

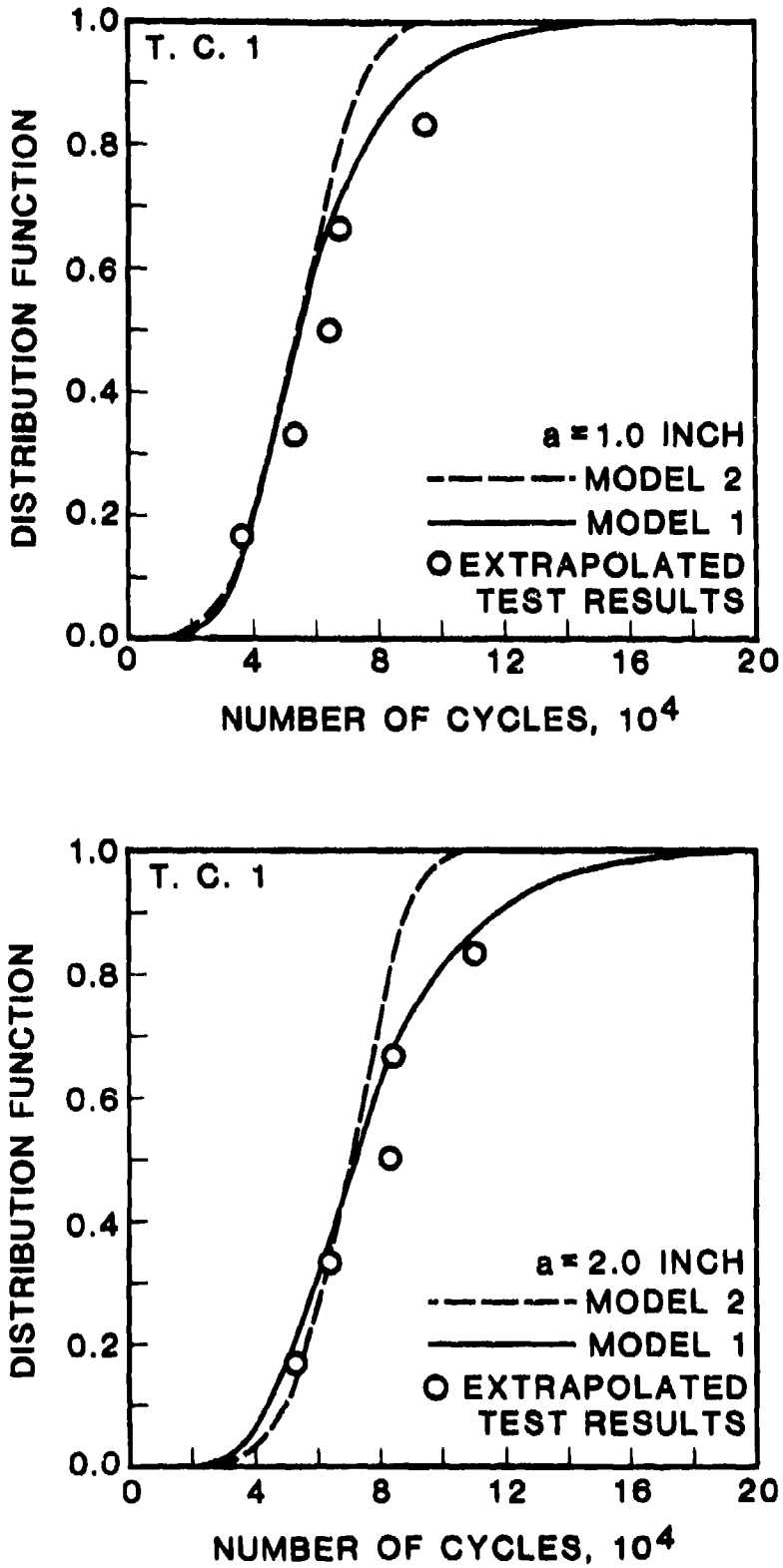

Figure 27. Distribution of Cycles to Reach a Given Crack Size for Test Condition No. 1

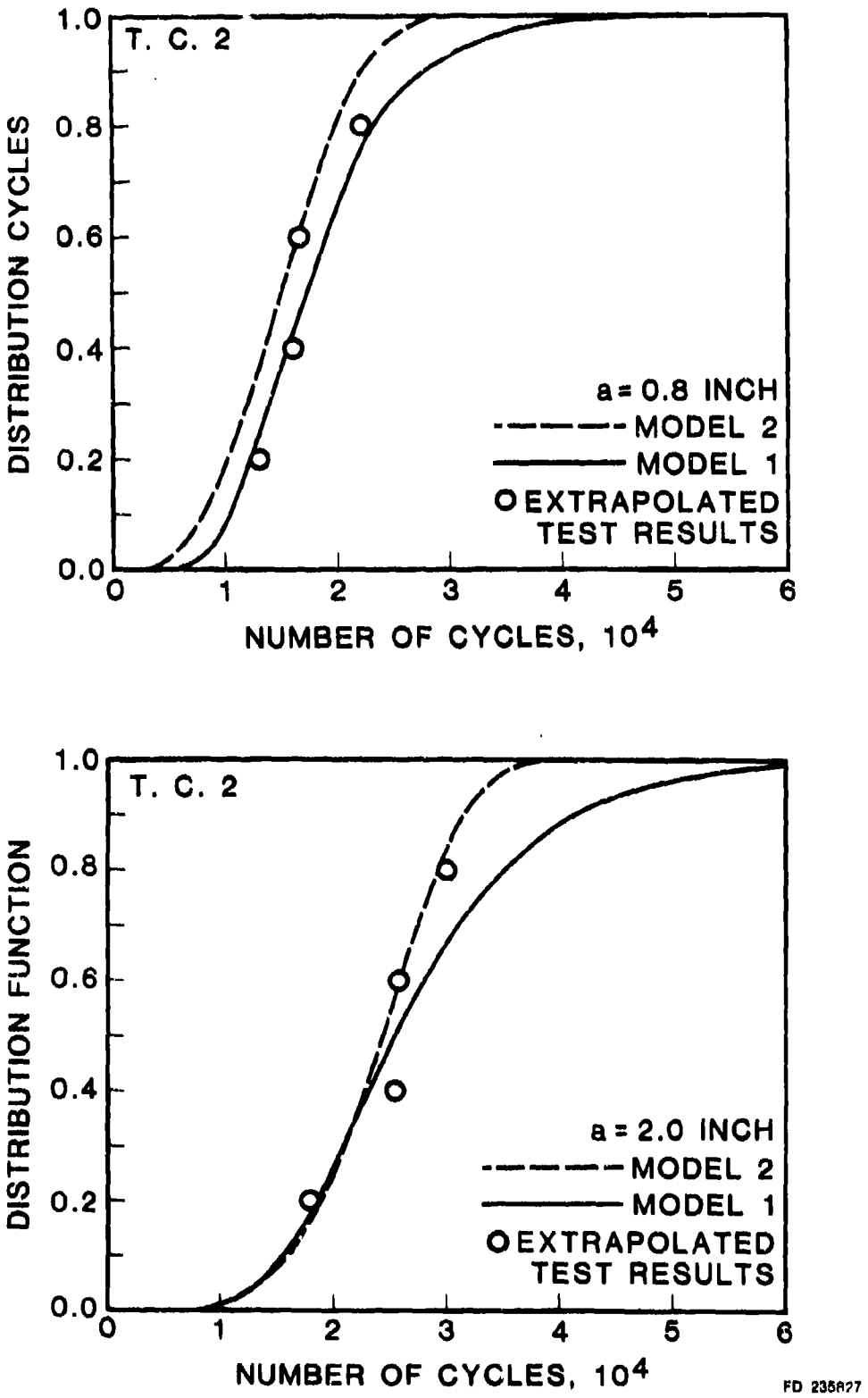

Figure 28. Distribution of Cycles to Reach a Given Crack Size for Test Condition No. 2

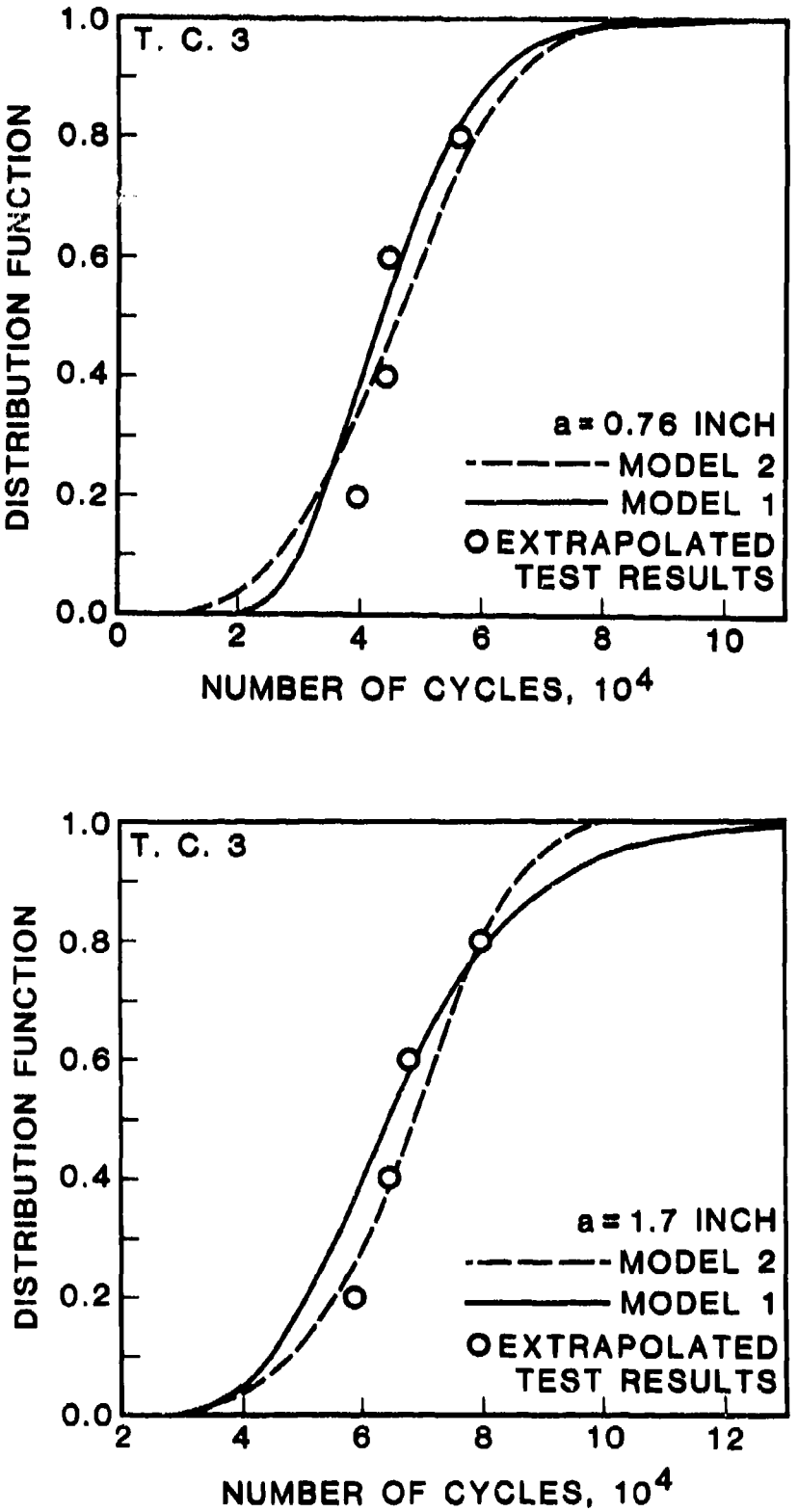

Figure 29. Distribution of Cycles to Reach a Given Crack Size for Test Condition No. 3

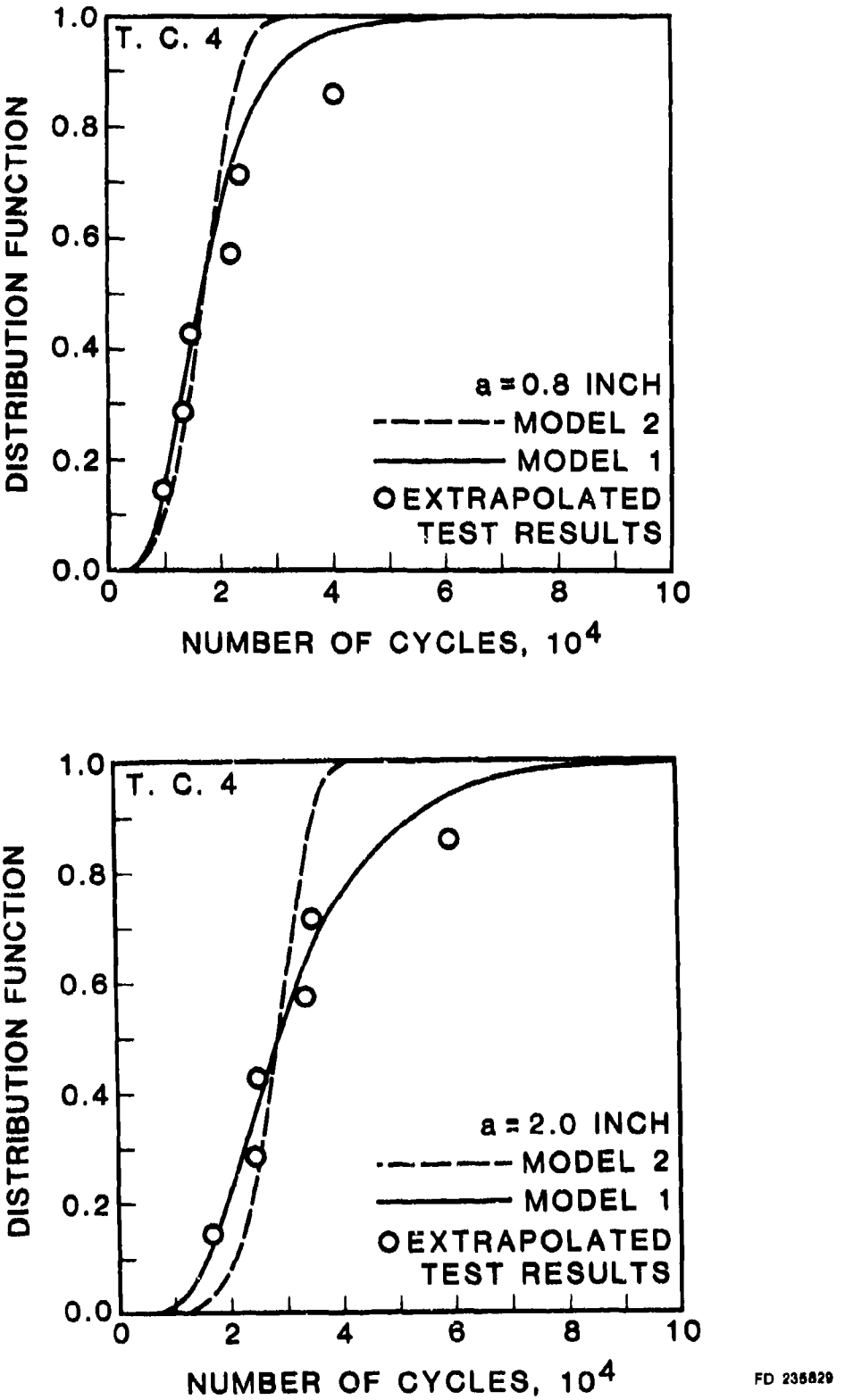

Figure 30. Distribution of Cycles to Reach a Given Crack Size for Test Condition No. 4

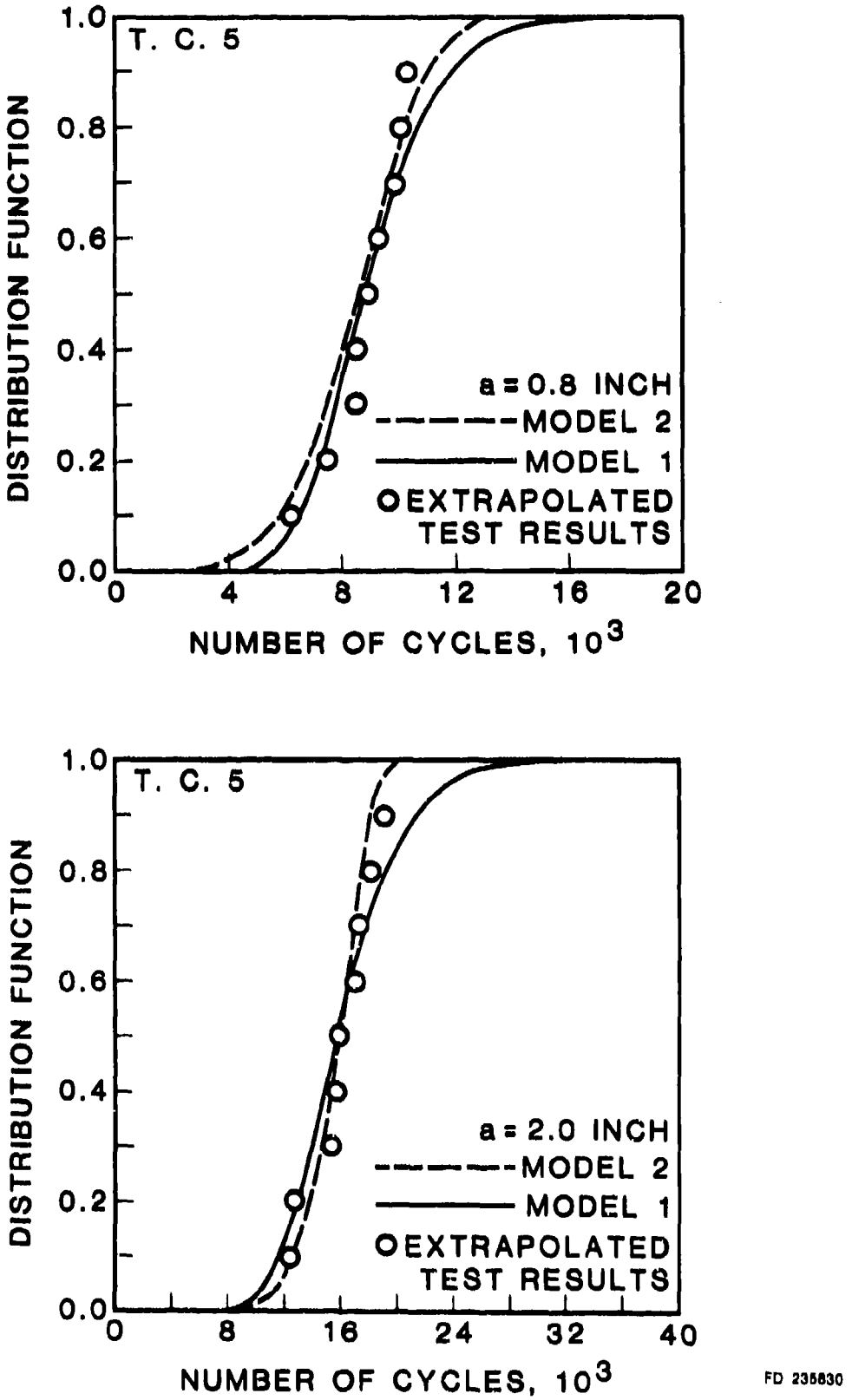

Figure 31. Distribution of Cycles to Reach a Given Crack Size for Test Condition No. 5

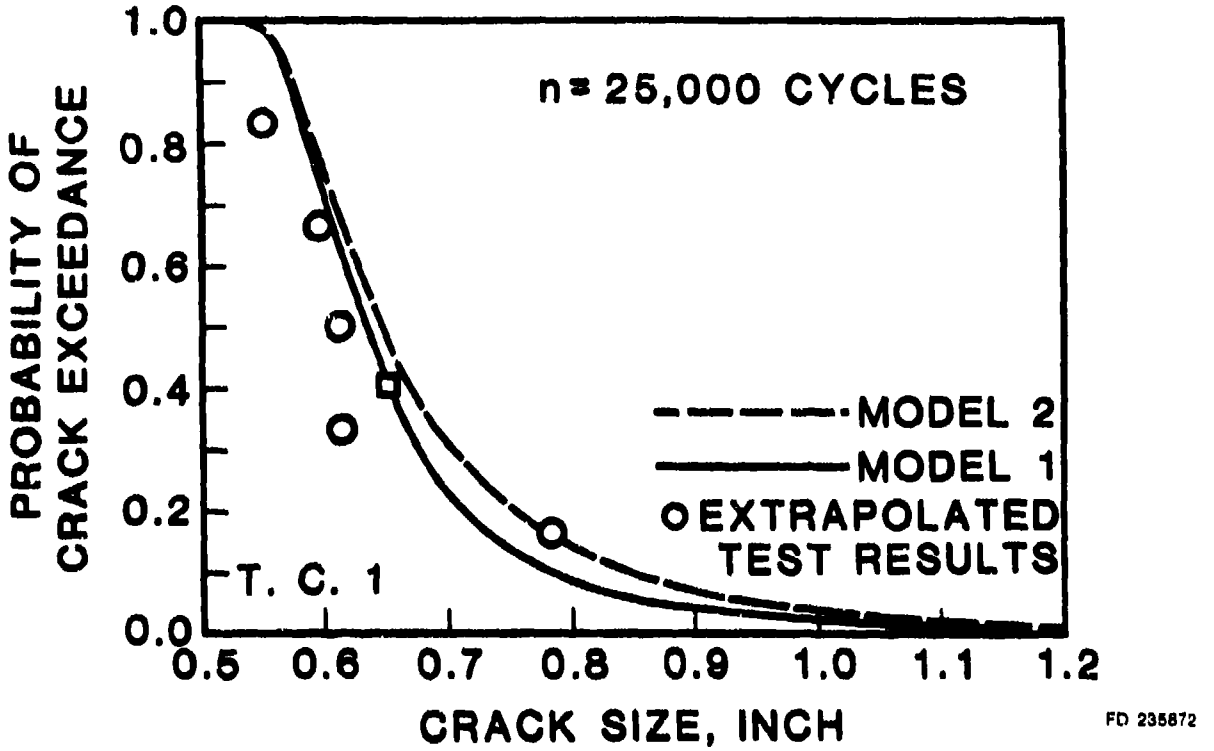

Figure 32. Probability of Crack Exceedance at n=25,000 Load Cycles for Test Condition No. 1

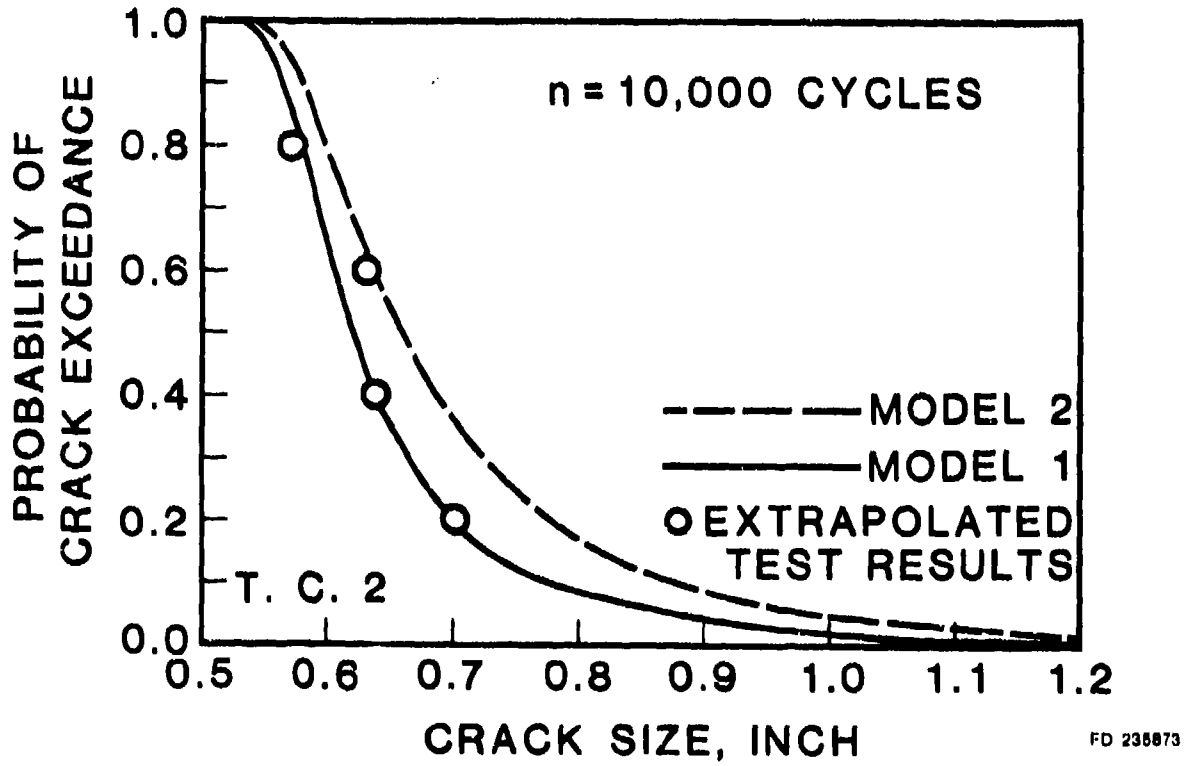

Figure 33. Probability of Crack Exceedance at n=10,000 Load Cycles for Test Condition No. 2

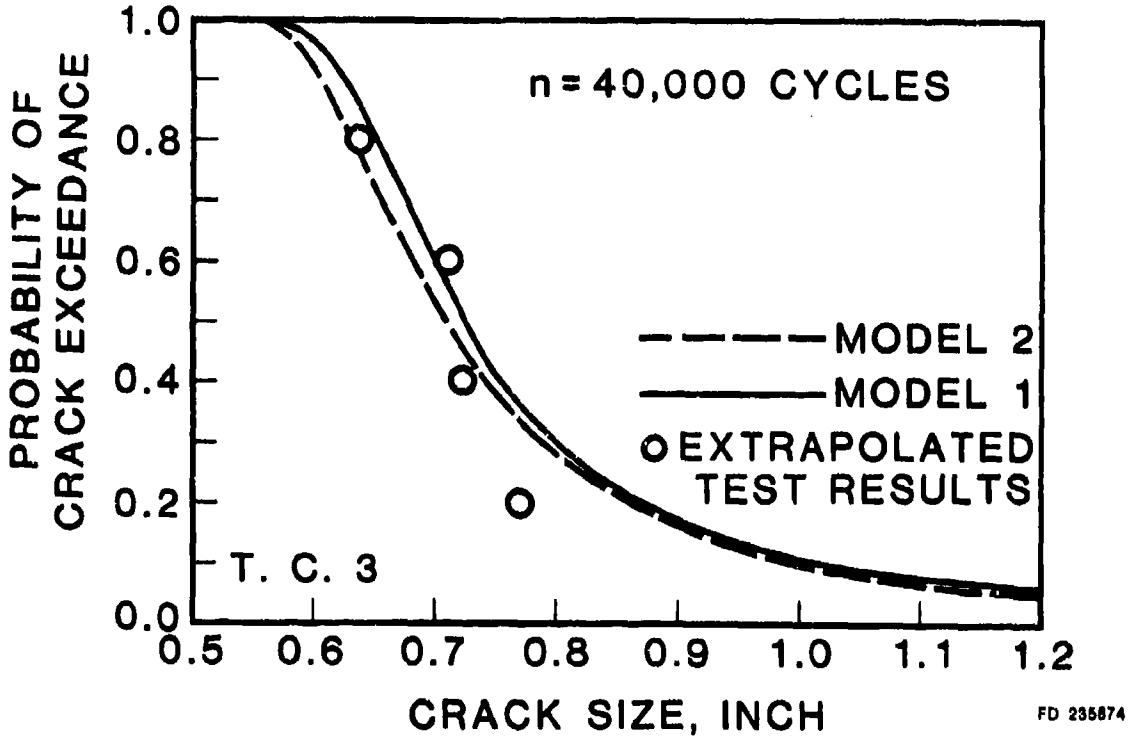

Figure 34. Probability of Crack Exceedance at n=40,000 Load Cycles for Test Condition No. 3

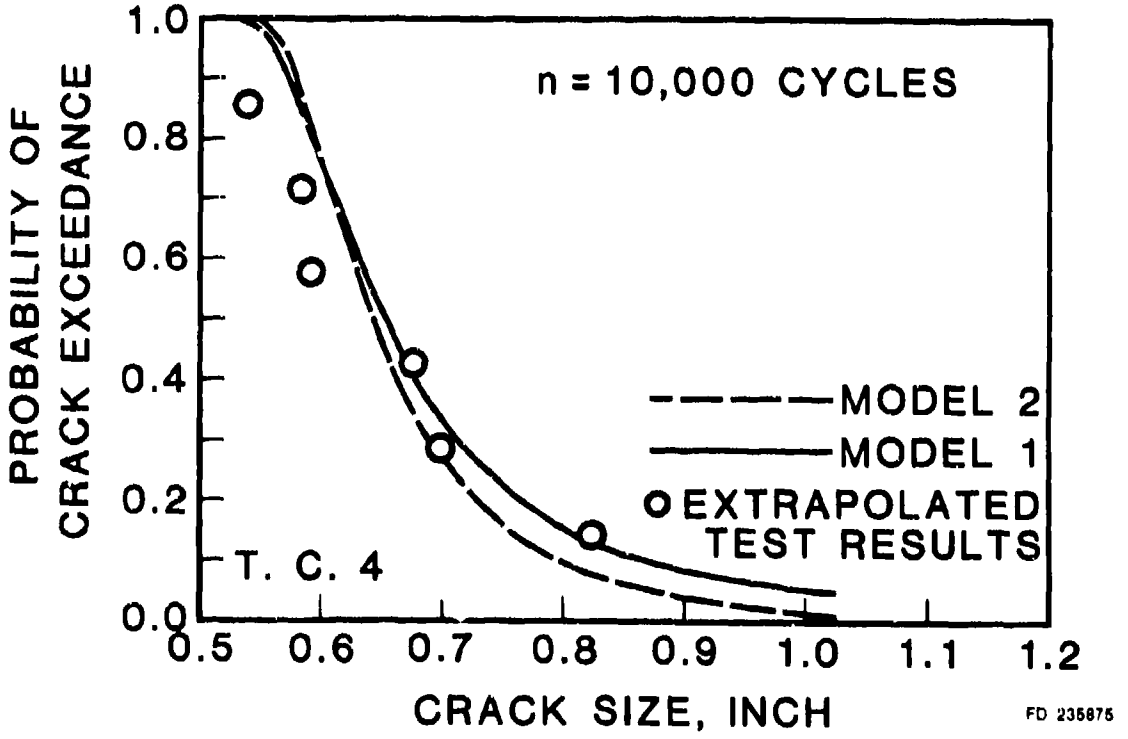

Figure 35. Probability of Crack Exceedance at n=10,000 Load Cycles for Test Condition No. 4

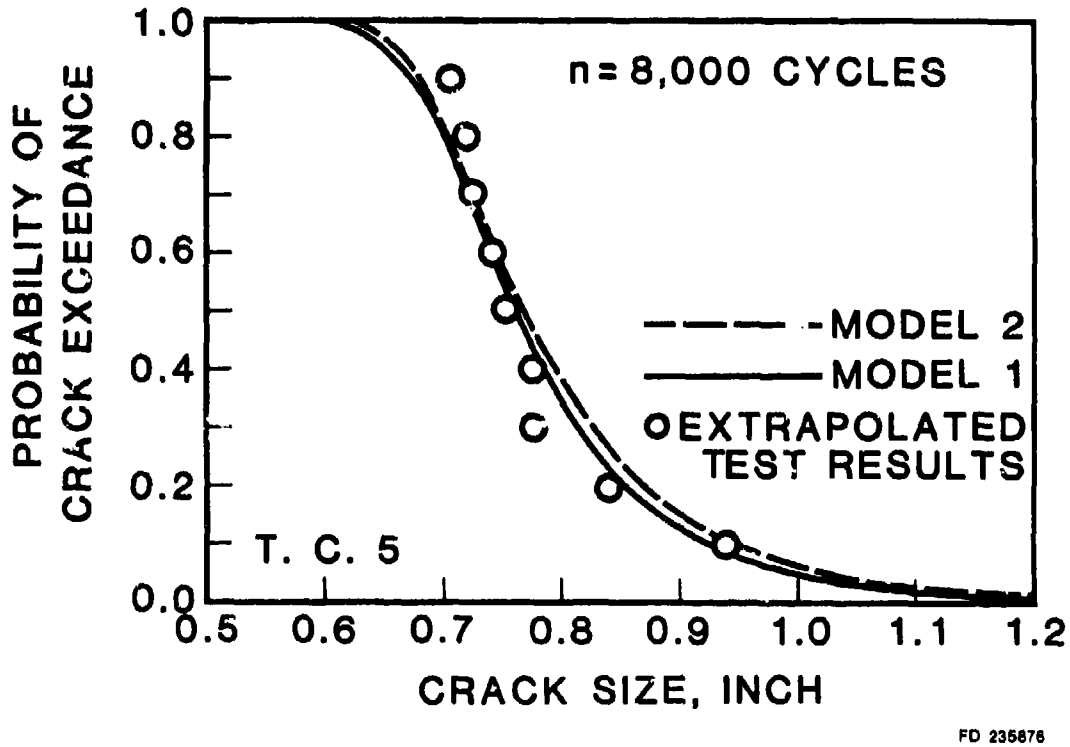

Figure 36. Probability of Crack Exceedance at n=8,000 Load Cycles for Test Condition No. 5

SECTION III

RANDOMIZATION OF PARAMETERS

Statistical Model

The second statistical model is expressed as

$$Y = C_1 \sinh|C_2(X+C_3)| + C_4 \tag{34}$$

in which C_2, C_3 and C_4 are considered as random variables, i.e., values of C_2, C_3, and C_4 vary from specimen to specimen. Thus each test specimen results in a set of sample values of C_2, C_3 and C_4.

To characterize the statistical distributions of C_2, C_3 and C_4 as well as their correlations, test results of crack growth rates for each specimen are best fitted by Eq. 34 using the method of least squares to estimate sample values of C_2, C_3 and C_4. The least squares best fit procedures have been discussed in Ref. 1. Sample values of C_i (i=2,3,4) are approximated by their estimates and are presented in Table 5 for various test conditions. For instance, the best-fitted crack growth rate for five specimens in the test condition No. 1 are plotted in Figure 16 using Eq. 34 as well as the C_i (i=2,3,4) values given in Table 5.

The mean values (μ_2,μ_3,μ_4), the standard deviations ($\sigma_2,\sigma_3,\sigma_4$), and the coefficients of variations (V_2,V_3,V_4) of those data given in Table 6 have been computed in the following manner:

$$\mu_2 = \frac{1}{m}\sum_{i=1}^{m} C_{2i},\ \mu_3 = \frac{1}{m}\sum_{i=1}^{m} C_{3i},\ \mu_4 = \frac{1}{m}\sum_{i=1}^{m} C_{4i} \tag{35}$$

$$\sigma^2_2 = \frac{1}{m}\sum_{i=1}^{m}(C_{2i}-\mu_2)^2,\ \sigma^2_3 = \frac{1}{m}\sum_{i=1}^{m}(C_{3i}-\mu_3)^2$$
$$\sigma^2_4 = \frac{1}{m}\sum_{i=1}^{m}(C_{4i}-\mu_4)^2 \tag{36}$$

$$V_2 = \sigma_2/\mu_2,\ V_3 = \sigma_3/\mu_3,\ V_4 = \sigma_4/\mu_4 \tag{37}$$

in which (C_{2i},C_{3i},C_{4i}) are the ith sample values of (C_2,C_3,C_4) associated with the ith specimen, and m is the total number of samples (specimens) for a test condition.

The correlation coefficients ρ_{23}, ρ_{34}, ρ_{42} among C_j (j=2,3,4) are obtained as follows:

$$\rho_{23} = \frac{1}{\sigma_2\sigma_3} \frac{1}{m} \sum_{i=1}^{m} (C_{2i}-\mu_2)(C_{3i}-\mu_3) \tag{38}$$

$$\rho_{34} = \frac{1}{\sigma_3\sigma_4} \frac{1}{m} \sum_{i=1}^{m} (C_{3i}-\mu_3)(C_{4i}-\mu_4) \tag{39}$$

$$\rho_{42} = \frac{1}{\sigma_4\sigma_2} \frac{1}{m} \sum_{i=1}^{m} (C_{4i}-\mu_4)(C_{2i}-\mu_2) \tag{40}$$

values of ρ_{23}, ρ_{34} and ρ_{42} thus computed are also given in Table 6 for various test conditions. To show the correlations among C_2, C_3 and C_4 under different test conditions, test data presented in Table 5 are shown in Figure 37 for C_2 vs C_3, C_3 vs C_4 and C_4 vs C_2.

TABLE 6. MEAN VALUES, STANDARD DEVIATIONS, COEFFICIENTS OF VARIATION AND CORRELATION COEFFICIENTS OF C_2, C_3 AND C_4

Test Condition	C_2	C_3	C_4
	Mean Values		
1	4.081	−1.467	−4.470
2	4.885	−1.358	−4.151
3	4.718	−1.247	−4.600
4	4.430	−1.459	−4.215
5	3.802	−1.529	−3.960
	Standard Deviations		
1	0.544	0.101	0.205
2	0.670	0.161	0.414
3	0.432	0.073	0.208
4	0.561	0.092	0.134
5	0.299	0.070	0.180
	Coefficients of Variation		
1	0.133	−0.069	−0.046
2	0.137	−0.119	−0.100
3	0.091	−0.058	−0.045
4	0.127	−0.063	−0.032
5	0.079	−0.046	−0.045
	Correlation Coefficients		
Test Condition	ρ_{23}	ρ_{34}	ρ_{42}
1	0.123	−0.982	−0.121
2	0.651	−0.992	−0.552
3	0.773	−0.990	−0.721
4	0.086	−0.918	−0.264
5	0.162	−0.938	−0.047

From the results presented in Table 6 and Figure 37 it is clear that the number of specimens tested under each condition (υ, R, T) is too small to characterize the statistical distributions of C_2, C_3 and C_4. Nevertheless, from the analysis results presented above, several interesting trends have been observed as follows:

(1) The mean values (μ_2,μ_3,μ_4) are functions of the test condition (υ,R,T).

(2) The statistical dispersions or the coefficients of variation (V_2,V_3,V_4) are fairly constant over various test conditions, such that (V_2,V_3,V_4) may be assumed to be independent of the test condition (υ,R,T).

(3) The correlations ρ_{23} and ρ_{42} between C_2 and C_3, and C_2 and C_4 are very small except in the third test condition, indicating that C_2 is almost uncorrelated with C_3 and C_4.

(4) The correlation ρ_{34} between C_3 and C_4 is almost unity, indicating that C_3 and C_4 may be linearly related.

Because of the difficulty associated with the small sample size as well as the observations made above, the following assumptions are made so that all the test results under different test conditions can be pooled together to characterize the distributions of C_2, C_3 and C_4.

(1) The mean values (μ_2,μ_3,μ_4) of C_2, C_3 and C_4 are functions of (υ,R,T), i.e., (μ_2,μ_3,μ_4) vary from test condition to test condition and their values are given in Table 6.

(2) The coefficients of variation (V_2,V_3,V_4) of C_2, C_3 and C_4 are independent of (υ,R,T), i.e., (V_2,V_3,V_4) are constants.

Based on these assumptions we normalize all the sample values of C_2, C_3 and C_4 by their respective mean values (μ_2,μ_3,μ_4). The resulting data will have the mean value equal to unity and the same standard deviation. Thus, all the normalized data under different test conditions can be pooled together to determine (1) the coefficients of variation (V_2,V_3,V_4), (2) the correlation coefficients among C_2, C_3 and C_4, and (3) the statistical distributions of C_2, C_3 and C_4.

Let m_j be the total number of test specimens under the jth test condition (υ_j,R_j,T_j) and J be the total number of test conditions. Then the total number of test specimens M is given by

$$M = \sum_{j=1}^{J} m_j \tag{41}$$

Let $\tilde{C}_2$, $\tilde{C}_3$ and $\tilde{C}_4$ be, respectively, the normalized random variables of $C_2(\upsilon,R,T)$, $C_3(\upsilon,R,T)$ and $C_4(\upsilon,R,T)$ with respect to their mean values, i.e.,

$$\begin{aligned} \tilde{C}_2 &= C_2(\upsilon,R,T)/\mu_2(\upsilon,R,T) \\ \tilde{C}_3 &= C_3(\upsilon,R,T)/\mu_3(\upsilon,R,T) \\ \tilde{C}_4 &= C_4(\upsilon,R,T)/\mu_4(\upsilon,R,T) \end{aligned} \tag{42}$$

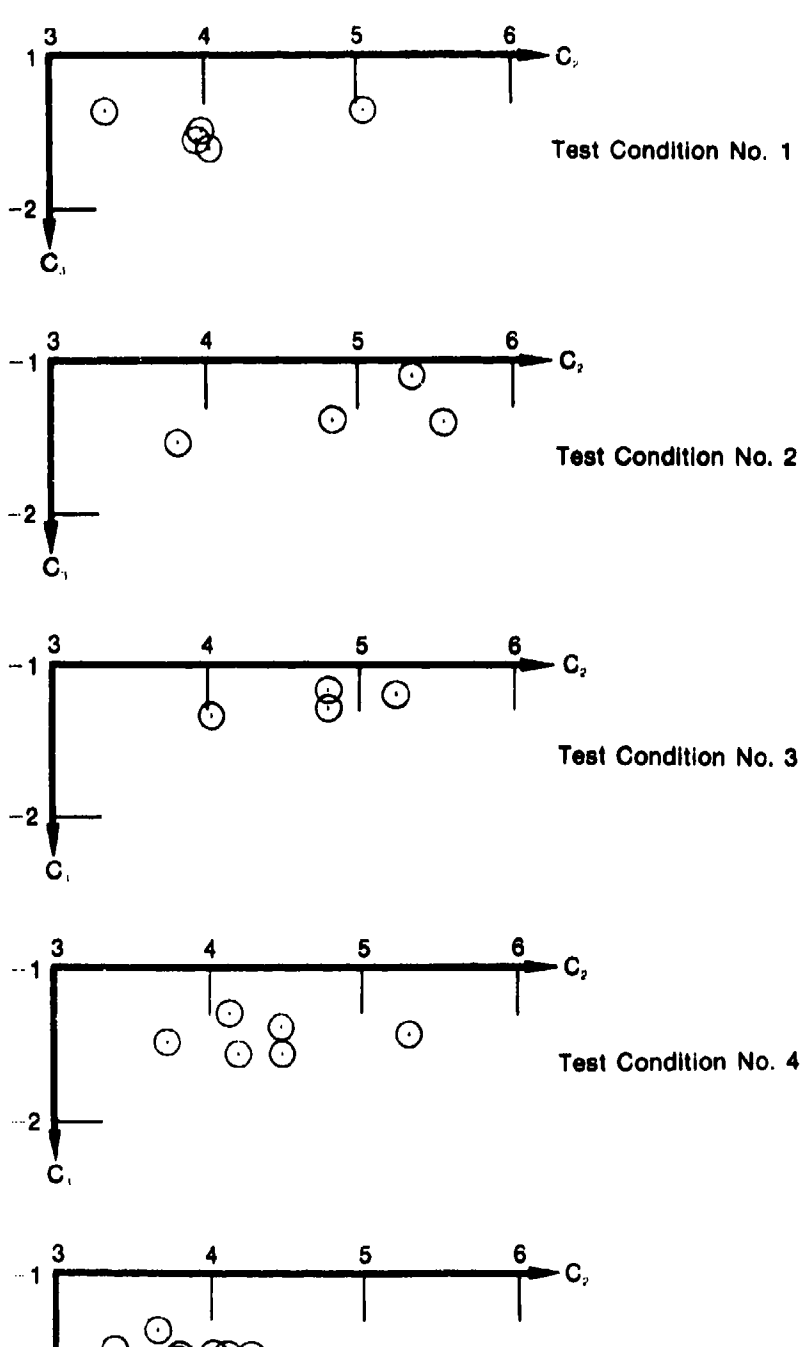

Figure 37a. Correlation Between C_2 and C_3 for Various Test Conditions

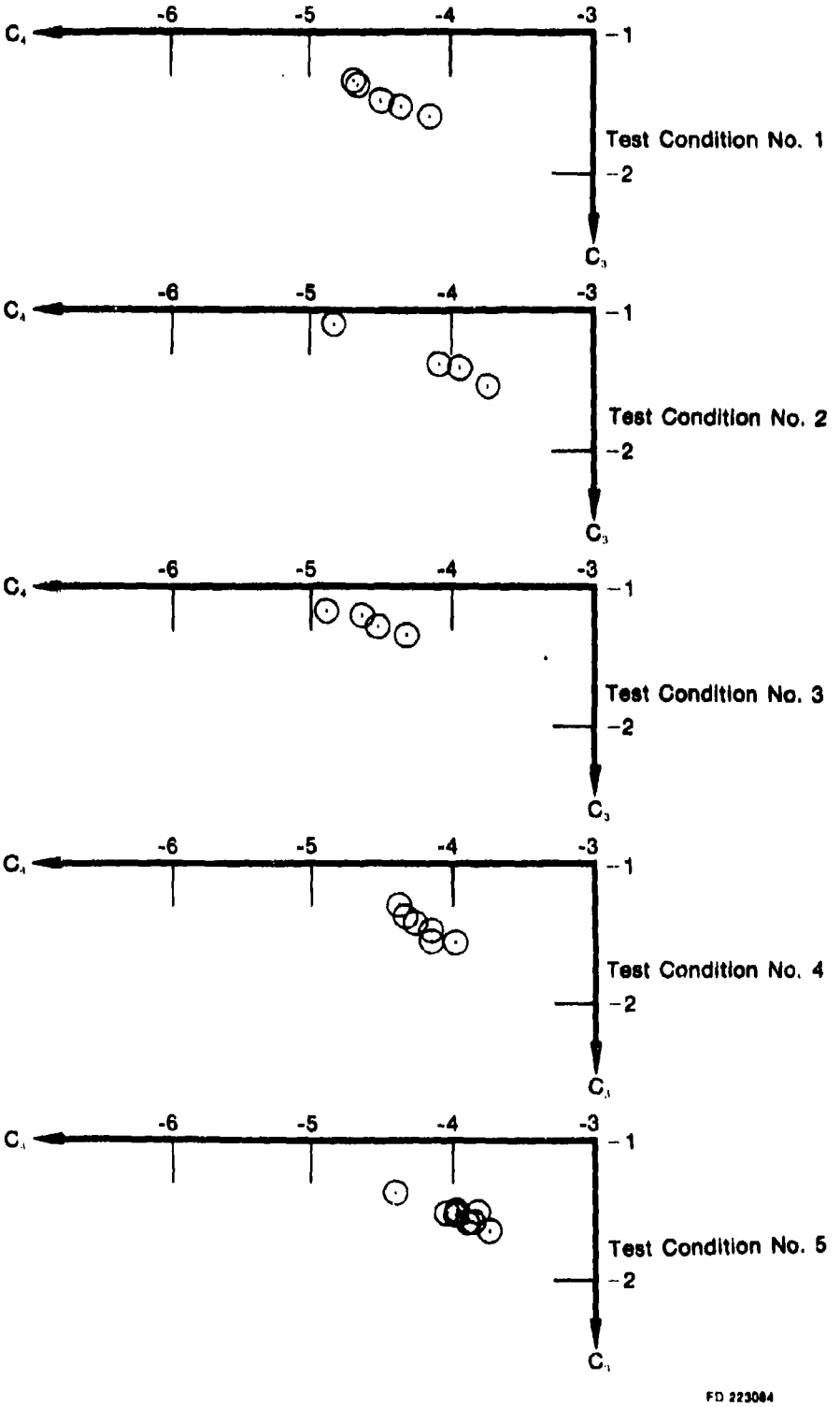

Figure 37b. Correlation Between C_3 and C_4 for Various Test Conditions

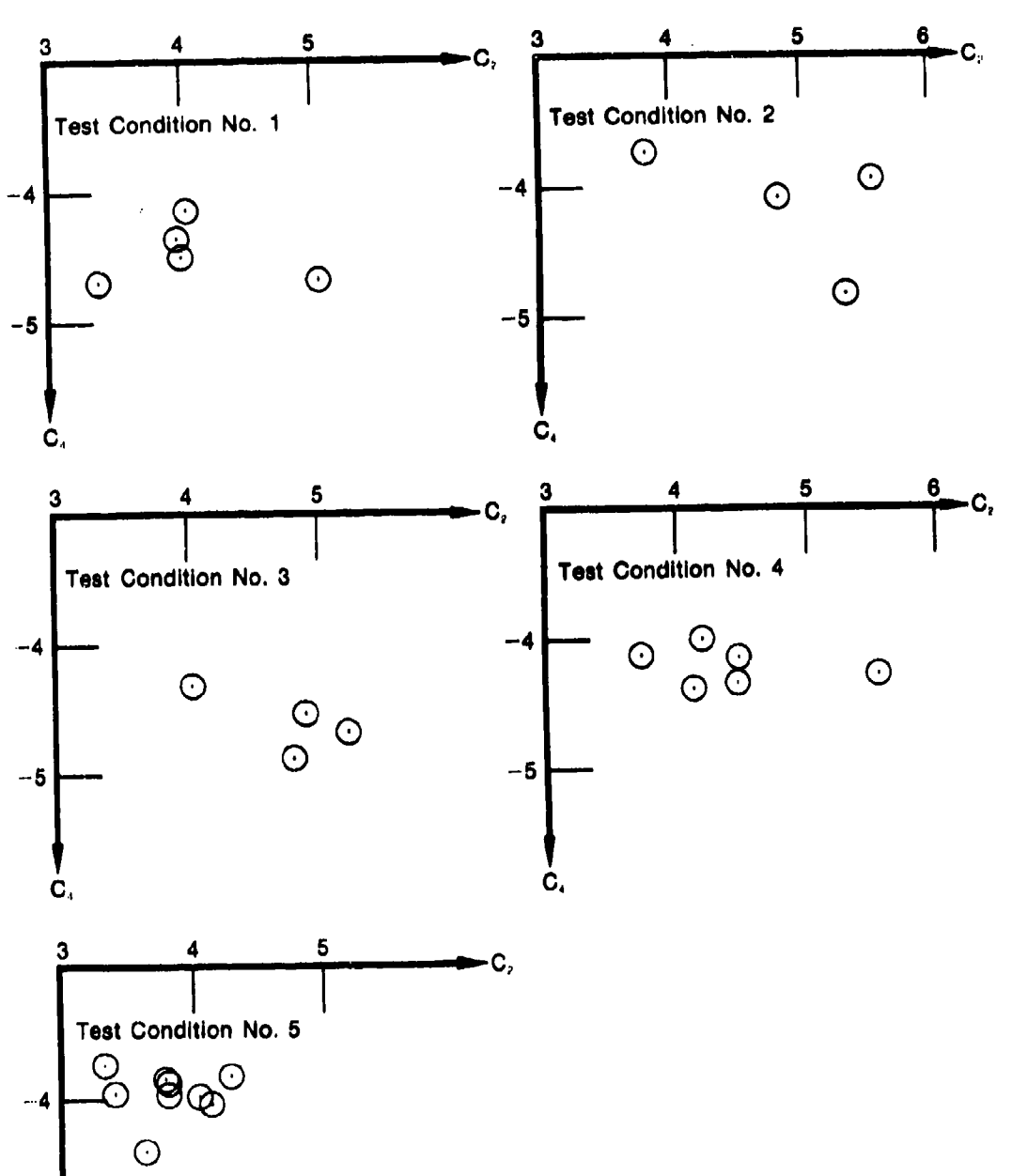

Figure 37c. Correlation Between C_2 and C_4 for Various Test Conditions

Sample values of $\tilde{C}_2$, $\tilde{C}_3$ and $\tilde{C}_4$ are obtained by dividing each data point in Table 5 by its corresponding mean value. The resulting data are pooled together and presented in Table 7. The coefficients of variation (V_2,V_3,V_4) and the correlation coefficients (ρ_{23},ρ_{34},ρ_{42}) of the pooled data are computed and presented in Table 8. Furthermore, the normalized pooled sample data in Table 7 are plotted in Figure 38 for $\tilde{C}_3$ vs $\tilde{C}_4$, $\tilde{C}_2$ vs $\tilde{C}_4$ and $\tilde{C}_2$ vs $\tilde{C}_3$ to show their correlations.

It is clearly observed from Table 8 and Figure 38 that the correlations between C_2 and C_3, and between C_2 and C_4 are very small whereas a strong correlation exists between C_3 and C_4 (see Figure 38(a)). Consequently, the following assumptions are reasonably made to simplify the statistical analysis of C_2, C_3 and C_4: (1) C_2 is statistically independent of C_3 and C_4, and (2) C_3 and C_4 are completely correlated and hence they are linearly related:

$$C_3 = \alpha C_4 + \beta \tag{43}$$

in which α and β will be determined later.

Based on these assumptions, the statistical characterizations for C_2, C_3 and C_4 become tractable, since the establishment of a joint density function for C_2, C_3 and C_4 is almost impossible. Note that the joint density function is available for C_2, C_3 and C_4 only when they are Gaussian (normal) random variables. It will become apparent later that C_2 must be positive and hence it should not be a Gaussian random variable.

Taking the expectation of Eq. 43 and forming the standard deviation of C_3, one obtains

$$\mu_3(\upsilon,R,T) = \alpha\mu_4(\upsilon,R,T) + \beta \tag{44}$$

$$\sigma_3^2(\upsilon,R,T) = \alpha^2\,\sigma_4^2(\upsilon,R,T) \tag{45}$$

in which $\mu_3(\upsilon,R,T)$ and $\mu_4(\upsilon,R,T)$ are the mean values of C_3 and C_4, repectively, and $\sigma_3(\upsilon,R,T)$ and $\sigma_4(\upsilon,R,T)$ are the corresponding standard deviations.

The standard deviations in Eq. 45 can be replaced by the mean value multiplied by the coefficient of variation in order to determine α

$$\mu_3^2(\upsilon,R,T)\,V_3^2 = \alpha^2\,\mu_4^2(\upsilon,R,T)\,V_4^2 \tag{46}$$

or

$$\alpha = -\frac{\mu_3(\upsilon,R,T)V_3}{\mu_4(\upsilon,R,T)V_4} \tag{47}$$

In Eq. 47, a negative sign is chosen because the correlation between C_3 and C_4 is negative (see Figure 38(a)).

Now β can be obtained by substituting Eq. 47 into Eq. 44; with the result

$$\beta = \mu_3(\upsilon,R,T)\left[1 + \frac{V_3}{V_4}\right] \tag{48}$$

It is obvious from Eqs. 47 and 48 that $\alpha = \alpha(\upsilon,R,T)$ and $\beta = \beta(\upsilon, R, T)$ depend on the test conditions (υ,R,T). Values of α and β under various test conditions are computed from Eqs. 47 and 48 as well as Tables 6 and 8, and they are presented in Table 9.

TABLE 7. NORMALIZED POOLED DATA OF C_2 C_3 AND C_4, M = 28

C_4	C_3	C_2
0.78200E 00	0.80810E 00	0.90182E 00
0.82382E 00	0.89562E 00	0.92796E 00
0.84263E 00	0.89582E 00	0.93691E 00
0.85554E 00	0.91684E 00	0.94215E 00
0.87383E 00	0.92570E 00	0.94761E 00
0.89198E 00	0.92882E 00	0.94880E 00
0.93428E 00	0.95750E 00	0.96588E 00
0.94827E 00	0.96411E 00	0.97226E 00
0.96642E 00	0.97936E 00	0.97422E 00
0.97084E 00	0.98218E 00	0.97901E 00
0.97746E 00	0.98786E 00	0.98319E 00
0.98737E 00	0.99964E 00	0.98422E 00
0.99020E 00	0.10029E 01	0.98438E 00
0.99430E 00	0.10068E 01	0.98495E 00
0.99930E 00	0.10157E 01	0.99997E 00
0.10006E 01	0.10212E 01	0.10028E 01
0.10090E 01	0.10225E 01	0.10030E 01
0.10122E 01	0.10245E 01	0.10045E 01
0.10162E 01	0.10245E 01	0.10145E 01
0.10188E 01	0.10267E 01	0.10176E 01
0.10645E 01	0.10367E 01	0.10214E 01
0.10853E 01	0.10477E 01	0.10287E 01
0.10941E 01	0.10699E 01	0 10416E 01
0.11095E 01	0.10733E 01	0.10461E 01
0.11237E 01	0.10788E 01	0.10492E 01
0.11365E 01	0.10804E 01	0.10606E 01
0.12377E 01	0.10941E 01	0.11116E 01
0.12537E 01	0.11330E 01	0.11652E 01

TABLE 8. COEFFICIENTS OF VARIATION AND CORRELATION COEFFICIENTS OF C_2, C_3 AND C_4 OF POOLED DATA

Coefficients of Variation		
V_2	V_3	V_4
0.1117	−0.0698	−0.0545
Correlation Coefficients		
ρ_{23}	ρ_{34}	ρ_{24}
−0.3384	−0.9536	0.3151

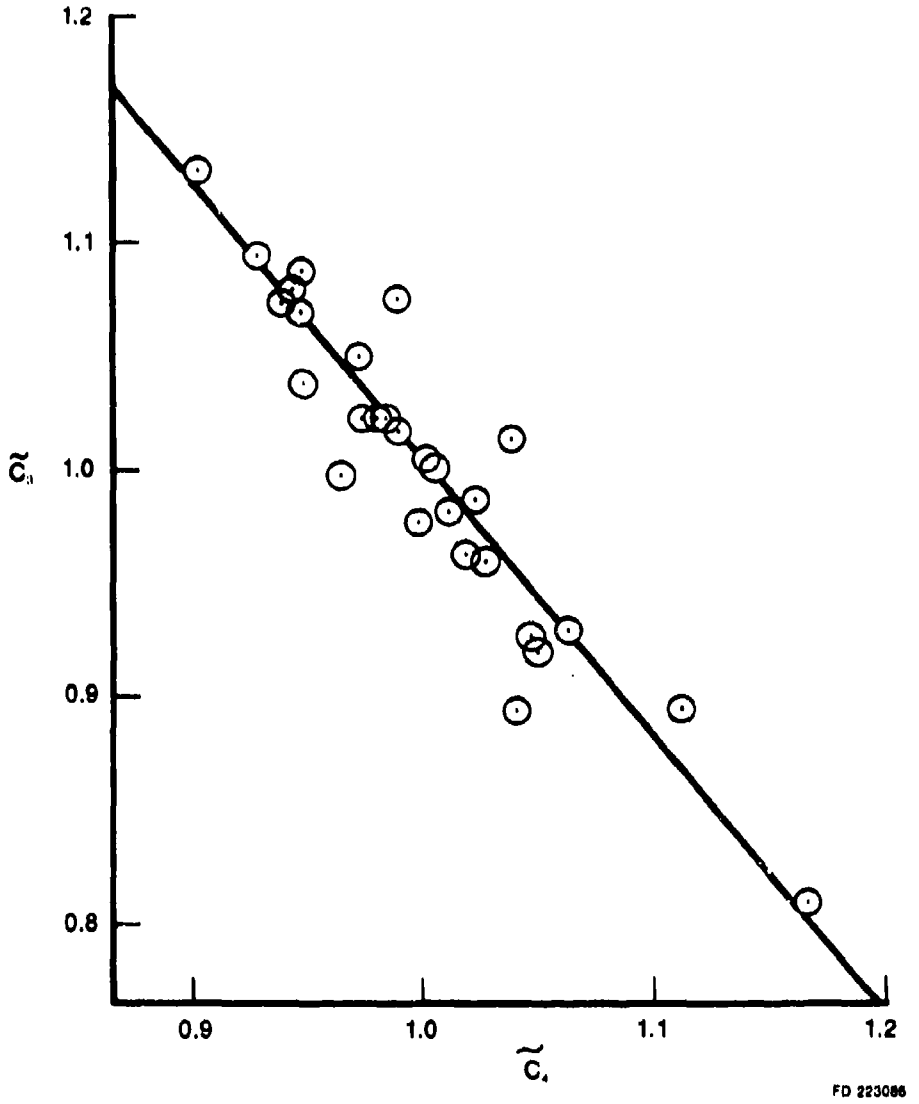

Figure 38a. Correlation Between $\tilde{C}_3$ and $\tilde{C}_4$ for Pooled Data

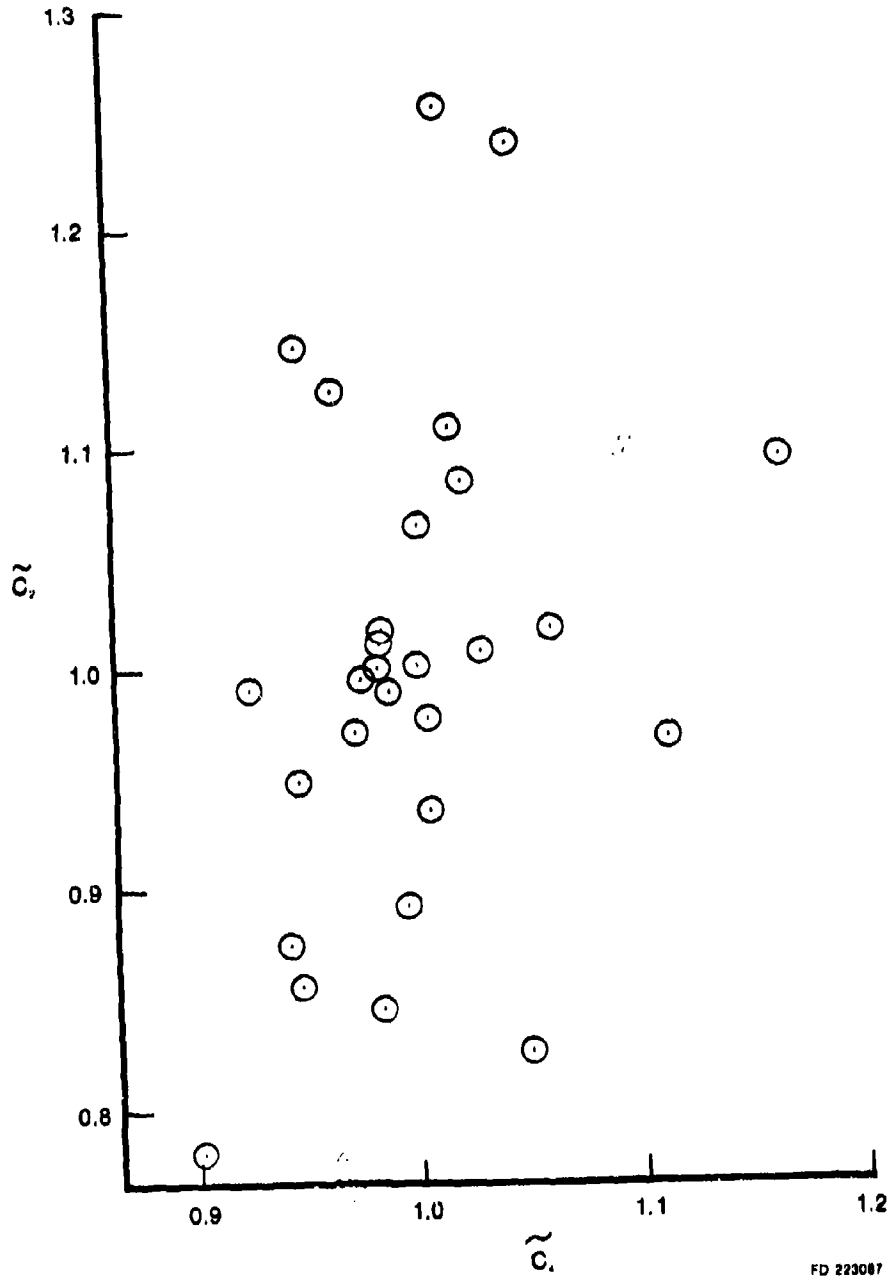

Figure 38b. Correlation Between $\tilde{C}_2$ and $\tilde{C}_4$ for Pooled Data

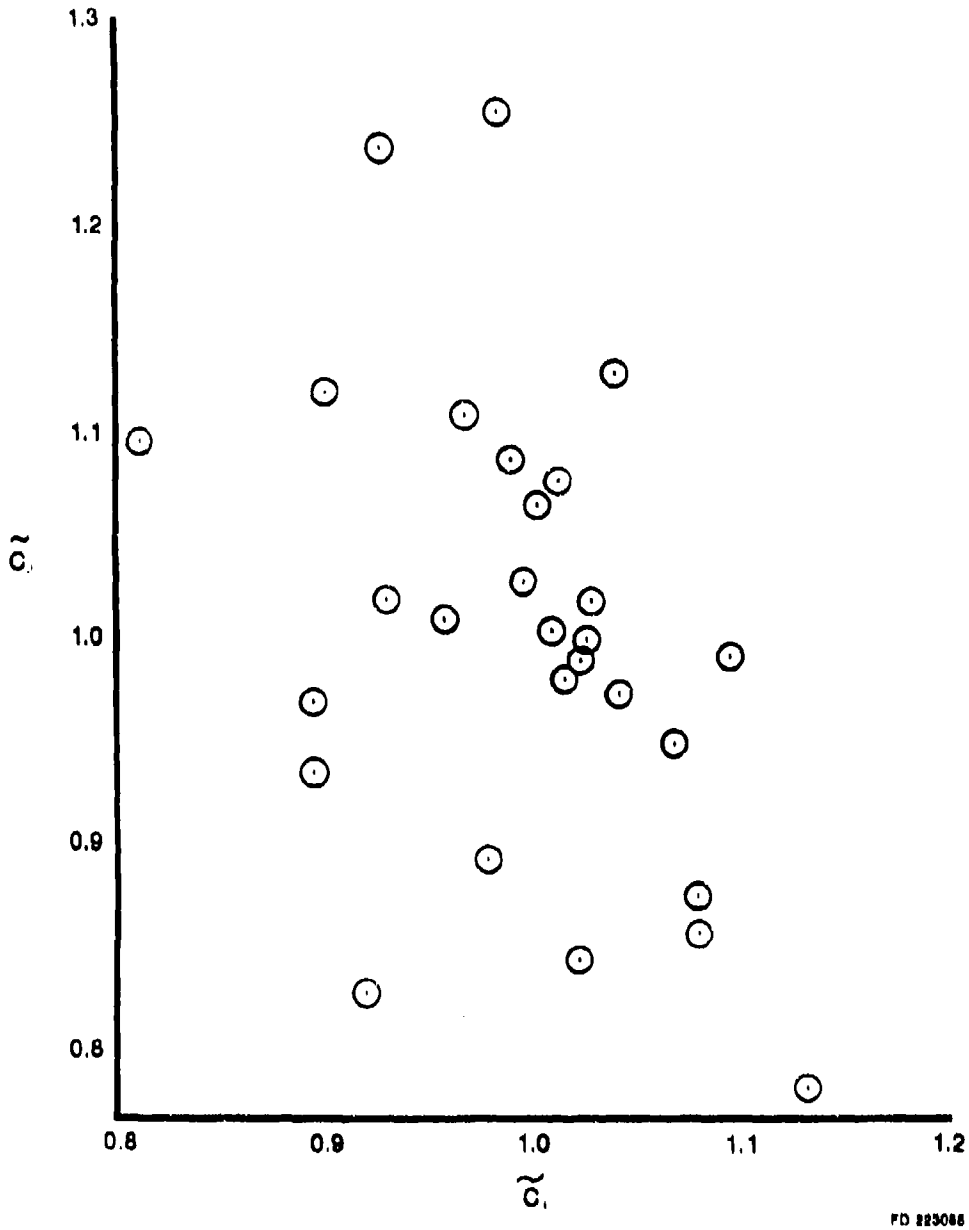

Figure 38c. Correlation Between $\tilde{C}_x$ and $\tilde{C}_y$ for Pooled Data

TABLE 9. VALUES OF α AND β UNDER VARIOUS TEST CONDITION

Test Condition	*1*	*2*	*3*	*4*	*5*
α	−0.4203	−0.4190	−0.3472	−0.4433	−0.4945
β	−3.3458	−3.0972	−2.844	−3.3276	−3.4872

After determining the mean values $\mu_2(v,R,T)$, $\mu_3(v,R,T)$ and $\mu_4(v,R,T)$, and the coefficients of variation (V_2,V_3,V_4) of C_2, C_3 and C_4 (Tables 6 and 8), as well as α and β (Table 9), we are in the position to estimate the distribution functions for C_2, C_3 and C_4. From the physical standpoint, the crack growth rate da/dn (or Y) should be a monotonically increasing function of the stress intensity range ΔK (or X). Hence, it follows from Eq. 1 that C_2 should be positive. We shall select a most appropriate distribution function of C_2 which is defined in the positive domain. Distribution functions, such as lognormal, Weibull, gamma and beta, are all defined in the positive domain. Normalized pooled data presented in Table 7 for C_2 are fitted by (1) lognormal, (2) Weibull, (3) gamma, and (4) beta distributions.

The Kolmogorov-Smirnov (K-S) test for the goodness-of-fit indicates that the lognormal distribution fits the data for C_2 better. However, both the normal and the lognormal distributions fit the data sets of C_3 and C_4 equally well. The normalized data set for C_2 is shown on the lognormal probability paper in Figure 39(a). The corresponding K-S statistics D_n is also given in the figure. The normalized data sets for C_3 and C_4 are plotted on the normal probability paper in Figure 39(b)-39(c), along with their corresponding D_n values. The total number of pooled data sets is 28. With the D_n value given in Figure 39, the lognormal distribution is acceptable for C_2 at a significance level much higher than 20%. Likewise the normal distribution is acceptable for C_3 and C_4 at the same level of significance.

We shall summarize the results obtained from the statistical analyses of the test data for C_2, C_3 and C_4 in the following:

1. C_2 is a lognormal random variable. The mean value, $\mu_2(v,R,T)$ as given by Table 6, is a function of the test conditions (v,R,T) whereas the coefficient of variation, V_2, given in Table 8, is independent of (v,R,T).

2. C_2 is statistically independent of C_3 and C_4.

3. C_3 and C_4 are normal random variables. The mean values, $\mu_3(v,R,T)$ and $\mu_4(v,R,T)$, as given by Table 6, are functions of the test conditions (v,R,T) whereas the coefficients of variation, V_3 and V_4, given in Table 8, are independent of (v,R,T).

4. C_3 and C_4 are completely correlated and hence they are functionally related as

$$C_3 = \alpha(v,R,T)\, C_4 + \beta(v,R,T) \qquad (49)$$

in which $\alpha(v,R,T)$ and $\beta(v,R,T)$ are functions of test conditions (v,R,T) and they are given by Eqs. 47 and 48, as well as Table 9.

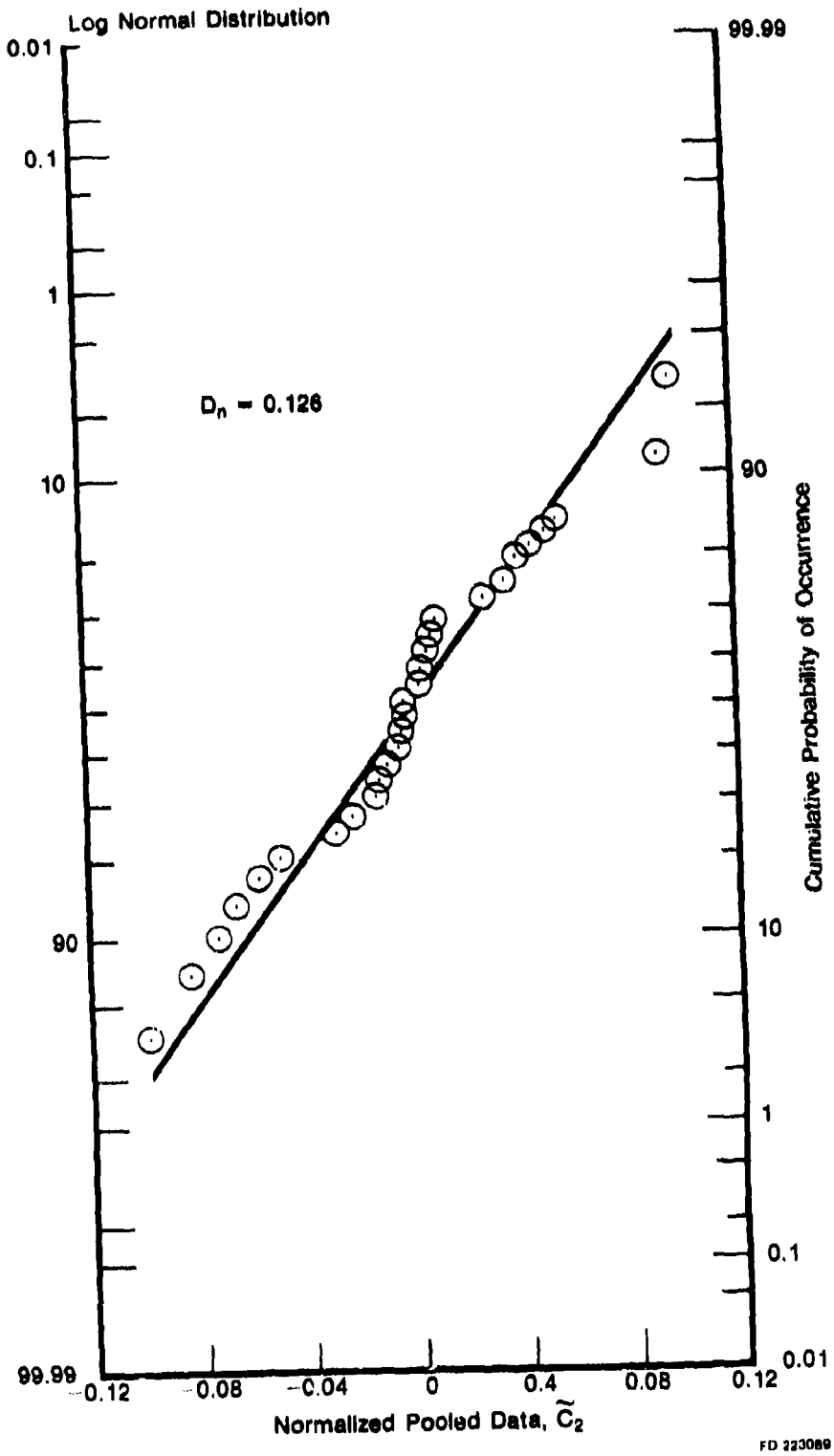

Figure 39a. Log Normal Probability Plot for $\tilde{C}_2$

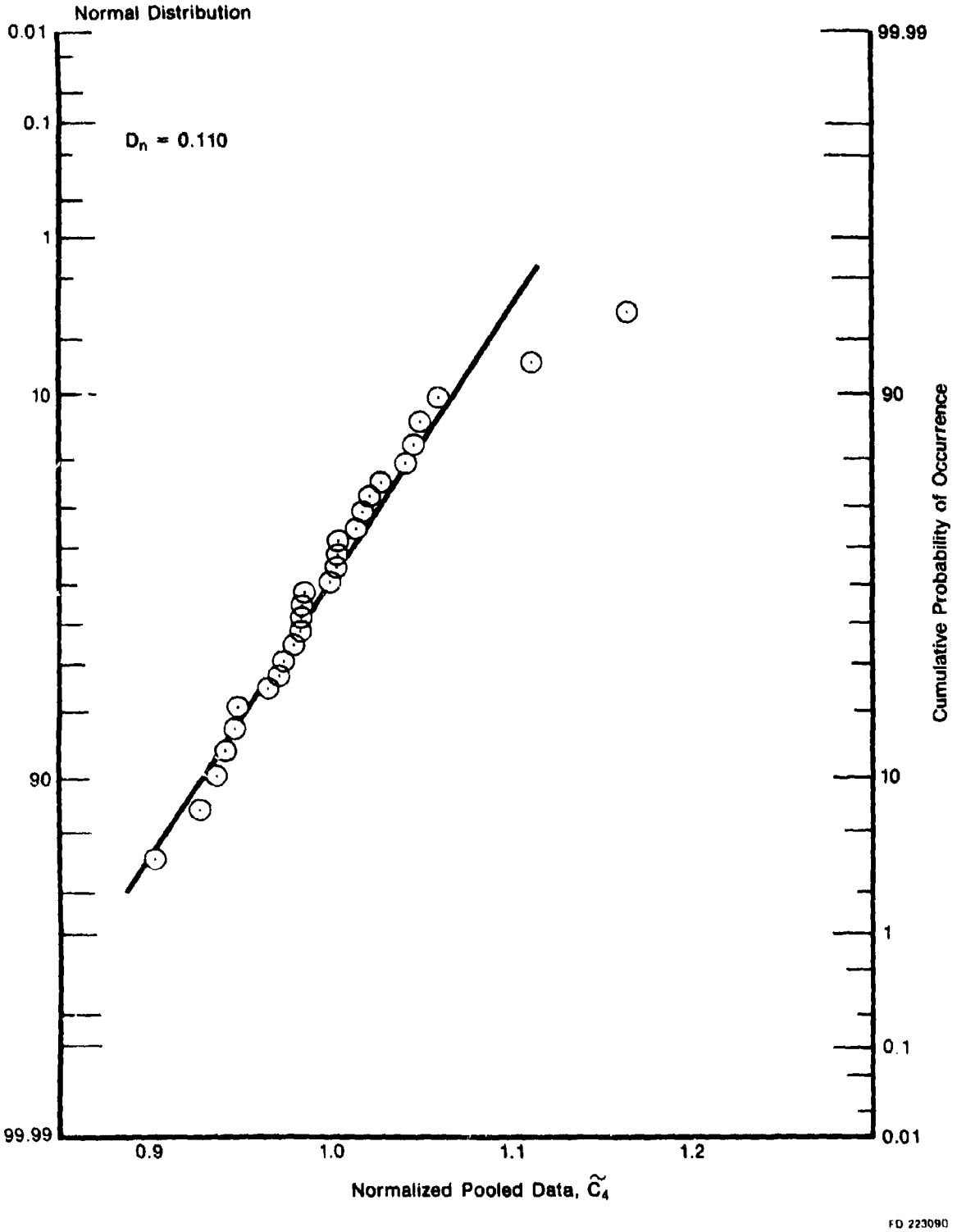

Figure 39b. Normal Probability Plot for $\widetilde{C}_4$

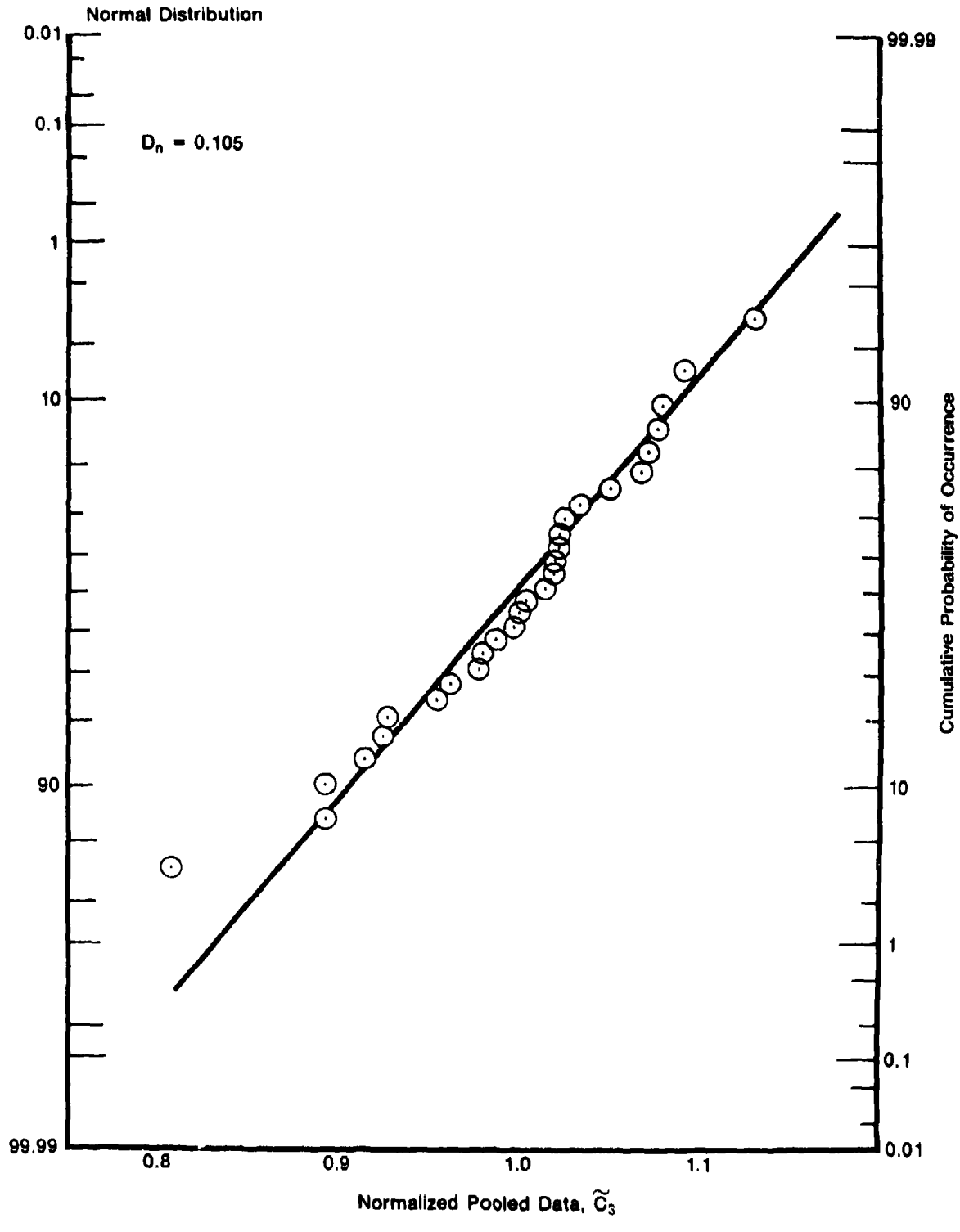

Figure 39c. Normal Probability Plot for $\widetilde{C}_3$

The distribution functions of C_2 and C_4, denoted by $F_{C2}(x_2)$ and $F_{C4}(x_4)$, can be expressed as follows:

$$F_{C_2}(x_2) = P[C_2 \leq x_2] = \Phi\left(\frac{\log x_2 - \mu_2^*(\upsilon,R,T)}{\sigma_2^*(\upsilon,R,T)}\right) \tag{50}$$

$$F_{C_4}(x_4) = P[C_4 \leq x_4] = \Phi\left(\frac{x_4 - \mu_4(\upsilon,R,T)}{\mu_4(\upsilon,R,T)V_4}\right) \tag{51}$$

in which $\Phi(\ )$ is the standardized normal distribution function and

$$\mu^*_2(\upsilon,R,T) = \ell n\left(\frac{\mu_2(\upsilon,R,T)}{\sqrt{1+V_2^2}}\right) \Big/ \ell n10 \tag{52}$$

$$\sigma^*_2(\upsilon,R,T) = \sqrt{\ell n(1+V^2_2)} \Big/ \ell n10 \tag{53}$$

where $\mu_2(\upsilon,R,T)$, $\mu_4(\upsilon,R,T)$, V_2 and V_4 are given in Tables 6 and 8.

The distribution function of C_3 is also normal with the mean value $\mu_3(\upsilon,R,T)$ and the coefficient of variation V_3 given, respectively, in Tables 6 and 8.

Statistical Distribution of Crack Growth Rate

Substitution of Eq. 43 into Eq. 34 yields the log crack growth rate Y

$$Y = C_1\sinh[C_2(X + \alpha C_4 + \beta)] + C_4 \tag{54}$$

Given the statistical distributions of C_2 and C_4, in which C_2 and C_4 are statistically independent lognormal and normal random variables, respectively, the distribution of the log crack growth rate Y can be obtained from the transformation of Eq. 54 as follows:

$$F_Y(y) = P[Y \leq y] = P[C_1\sinh[C_2(X + \alpha C_4 + \beta)] + C_4 \leq y]$$

$$= P\left[C_2(X + \alpha C_4 + \beta) \leq \sinh^{-1}\left(\frac{y-C_4}{C_1}\right)\right]$$

$$= P\left[C_2 \leq \frac{\sinh^{-1}\left(\frac{y-C_4}{C_1}\right)}{(X + \alpha C_4 + \beta)}\right] \tag{55}$$

Substituting Eq. 50 into Eq. 55 and using the theory of total probability, one obtains

$$F_Y(y) = \int_{-\infty}^{\infty} f_{C_4}(\xi)\ \Phi\left\{\frac{\log \sinh^{-1}\left(\frac{y-\xi}{C_1}\right) - \log(X + \alpha\xi + \beta) - \mu_2^*}{\sigma_2^*}\right\} d\xi \quad (56)$$

in which $f_{C_4}(\xi)$ is the probability density function C_4 obtained from Eq. 51

$$f_{C_4}(\xi) = \frac{1}{\sqrt{2\pi}\,\mu_4 V_4} \exp\left\{-\frac{1}{2}\left(\frac{\xi - \mu_4}{\mu_4 V_4}\right)^2\right\} \quad (57)$$

and $\mu^*_2 = \mu^*_2(\upsilon,R,T)$, $\sigma^*_2 = \sigma^*_2(\upsilon, R, T)$ and $\mu_4 = \mu_4(\upsilon,R,T)$ are functions of (υ,R,T) given by Eqs. 52, 53 and Table 6. The distribution function of the log crack growth rate Y given by Eq. 56 can be evaluated easily by a straightforward numerical integration.

The distribution of the log crack growth rate, however, is not the main objective of our research program. What is important in the present research effort is the life (or time) to reach a given crack size. However, any reasonable statistical model should be capable of describing the physical behavior of test results. Hence nineteen (19) sample functions of the log-crack growth rate Y given by Eq. 54 have been simulated and only the first 10 of them are displayed in Figure 40. These sample functions are simulated from Eq. 54 using the statistical distributions of C_2 and C_4 under the test condition No. 1.

Relation Between Distributions of Crack Size and Cycles To Reach a Given Crack Size

The distribution of the crack size $a(n_1)$ at any number of load cycles n_1 (or any service time) is the important information needed in the analysis of Retirement for Cause for engine components. Likewise, the distribution of the number of load cycles $N(a_1)$ (or life) to reach a given crack size a_1 is also very useful information. In fact, both distributions mentioned above are related to each other as will be described in the following.

Let $f_{a(n_1)}(x)$ be the probability density function of the crack size $a(n_1)$ at n_1 load cycles, and $f_{N(a_1)}(n)$ be the probability density function of the number of cycles $N(a_1)$ to reach a given crack size a_1. Both density functions are schematically shown in Figure 41. The probability that the crack size $a(n_1)$ at n_1 load cycles will exceed a_1 is equal to the probability that the number of load cycles $N(a_1)$ to reach the same crack size a_1 is less than n_1 cycles, i.e.,

$$P[a(n_1) > a_1] = P[N(a_1) \leq n_1] \quad (58)$$

It follows from Eq. 58 that

$$\int_{a_1}^{\infty} f_{a(n_1)}(x)dx = \int_0^{n_1} f_{N(a_1)}(n)dn \quad (59)$$

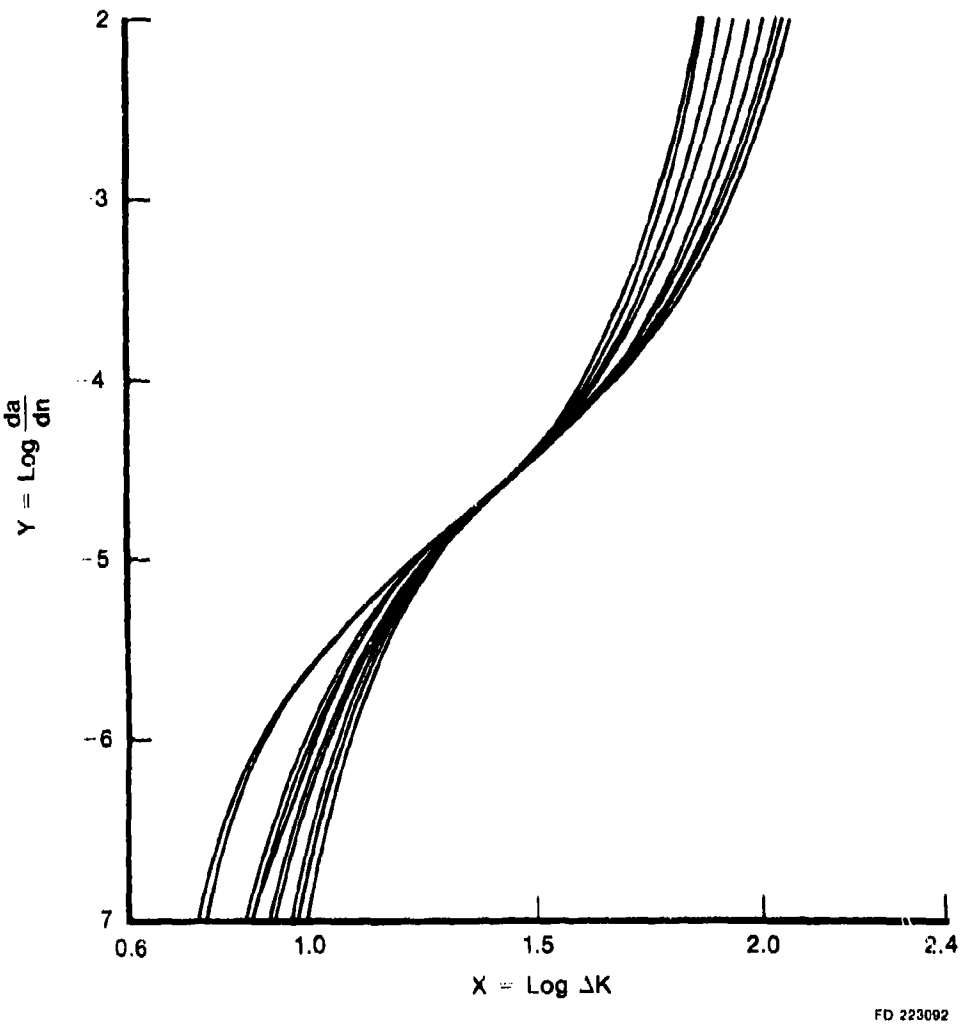

Figure 40. Simulated Log Crack Growth Rate Y as Function of Log Stress Intensity Range X Using Model 2 for Test Condition No. 1

Equations 58 and 59 indicate that the shaded areas shown in Figure 41 under both density functions are equal. Consequently, if the distribution of the number of load cycles to reach a crack size a_i is obtained for all values of a_i, then the distribution of the crack size at any load cycle n_i (or service time) can be derived from it, as schematically shown in Figure 42. From Figure 42, the following relationships can be used to determine $f_{a(n_i)}(x)$ as follows:

$$\int_{a_1}^{\infty} f_{a(n_1)}(x)dx = \int_{0}^{n_1} f_{N(a_1)}(n)dn \qquad (60)$$

$$\int_{a_2}^{\infty} f_{a(n_1)}(x)dx = \int_{0}^{n_1} f_{N(a_2)}(n)dn$$

$$\int_{a_3}^{\infty} f_{a(n_1)}(x)dx = \int_{0}^{n_1} f_{N(a_3)}(n)dn$$

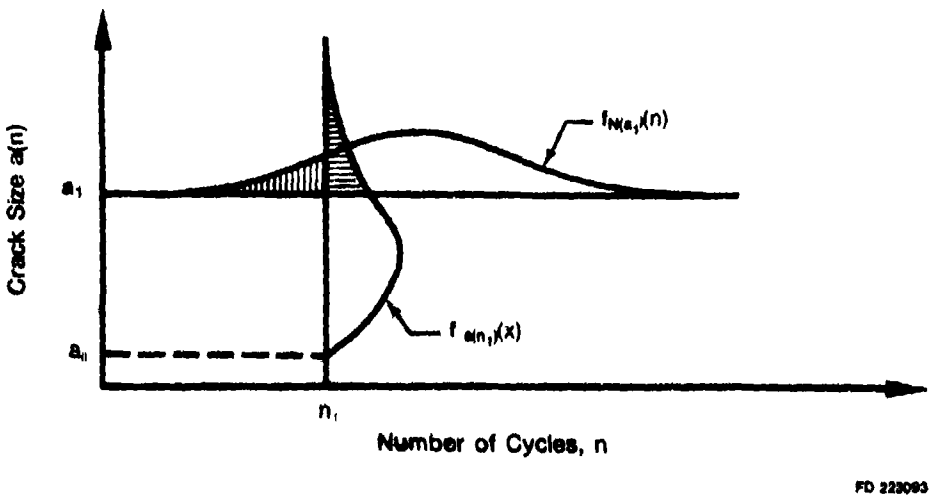

Figure 41. Relation Between Probability for n_1 Load Cycles to Reach a_1 and Probability for the Crack Size at n_1 To Be Larger Than a_1

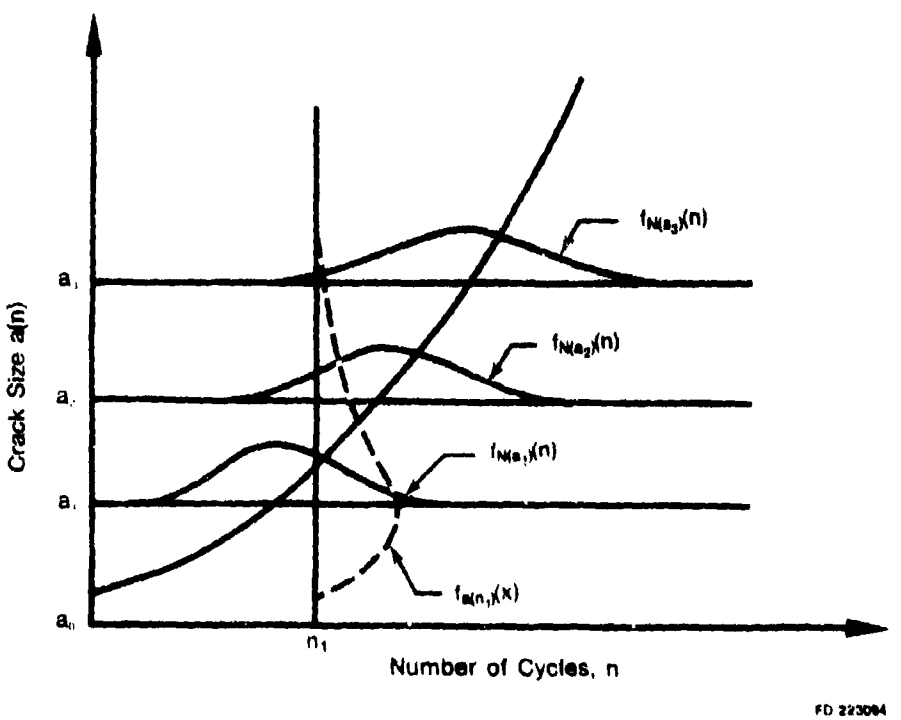

Figure 42. Relation Between Distributions of Crack Size and Cycles to Reach Given Crack Sizes

Frequently, the distribution function of the crack size at any service time cannot be easily determined, but the distribution of the time to reach a crack size can be estimated in approximation in a relatively simple manner. In such a situation, the distribution of the crack size or the probability of crack exceedance will be determined from that of the time to reach a given crack size using Eq. 60 as will be described later.

To show the crack growth behavior based on the present statistical model given by Eq. 54, referred to as model 2, nineteen (19) simulated sample functions of the crack growth rate Y presented above have been integrated numerically to obtain the crack growth curves a(n) versus n using the assumed homogeneous test environment given in Table 4 for the test condition No. 1. The results are depicted in Figure 43. It is observed that the simulated sample functions of the crack growth curves do intermingle.

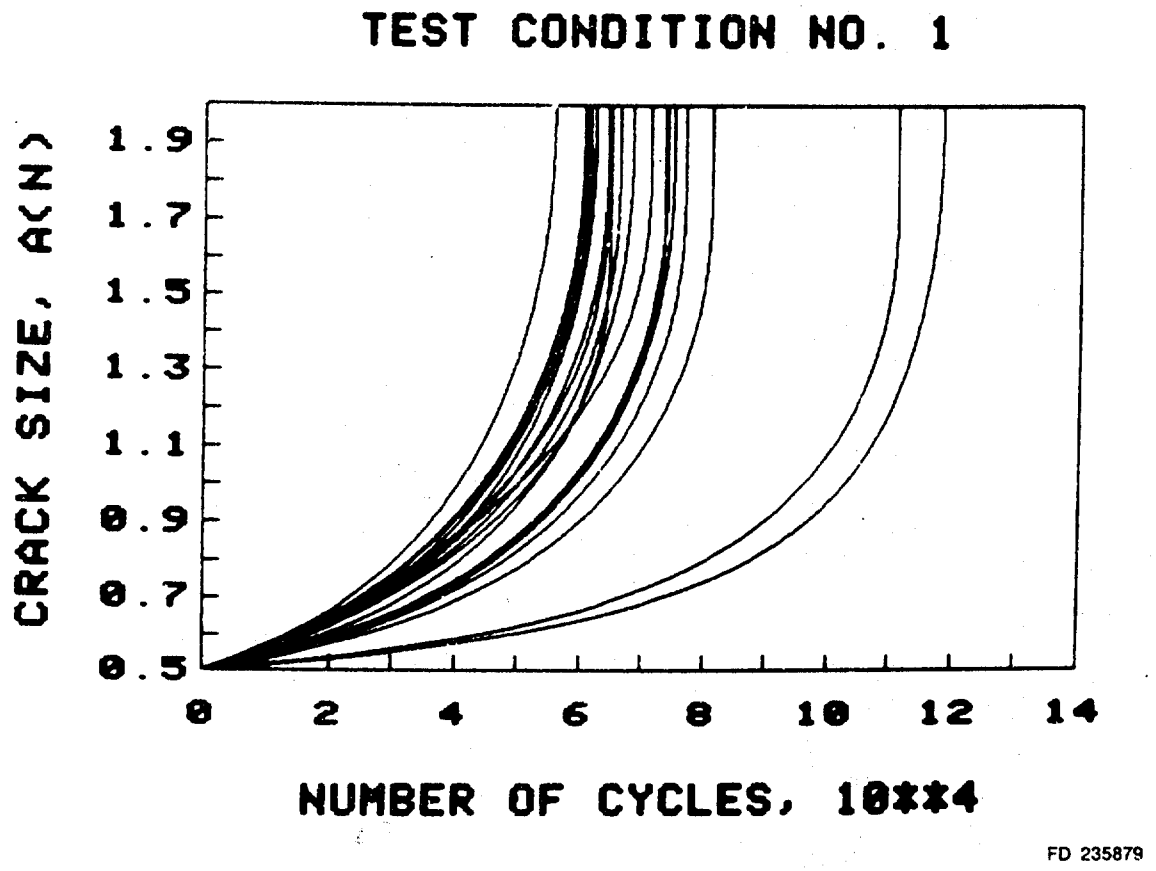

Figure 43. Simulated Crack Growth Damage Accumulation Using Model 2 for Test Condition No. 1

Statistical Distribution of Time to Reach Given Crack Size

Given the statistical distributions of C_2 and C_4, the distribution of the log crack growth rate Y has been derived analytically in Eq. 56. However, the distribution of either the crack size, a(n), at any number of load cycles, n, or the number of cycles, N(a), to reach any crack size "a" cannot be obtained analytically. This is because Eq. 54 cannot be integrated in a closed form to yield the analytical relation among a(n), N(a), C_2 and C_4. As a result, the method of perturbation will be used to estimate the first four central moments of N(a) as follows.

The crack size a(n) at any number of load cycles, n, can be obtained by numerically integrating Eq. 54 and expressed symbolically as

$$a(n) = a(n;C_2,C_4) \tag{61}$$

It is obvious that the crack size $a(n;C_2,C_4)$ is a statistical variable, since both C_2 and C_4 are statistical variables.

On the other hand, Eq. 54 can be integrated numerically to arrive at the number of load cycles N(a) to reach any given crack size "a", which is symbolically denoted by

$$N(a) = N(a;C_2,C_4) \tag{62}$$

Again, $N(a;C_2,C_4)$ is a statistical variable.

Let the first four central moments of C_2 and C_4 be denoted by $(\mu_2,\sigma_2^2,\zeta_2,\eta_2)$ and $(\mu_4,\sigma_4^2,\zeta_4,\eta_4)$, respectively. Since C_2 and C_4 follow the lognormal and normal distributions, respectively, their first four central moments can easily be computed from the respective mean values and coefficients of variation given in Tables 6 and 8. The results are shown in Tables 10 and 11. Then, the first four central moments of N(a), denoted by $(\mu_{N(a)},\sigma^2_{N(a)},\zeta_{N(a)},\eta_{N(a)})$, can be obtained by the method of perturbation as follows [Ref. 46],

$$\begin{aligned}
\mu_{N(a)} &\simeq N(a;\mu_2,\mu_4) + \frac{1}{2}\left(\frac{\partial^2\bar{N}}{\partial C_2^2}\right)\sigma_2^2 + \frac{1}{2}\left(\frac{\partial^2\bar{N}}{\partial C_4^2}\right)\sigma_4^2 \\
\sigma^2_{N(a)} &\simeq \left(\frac{\partial\bar{N}}{\partial C_2}\right)^2\sigma_2^2 + \left(\frac{\partial\bar{N}}{\partial C_4}\right)^2\sigma_4^2 + \left(\frac{\partial\bar{N}}{\partial C_2}\right)\left(\frac{\partial^2\bar{N}}{\partial C_2^2}\right)\zeta_2 \\
\zeta_{N(a)} &\simeq \left(\frac{\partial\bar{N}}{\partial C_2}\right)^3\zeta_2 \\
\eta_{N(a)} &\simeq \left(\frac{\partial\bar{N}}{\partial C_2}\right)^4\eta_2 + \left(\frac{\partial\bar{N}}{\partial C_4}\right)^4\eta_4 + 6\left(\frac{\partial\bar{N}}{\partial C_2}\right)^2\left(\frac{\partial\bar{N}}{\partial C_4^2}\right)^2\sigma_2^2\,\sigma_4^2
\end{aligned} \tag{63}$$

in which $N(a;\mu_2,\mu_4)$ is the value of N(a) evaluated by integrating Eq. 54 with $C_2=\mu_2$, $C_4=\mu_4$, and

$$\begin{aligned}
\frac{\partial\bar{N}}{\partial C_2} &= \left.\frac{\partial N(a;C_2,C_4)}{\partial C_2}\right|_{\substack{C_2=\mu_2\\C_4=\mu_4}}, \quad \frac{\partial\bar{N}}{\partial C_4} = \left.\frac{\partial N(a;C_2,C_4)}{\partial C_4}\right|_{\substack{C_2=\mu_2\\C_4=\mu_4}} \\
\frac{\partial^2\bar{N}}{\partial C_2^2} &= \left.\frac{\partial^2 N(a;C_2,C_4)}{\partial C_2^2}\right|_{\substack{C_2=\mu_2\\C_4=\mu_4}}, \quad \frac{\partial^2\bar{N}}{\partial C_4^2} = \left.\frac{\partial^2 N(a;C_2,C_4)}{\partial C_4^2}\right|_{\substack{C_2=\mu_2\\C_4=\mu_4}}
\end{aligned} \tag{64}$$

Since C_4 is a normal random variable, the property that $\zeta_4=0$ has been used in Eq. 63.

TABLE 10. FIRST FOUR CENTRAL MOMENTS OF C_2 FOR EACH TEST CONDITION

Test Condition	μ_2	σ_2^2	ζ_2	η_2
1	4.081	0.2078	0.03186	0.1382
2	4.888	0.2981	0.0548	0.2846
3	4.718	0.2777	0.0492	0.2470
4	4.43	0.2450	0.0408	0.1922
5	3.802	0.179	0.0255	0.1029

TABLE 11. FIRST FOUR CENTRAL MOMENTS OF C_4 FOR EACH TEST CONDITION

Test Condition	μ_4	σ_4^2	ζ_4	η_4
1	−4.47	0.0593	0	0.01056
2	−4.151	0.0511	0	0.00783
3	−4.60	0.0629	0	0.01185
4	−4.215	0.0514	0	0.00791
5	−3.96	0.0466	0	0.00651

The evaluation of the first four central moments for N(a) from Eq. 63 involves the partial derivatives $(\partial\bar{N}/\partial C_2)$, $(\partial\bar{N}/\partial C_4)$, $(\partial^2\bar{N}/\partial C^2_2)$, and $(\partial_2\bar{N}/\partial C^2_4)$ evaluated at $C_2=\mu_2$ and $C_4=\mu_4$, Eq. 64. These partial derivatives can be computed using the finite-difference scheme as follows;

$$\frac{\partial\bar{N}}{\partial C_2} = \frac{1}{2\Delta}\,[N(a;\mu_2+\Delta,\mu_4) - N(a;\mu_2-\Delta,\mu_4)]$$

$$\frac{\partial\bar{N}}{\partial C_4} = \frac{1}{2\Delta}\,[N(a;\mu_2,\mu_4+\Delta) - N(a;\mu_2,\mu_4-\Delta)] \qquad (65)$$

$$\frac{\partial^2\bar{N}}{\partial C_2^2} = \frac{1}{4\Delta^2}[N(a;\mu_2+2\Delta,\mu_4) - 2N(a;\mu_2,\mu_4) + N(a;\mu_2-2\Delta,\mu_4)]$$

$$\frac{\partial^2\bar{N}}{\partial C_4^2} = \frac{1}{4\Delta^2}[N(a;\mu_2,\mu_4+2\Delta) - 2N(a;\mu_2,\mu_4) + N(a;\mu_2,\mu_4-2\Delta)]$$

in which Δ is chosen to be a reasonably small number such that all the partial derivatives converge. In the present investigation, the second derivative terms in Eq. 63 have been neglected and it is found that $\Delta=0.005$ is sufficient. Equation 65 involves various N(a) values which can be determined in a straightforward numerical integration using Eq. 54. For instance, the quantity $N(a;\mu_2+\Delta,\mu_4)$ is estimated by setting $C_2=\mu_2+\Delta$ and $C_4=\mu_4$ in Eq. 54 and carrying out the numerical integration.

The first central moment $\mu_{N(a)}$ indicates the mean number of cycles to reach a given crack size "a", and the second central moment $\sigma^2_{N(a)}$ represents the variance of N(a). The third central moment $\zeta_{N(a)}$ is a measure of skewness (or symmetry) of the distribution whereas the fourth central moment $\eta_{N(a)}$ is related to the peakedness of the distribution of N(a), called kurtosis. The following nondimensional quantities are commonly used as measures of skewness and kurtosis of the distribution,

$$\sqrt{\beta_1} = \zeta_{N(a)}/\sigma^3_{N(a)} \tag{66}$$

$$\beta_2 = \eta_{N(a)}/\sigma^4_{N(a)} \tag{67}$$

With the assumed homogeneous test environment given in Table 4, the mean values, $\mu_{N(a)}$, the standard deviations, $\sigma_{N(a)}$, the skewness, $\sqrt{\beta_1}$ and the kurtosis, β_2, have been computed and presented in Tables 12 and 13 for two particular crack sizes. The mean value $\mu_{N(a)}$, the mean value ± one standard deviation, $\mu_{N(a)} \pm \sigma_{N(a)}$, and the coefficient of variation, $V_{N(a)} = \sigma_{N(a)}/\mu_{N(a)}$, for test condition No. 1 are plotted in Figure 44 and 45, respectively. From these figures, as well as Tables 12 and 13, two interesting observations are made in the following:

(1) Although the standard deviation $\sigma_{N(a)}$ increases as the number of cycles n increases, the coefficient of variation $V_{N(a)}$ (a measure of dispersion) actually reduces as n increases.

(ii) The skewness $\sqrt{\beta_1}$ of N(a) is quite small because the perturbation approximation made in Eq. 63 takes into account only the first term in the series expansion. Hence $\sqrt{\beta_1}$ thus obtained is not very accurate.

TABLE 12. VALUES OF DISTRIBUTION PARAMETER FOR WEIBULL, LOGNORMAL AND GAMMA DISTRIBUTIONS

Distribution								*Perturbations*	
Test	*Crack*	*Weibull*		*Lognormal*		*Gamma*		*Results*	
Condition	*Size*	α_0	β_0	$\mu_{\ell nN(a)}$	$\sigma_{\ell nN(a)}$	η	λ	$\mu_{N(a)}$	$\sigma_{N(a)}$
1	1.6	3.783	59,763	10.855	0.289	11.491	0.000212	53,780	16,018
	2.0	5.192	75,894	11.130	0.219	20.419	0.000292	69,660	15,447
2	0.8	3.072	16,990	9.56	0.345	7.902	0.00052	15,101	5,400
	2.0	4.572	26,291	20.056	0.245	16.195	0.00067	24,000	5,967
3	0.76	3.362	50,972	10.680	0.319	9.291	0.00020	45,594	15,007
	1.7	5.349	73,453	11.100	0.212	21.569	0.00031	67,520	14,571
4	0.8	2.612	18,889	9.685	0.300	10.563	0.00062	16,740	5,171
	2.0	5.790	30,423	10.226	0.198	24.938	0.00085	28,082	5,636
5	0.8	4.794	9,291	9.021	0.235	17.654	0.00207	8,500	2,026
	2.0	8.711	16,498	9.646	0.136	53.279	0.00341	15,600	2,144

Theoretically, the four-parameter Johnson distribution can be employed for the distribution of the number of cycles N(a) to reach a given crack size "a." The four central moments, $\mu_{N(a)}$, $\sigma^2_{N(a)}$, $\zeta_{N(a)}$ and $\eta_{N(a)}$, obtained above can be used to determine the four parameters involved in the Johnson distribution. For the practical analysis and design purpose, however, it is highly desirable to simplify the approach as much as possible. As a result, the lognormal, Weibull and gamma distributions have been chosen as possible candidates for the distribution of N(a). The reasons for the choice of these distributions is given as follows; (i) they are well-known to engineers, (ii) they are defined in the positive domain, and (iii) they involve only two distribution parameters.

TABLE 13. SKEWNESS AND KURTOSIS OF WEIBULL, LOGNORMAL AND GAMMA DISTRIBUTIONS

Distribution								*Perturbations*	
Test	*Crack*	*Weibull*		*Lognormal*		*Gamma*		*Results*	
Condition	*Size*	β_1	β_2	β_1	β_2	β_1	β_2	β_1	β_2
1	1.0	0.041	2.728	0.910	4.510	0.590	3.522	0.126	3.054
	2.0	0.280	2.910	0.674	3.820	0.443	3.294	0.124	3.053
2	0.8	0.145	2.722	1.112	5.277	0.711	3.76	0.0548	3.018
	2.0	0.190	2.818	0.761	4.046	0.507	3.37	0.0363	3.010
3	0.76	0.0801	2.710	1.019	4.903	0.656	3.645	0.1369	3.061
	1.7	0.209	2.934	0.656	3.774	0.430	3.278	0.1560	3.072
4	0.8	0.002	2.717	0.952	4.653	0.615	3.567	0.0738	3.027
	2.0	0.350	3.003	0.608	3.666	0.400	3.241	0.0517	3.016
5	0.8	0.224	2.850	0.727	3.955	0.476	3.340	0.110	3.045
	2.0	0.574	3.417	0.413	3.305	0.274	3.112	0.085	3.032

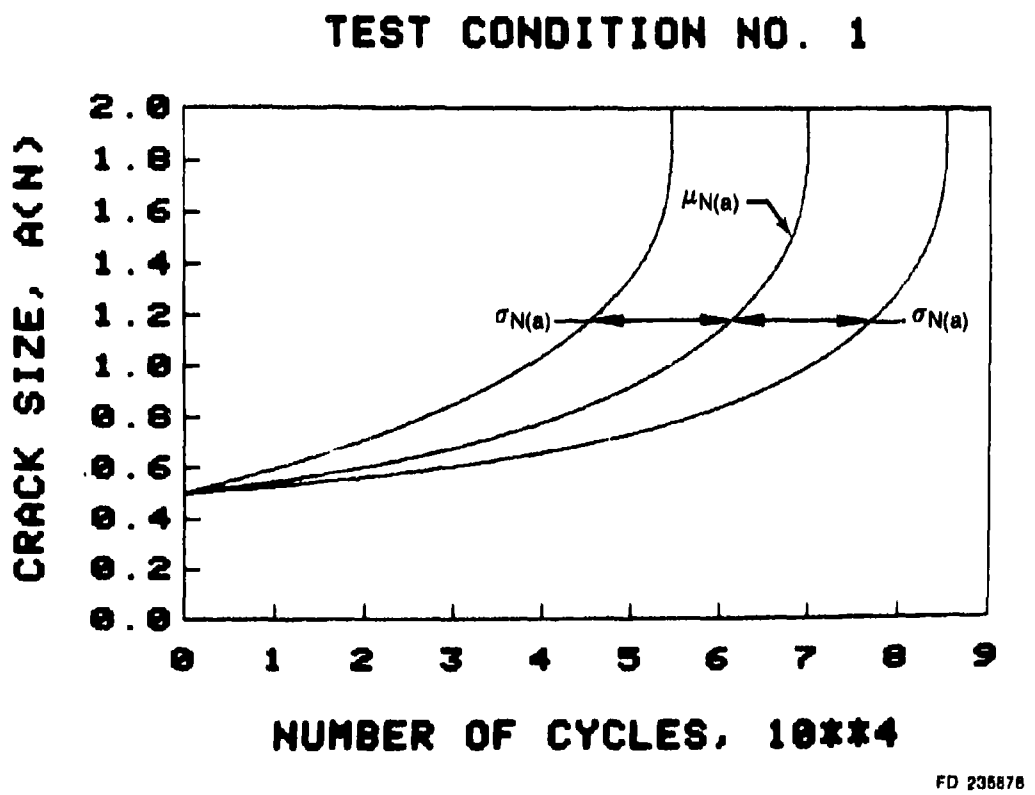

Figure 44. Average Number of Load Cycles $\mu_{N(a)}$ to Reach a Crack Size and Average ± One Standard Deviation $\mu_{N(a)} \pm \sigma_{N(a)}$ for Test Condition No. 1

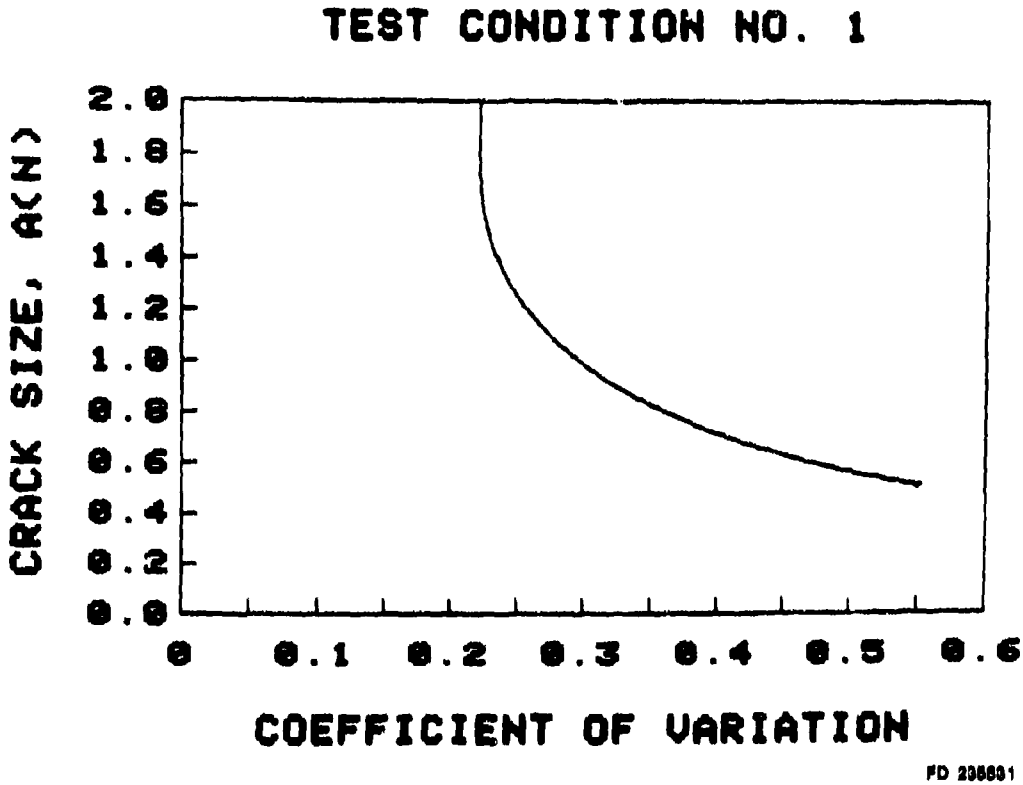

Figure 45. Coefficient of Variation of the Number of Load Cycles to Reach Given Crack Size for Test Condition No. 1

The three distribution functions chosen above are given in the following:

(1) Weibull distribution

$$F_{N(a)}(n) = P[N(a) \leq n] = 1 - \left\{ \exp -(n/\beta_0)^{\alpha_0} \right\};\ n \geq 0 \tag{68}$$

(2) Lognormal distribution

$$F_{N(a)}(n) = \Phi\left(\frac{\ell nn - \mu_{\ell nN(a)}}{\sigma_{\ell nN(a)}} \right);\ n \geq 0 \tag{69}$$

(3) Gamma distribution

$$F_{N(a)}(n) = G(\eta;\lambda n)/\Gamma(\eta);\ n \geq 0 \tag{70}$$

in which α_0, β_0, $\mu_{\ell nN(a)}$, $\sigma_{\ell nN(a)}$, η, and λ are distribution parameters, $\Phi(\ )$ is the standardized normal distribution function, $\Gamma(\ )$ is the complete gamma function, and $G(\ )$ is the incomplete gamma function

$$\Gamma(\eta) = \int_0^{\infty} t^{\eta-1} e^{-t}\, dt \tag{71}$$

$$G(\eta;\lambda x) = \int_0^{\lambda x} t^{\eta-1} e^{-t}\, dt \tag{72}$$

in which $G(\eta;\lambda x) \to \Gamma(n)$ as $x \to \infty$.

Since each distribution function listed above involves only two parameters, the first two central moments of N(a), $\mu_{N(a)}$ and $\sigma^2_{N(a)}$, obtained from the method of perturbation (eq. 63) are used to estimate the two distribution parameters using the method of moment. The distribution parameters are shown in Table 12 for each test condition (c,R,T) at two crack sizes.

After determining the distribution parameters for each distribution function using the first two central moments from the perturbation results, the skewness $\sqrt{\beta_1}$ and the kurtosis β_2 can be computed from the respective distribution parameters. They are presented in Table 13 along with the perturbation results. Then, the goodness-of-fit for each distribution may be judged by comparing the $\sqrt{\beta_1}$ and β_2 values of each distribution with those of the perturbation results. It is observed from Table 13 that the Weibull distribution is the best of the three distributions considered above. Thus, the Weibull distribution is selected for the distribution of N(a), the number of cycles to reach a given crack size "a."

Correlation With Test Results

A qualitative correlation study is made of the second statistical model with respect to the extrapolated test results in this section. Although the statistical distribution of the log crack growth rate Y has been derived in Eqs. 56 and 57, it would be more relevant to examine the behavior of the sample functions of Y. In this connection, 19 sample functions of Y versus X have been simulated using Eq. 54 with the statistics of C_i (i=2,3,4) given by Tables 6 and 8. The results are presented in Figures 46-50 for all test conditions. With the assumed homogeneous test environments given in Table 4, the crack growth rates displayed in Figures 46-50 have been integrated to yield the simulated crack growth damage accumulation. The corresponding crack size a(n) versus the number of load cycles n are shown in Figures 51-55.

The average number of load cycles, $\mu_{N(a)}$, to reach any given crack size and the standard deviation, $\sigma_{N(a)}$, have been computed using the method of perturbation. The results for $\mu_{N(a)}$ and $\mu_{N(a)} \pm \sigma_{N(a)}$ are shown in Figures 56-60. A comparison between the corresponding results in Figures 56-60 and Figures 18(b), 23(b)-26(b) indicates that the correlation between the second statistical model and the extrapolated test results is reasonable.

As described previously, the Weibull distribution is suitable for the distribution of the number of load cycles to reach any crack size. With the Weibull parameters α_0 and β_0 estimated in Table 12, the distributions of N(a) for two crack sizes is depicted as dashed curves in Figures 27-31. Likewise, the crack exceedance curves based on the present model are shown in Figures 32-36 as dashed curves. It is observed from these figures, that the correlation between the second statistical model (dashed curves) and the extrapolated test results (circles) is also reasonable.

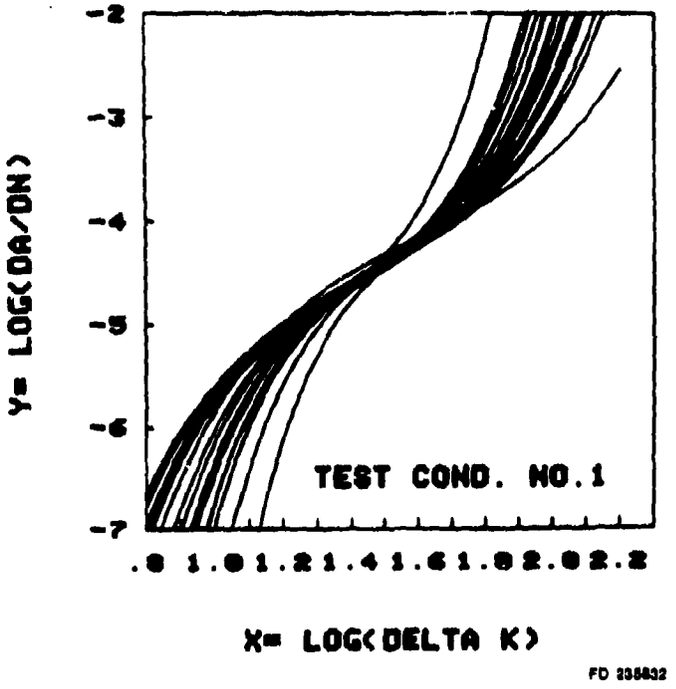

Figure 46. Simulated Log Crack Growth Rate Y as Function of Log Stress Intensity Range X Using Model 2 for Test Condition No. 1

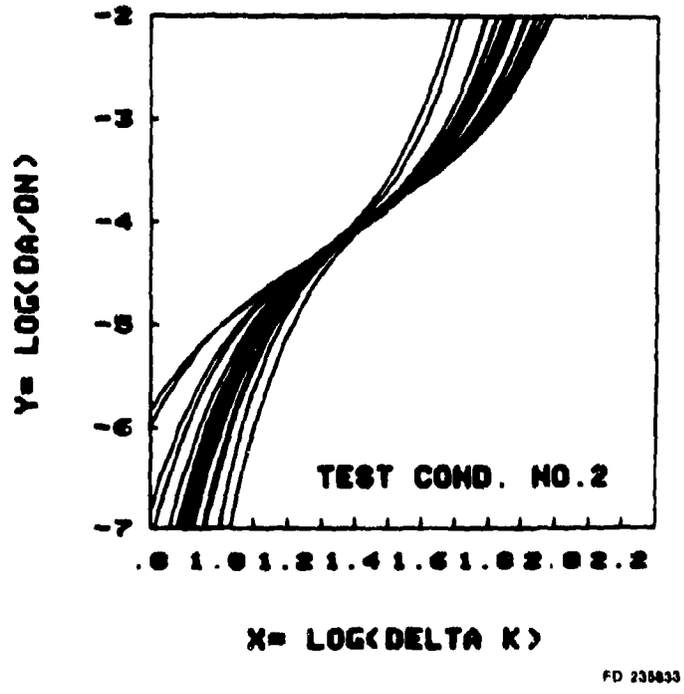

Figure 47. Simulated Log Crack Growth Rate Y as Function of Log Stress Intensity Range X Using Model 2 for Test Condition No. 2

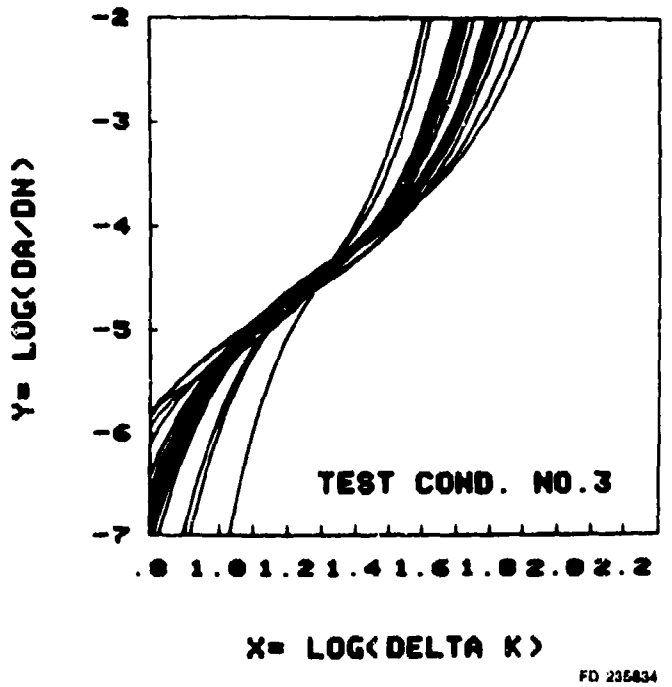

Figure 48. Simulated Log Crack Growth Rate Y as Function of Log Stress Intensity Range X Using Model 2 for Test Condition No. 3

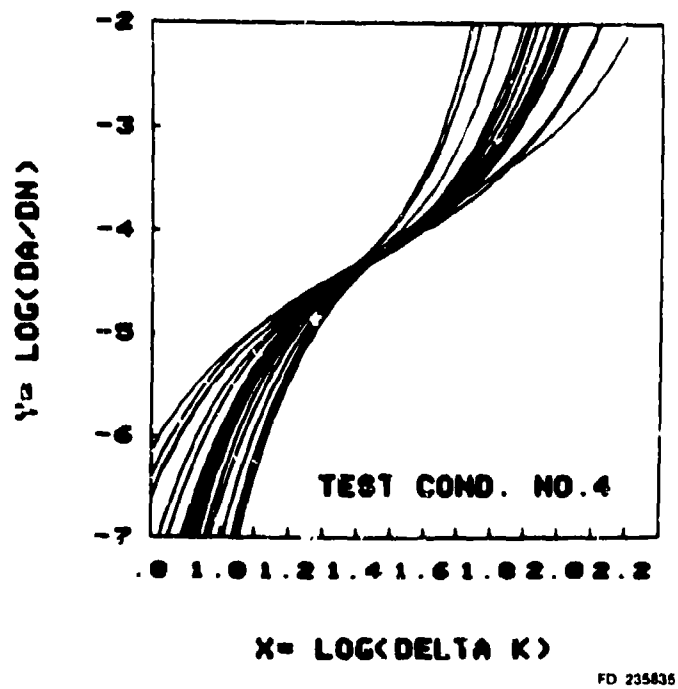

Figure 49 Simulated Log Crack Growth Rate Y as Function of Log Stress Intensity Range X Using Model 2 for Test Condition No. 4

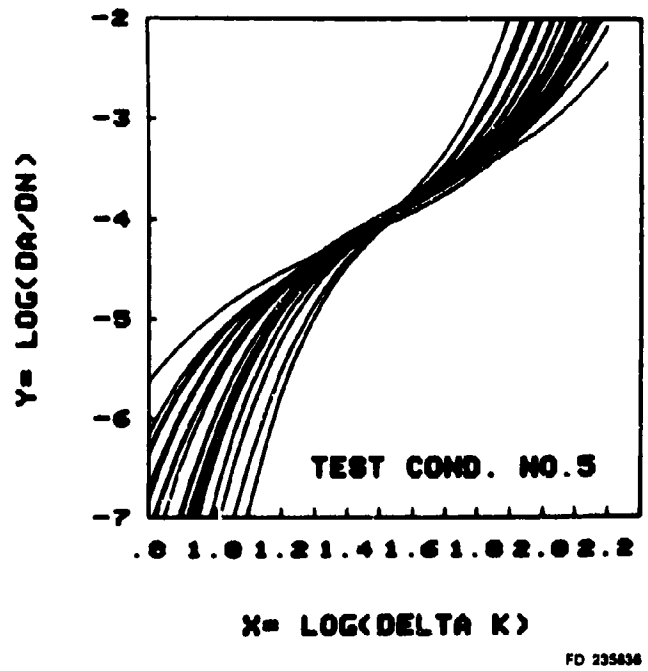

Figure 50. Simulated Log Crack Growth Rate Y as Function of Log Stress Intensity Range X Using Model 2 for Test Condition No. 5

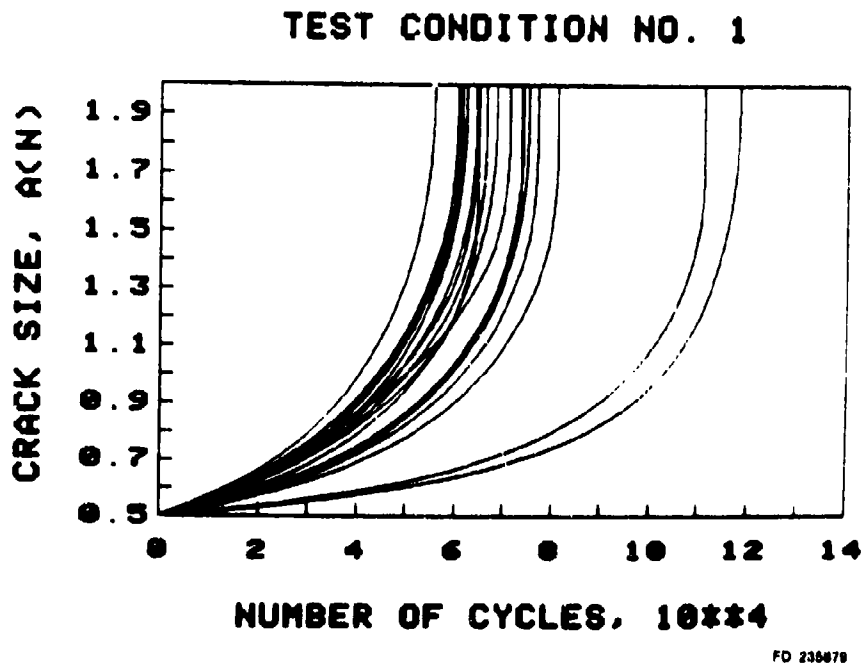

Figure 51. Simulated Crack Growth Damage Accumulation Using Model 2 for Test Condition No. 1

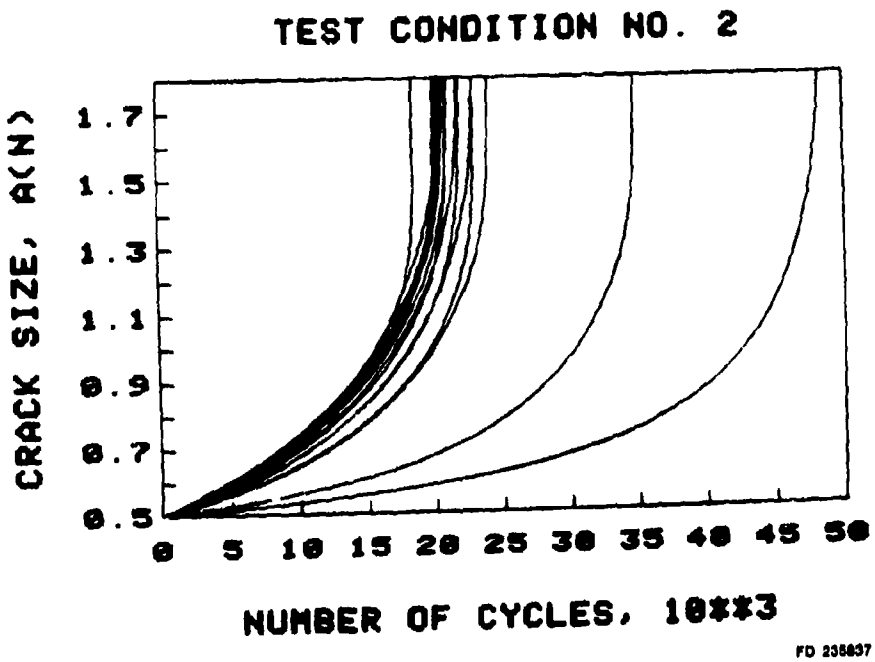

Figure 52. Simulated Crack Growth Damage Accumulation Using Model 2 for Test Condition No. 2

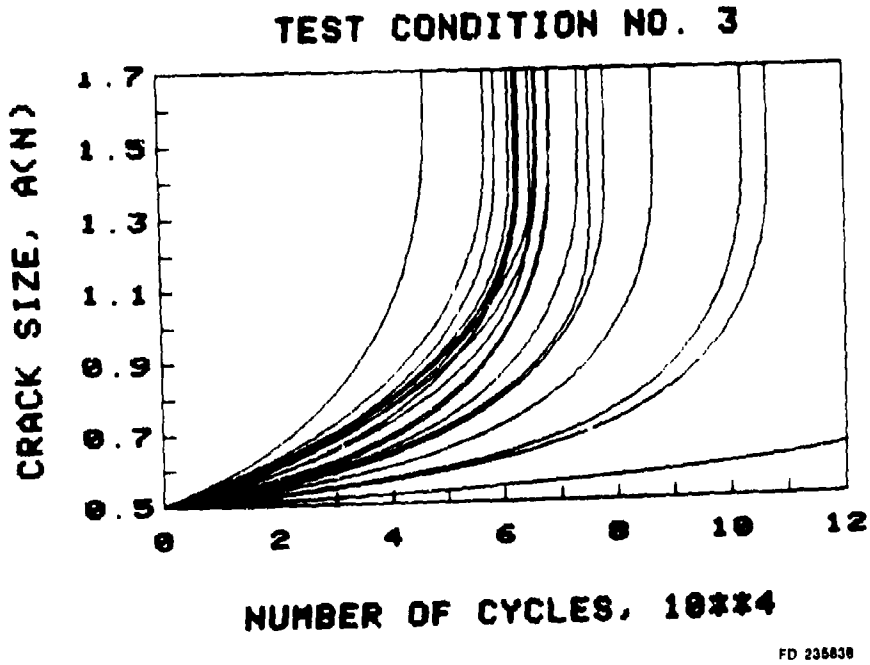

Figure 53. Simulated Crack Growth Damage Accumulation Using Model 2 for Test Condition No. 3

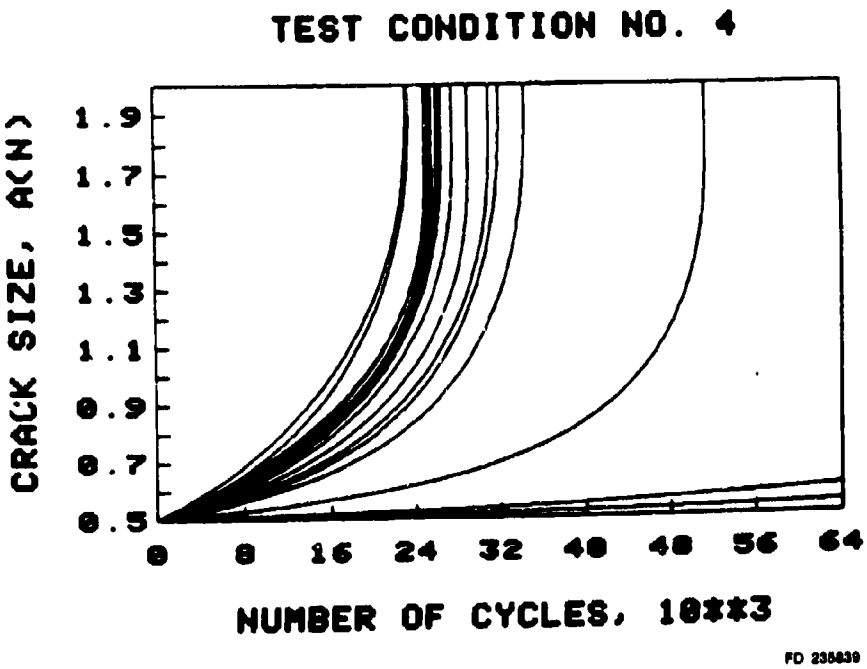

Figure 54. Simulated Crack Growth Damage Accumulation Using Model 2 for Test Condition No. 4

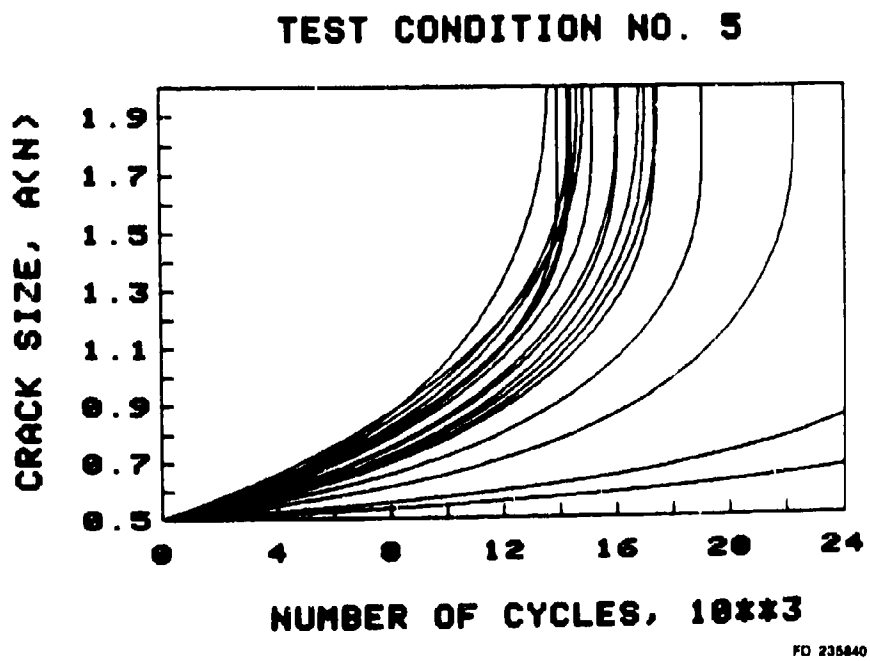

Figure 55. Simulated Crack Growth Damage Accumulation Using Model 2 for Test Condition No. 5

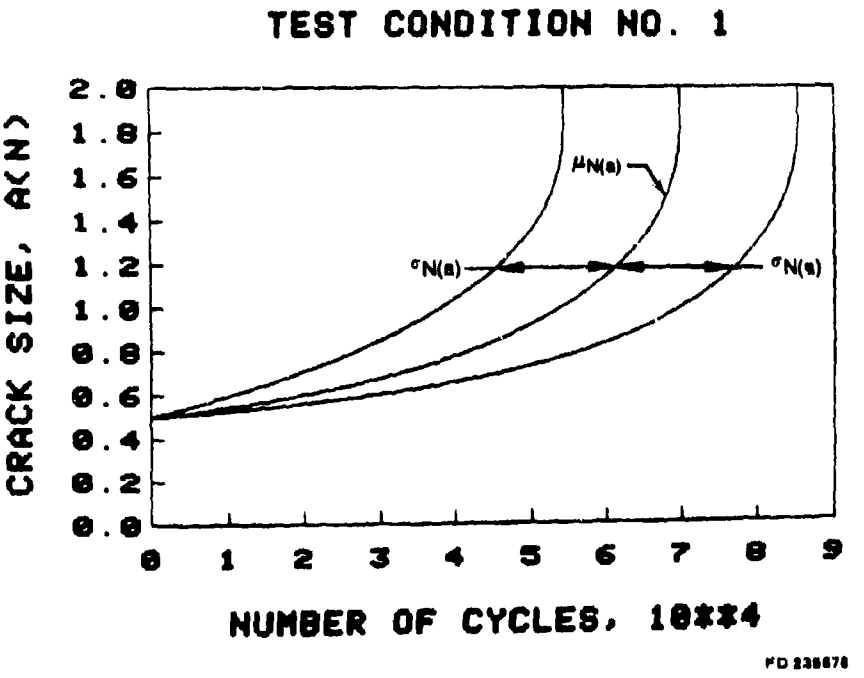

Figure 56. Average Number of Load Cycles $\mu_{N(a)}$ to Reach a Given Crack Size and Average ± One Standard Deviation $\mu_{N(a)} \pm \sigma_{N(a)}$ for Test Condition No. 1

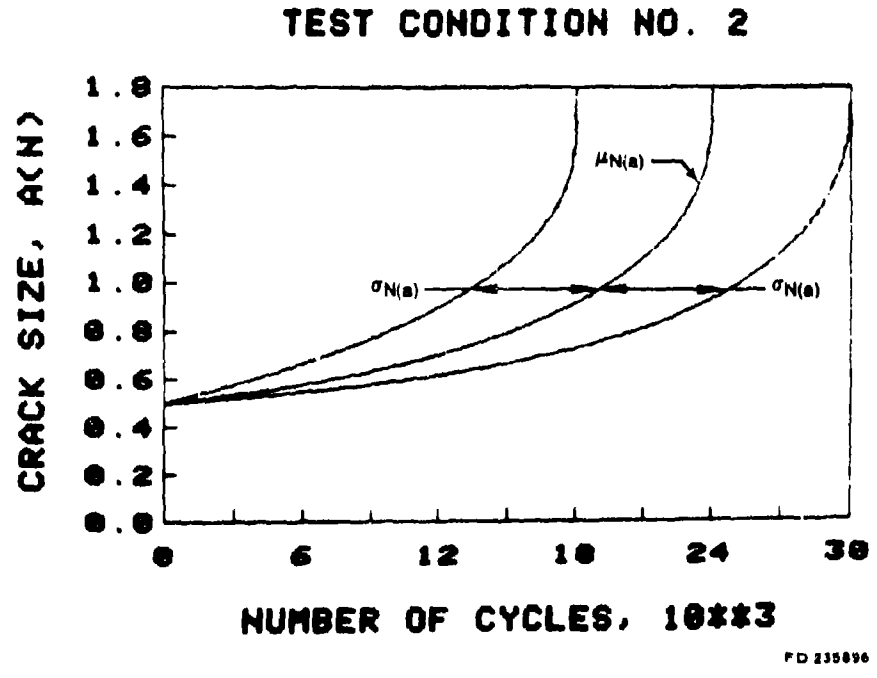

Figure 57. Average Number of Load Cycles $\mu_{N(a)}$ to Reach a Given Crack Size and Average ± One Standard Deviation $\mu_{N(a)} \pm \sigma_{N(a)}$ for Test Condition No. 2

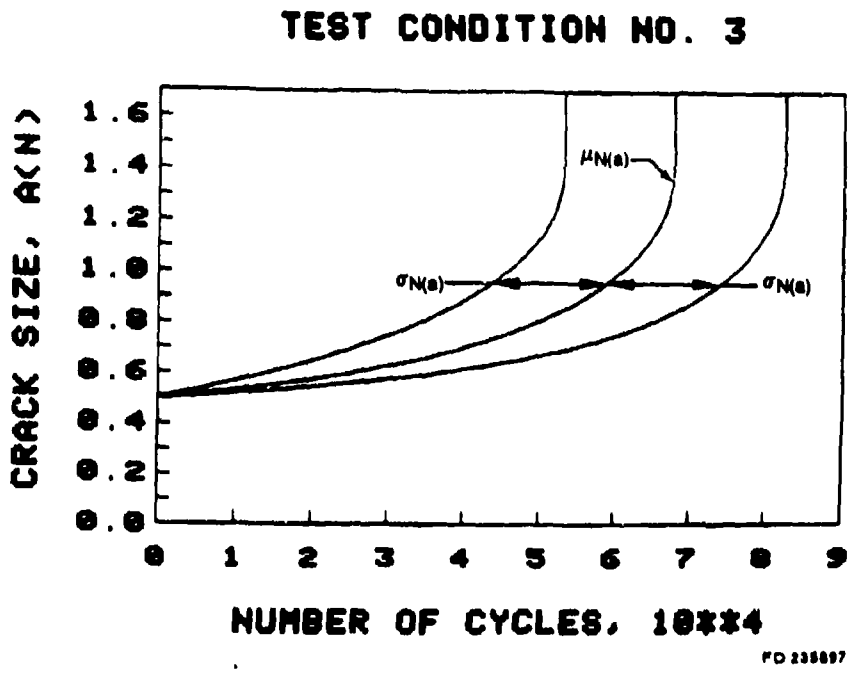

Figure 58. Average Number of Load Cycles $\mu_{N(a)}$ to Reach a Given Crack Size and Average ± One Standard Deviation $\mu_{N(a)} \pm \sigma_{N(a)}$ for Test Condition No. 3

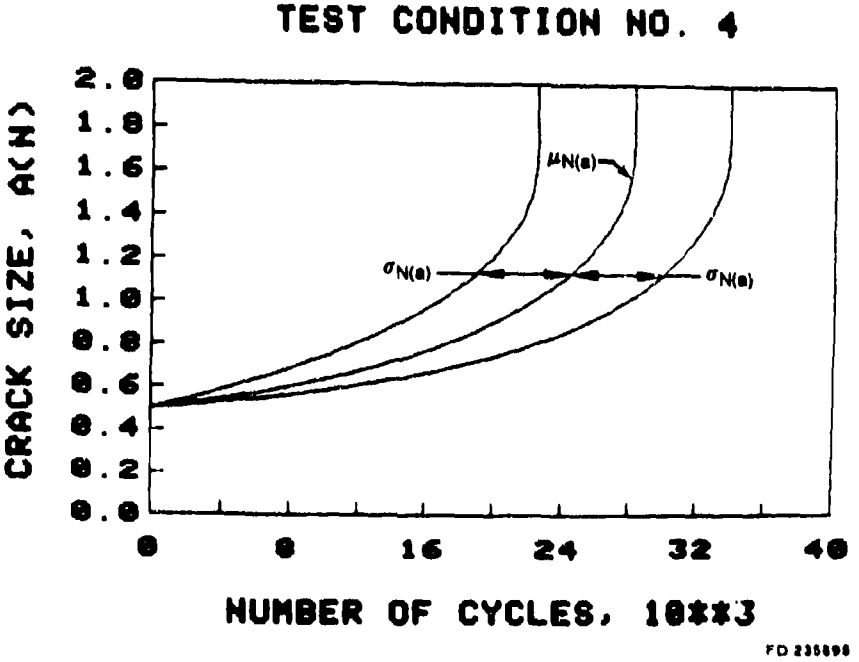

Figure 59. Average Number of Load Cycles $\mu_{N(a)}$ to Reach a Given Crack Size and Average ± One Standard Deviation $\mu_{N(a)} \pm \sigma_{N(a)}$ for Test Condition No. 4

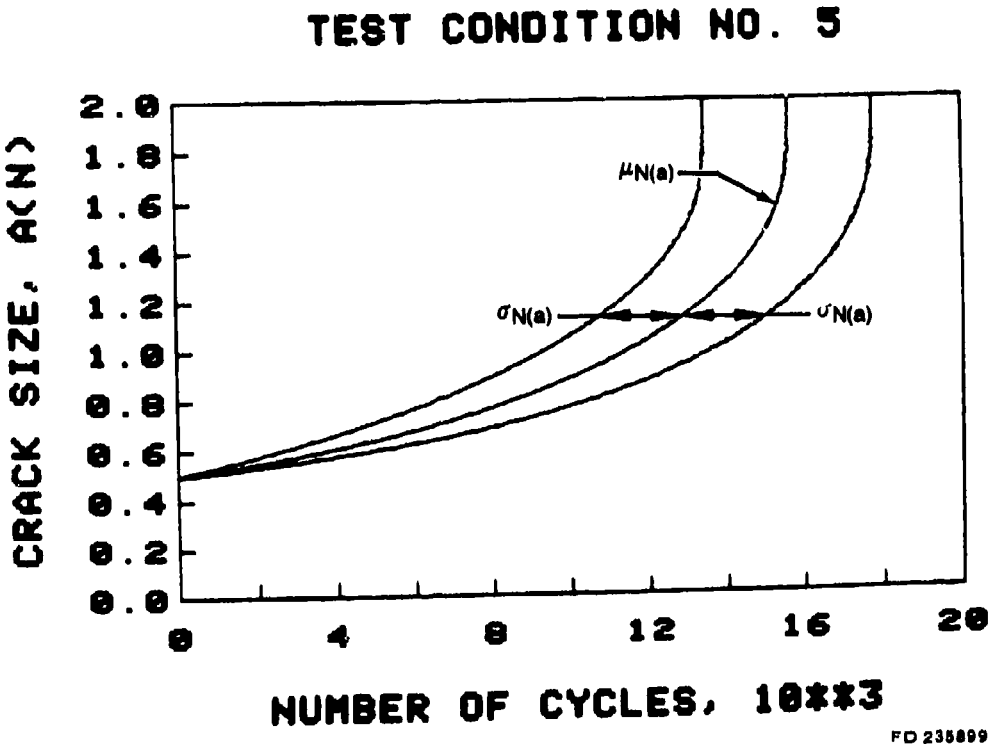

Figure 60. Average Number of Load Cycles $\mu_{N(a)}$ to Reach a Given Crack Size and Average ± One Standard Deviation $\mu_{N(a)} \pm \sigma_{N(a)}$ for Test Condition No. 5

Since each distribution function listed above involves only two parameters, the first two central moments of N(a), $\mu_{N(a)}$ and $\sigma^2_{N(a)}$, obtained from the method of perturbation (eq. 63) are used to estimate the two distribution parameters using the method of moment. The distribution parameters are shown in Table 12 for each test condition (σ,R,T) at two crack sizes.

After determining the distribution parameters for each distribution function using the first two central moments from the perturbation results, the skewness $\sqrt{\beta_1}$ and the kurtosis β_2 can be computed from the respective distribution parameters. They are presented in Table 13 along with the perturbation results. Then, the goodness-of-fit for each distribution may be judged by comparing the $\sqrt{\beta_1}$ and β_2 values of each distribution with those of the perturbation results. It is observed from Table 13 that the Weibull distribution is the best of the three distributions considered above. Thus, the Weibull distribution is selected for the distribution of N(a), the number of cycles to reach a given crack size "a."

Correlation With Test Results

A qualitative correlation study is made of the second statistical model with respect to the extrapolated test results in this section. Although the statistical distribution of the log crack growth rate Y has been derived in Eqs. 56 and 57, it would be more relevant to examine the behavior of the sample functions of Y. In this connection, 19 sample functions of Y versus X have been simulated using Eq. 54 with the statistics of C_i (i=2,3,4) given by Tables 6 and 8. The results are presented in Figures 46-50 for all test conditions. With the assumed homogeneous test environments given in Table 4, the crack growth rates displayed in Figures 46-50 have been integrated to yield the simulated crack growth damage accumulation. The corresponding crack size a(n) versus the number of load cycles n are shown in Figures 51-55.

The average number of load cycles, $\mu_{N(a)}$, to reach any given crack size and the standard deviation, $\sigma_{N(a)}$, have been computed using the method of perturbation. The results for $\mu_{N(a)}$ and $\mu_{N(a)} \pm \sigma_{N(a)}$ are shown in Figures 56-60. A comparison between the corresponding results in Figures 56-60 and Figures 18(b), 23(b)-26(b) indicates that the correlation between the second statistical model and the extrapolated test results is reasonable.

As described previously, the Weibull distribution is suitable for the distribution of the number of load cycles to reach any crack size. With the Weibull parameters α_0 and β_0 estimated in Table 12, the distributions of N(a) for two crack sizes is depicted as dashed curves in Figures 27-31. Likewise, the crack exceedance curves based on the present model are shown in Figures 32-36 as dashed curves. It is observed from these figures, that the correlation between the second statistical model (dashed curves) and the extrapolated test results (circles) is also reasonable.

SECTION V
REFERENCES

1. Larsen, J. M., B. J. Schwartz, and C. G. Annis, Jr., "Cumulative Fracture Mechanics Under Engine Spectra," Technical Report AFML-TR-79-4159, Air Force Materials Laboratory, WPAFB, Jan. 1980.

2. Annis, C. G., R. M. Wallace, and D. L. Sims, "An Interpolative Model for Elevated Temperature Fatigue Crack Propagation," AFML-TR-76-176, Part I, November 1976.

3. Wallace, R. M., C. G. Annis, and D. L. Sims, "Application of Fracture Mechanics at Elevated Temperature," AFML-TR-76-175, Part II, November 1976.

4. Sims, D. L., C. G. Annis, and R. M. Wallace, "Cumulative Damage Fracture Mechanics at Elevated Temperature," AFML-TR-76-176, Part III, November 1976.

5. Larsen, J. M., and C. G. Annis, "Observation of Crack Retardation Resulting From Load Sequencing Characteristic of Military Gas Turbine Operation," Submitted for Publication - American Society for Testing and Materials, 1979.

6. Cowles, B. A., D. L. Sims, and J. R. Warren, "Evaluation of the Cyclic Behavior of Aircraft Turbine Disk Alloys," NASA CR-159409, August 1978, Contract NAS3-20367.

7. Macha, D. E., A. F. Gandt, Jr., and B. J. Wicks, "Effects of Gas Turbine Engine Load Spectrum Variables on Crack Propagation," Submitted for Publication - American Society for Testing and Materials, 1979.

8. Damage Tolerant Design Handbook, MCIC-HB-1, Dec. 1972, Air Force Materials Laboratory, Air Force Flight Dynamics Laboratory, WPAFB.

9. Swanson, S. R., F. Cicci, and W. Hoppe, "Crack Propagation in Clad 7079-T6 Aluminum Alloy Sheet Under Constant and Random Amplitude Fatigue Loading, *Fatigue Crack Propagation*, ASTM-STP415, 1967, pp 312-362.

10. Paris, P. C., "The Fracture Mechanics Approach to Fatigue," *Proc. of the 8th Sagamore Army Materials Research Conf.*, Syracuse Univ. Press, 1964, pp 107-127.

11. Rice, J. R., and F. P. Beer, "On the Distribution of Rises and Falls in a Continuous Random Process," *Journal of Basic Engineering*, ASME, 1965, pp 398-404.

12. Rice, J. R., et al., "On the Prediction of Some Random Loading Characteristics Relevant to Fatigue," *Proc. of the Second Inter. Conf. on Accou. Fatigue in Aero. Structures*, Syracuse Univ. Press, 1965, pp 121-143.

13. Smith, S. H., "Fatigue Crack Growth Under Axial Narrow and Broad Band Random Loading," *Accoustical Fatigue in Aero. Structures*, Syracuse Univ. Press, 1965.

14. Smith, S. H., "Random Loading Fatigue Crack Growth Behavior of Some Aluminum and Titanium Alloys," *Structural Fatigue in Aircraft*, ASTM-STP 404, 1966.

15. Yang, J. N., "Statistics of Random Loading Relevant to the Fatigue," *Journal Engr. Mech. Div.*, ASCE, Vol. 100, No. EM3, 1974, pp 469-475.

16. Yang, J. N., and J. W. Trapp, "Reliability Analysis of Fatigue-Critical Aircraft Structures Under Random Loading and Periodic Inspections," Air Force Materials Lab., AFML-TR-75-29, WPAFB, 1975.

17. Yang, J. N., and W. H. Trapp, "Reliability Analysis of Aircraft Structures Under Random Loading and Periodic Inspection," *AIAA Journal*, Vol. 12, No. 12, 1974, pp 1623-1630.

18. Johnson, W. S., R. A. Heller, and J. N. Yang, "Flight Inspection Data, Crack Initiation Times, and Initial Crack Size," Proc. 1977 Annual Reliability and Maintainability Symposium, Jan. 1977.

19. Gallagher, J. P., and H. D. Stanaker, "Predicting Flight-by-Flight Crack Growth Rates," *J. Aircraft*, Vol. 12, 1975, pp 699-705.

20. Gallagher, J. P., and H. D. Stanaker, "Methods of Analyzing Fatigue Crack Growth Rate Behavior Associated with Flight-by-Flight Loading," AIAA Paper No. 74-367, Proc. AIAA/ASME/SAE 15th SDM Conf., 1974.

21. Gallagher, J. P., "Estimating Fatigue Crack Lives for Aircraft: Techniques," *Exper. Mech.*, Vol. 16, No. 11, 1976, pp 425-433.

22. Chang, J. B., et. al., "Improved Methods for Predicting Spectrum Loading Effects," Phase I Report, Vol. 1, Results and Discussion, AFFDL-TR-79-3036, 1978.

23. Levy, M., A. S. Kuo, and K. Grube, "Practical Method of Crack Growth Analyses for Fighter Aircraft," *Journal of Aircraft*, Vol. 18, No. 2, Feb. 1981, pp 150-157.

24. Wood, H. A., R. M. Engle, J. P. Gallagher, and J. M. Potter, "Current Practice on Estimating Crack Growth Damage Accumulation With Specific Application to Structural Safety, Durability and Reliability," U. S. Air Force Flight Dynamics Lab., AFFDL-TR-75-32, WPAFB, 1976.

25. Rudd, J. L., and T. D. Gray, "Equivalent Initial Quality Method," U. S. Air Force Flight Dynamics Lab., AFFDL-TM-76-83, WPAFB, 1976.

26. Rudd, J. L., and T. D. Gray, "Quantification of Fastener Hole Quality," Proc. 18th AIAA/ASME/SAE Structures, Structural Dynamics and Materials Conference, March 1977.

27. Norohna, P. J., et. al., "Fastener Hole Quality, Vol. I," Air Force Flight Dynamics Lab., AFFDL-TR-78-206, WPAFB, 1978.

28. Yang, J. N., and S. D. Manning, "Distribution of Equivalent Initial Flaw Size," 1980 Proceedings of Annual Reliability and Maintainability Symposium, Jan. 1980, pp 112-120.

29. Yang, J. N., "Statistical Estimation of Economic Life for Aircraft Structures," Proc. AIAA/ASME/ASCE/AHS SDM Conf., St. Louis, April 1979, pp 240-248; *Journal of Aircraft, AIAA*, Vol. 17, No. 7, July 1980, pp 528-535.

30. Manning, S. D., et al., "Durability Methods Development, Vol. I, Phase I Summary," Air Force Flight Dynamics Laboratory, AFFDL-TR-3118, Vol. 1, June 1979.

31. Yang, J. N., S. D. Manning, and W. R. Garver, "Durability Methods Development, Volume V - Durability Analysis Methodology Development," Air Force Flight Dynamics Laboratory, AFFDL-TR-3118, Vol. 5, Sept. 1979.

32. Rudd, J. L., J. N. Yang, S. D. Manning, and W. R. Garver, "Durability Design Requirements and Analysis for Metallic Airframe" in *Design of Fatigue and Fracture Resistant Structures*, ASTM, STP761, 1982, pp 133-151.

33. Yang, J. N., "Statistical Crack Growth in Durability and Damage Tolerant Analyses," Proc. AIAA/ASME/ASCE/AHS 22nd Structures, Structural Dynamics, and Materials Conference, April 1981, pp 38-44.

34. Virkler, D. A., B. M. Hillberry, and P. K. Goel, "The Statistical Nature of Fatigue Crack Propagation," *Journal of Engineering Materials and Technology*, ASME, Vol. 101, April 1979, pp 148-152.

35. Virkler, D. A., B. M. Hillberry, and P. K. Goel, "The Statistical Nature of Fatigue Crack Propagation," Air Force Flight Dynamics Laboratory, Technical Report AFFDL-TR-78-43, WPAFB, April 1978.

36. Birnbaum, Z. W., and S. C. Saunders, "A New Family of Life Distribution," *Journal of Applied Probability*, Vol. 6, 1969, pp 319-327.

37. Birnbaum, Z. W., and S. C. Saunders, "Estimation For a Family of Life Distributions With Applications to Fatigue," *Journal of Applied Probability*, Vol. 6, 1969, pp 328-347.

38. Bogdanoff, J., "A New Cumulative Damage Model - Part I," *Journal of Applied Mechanics*, ASME, Vol. 45, June 1978, pp 246-250.

39. Bogdanoff, J., and W. Krieger, "A New Cumulative Damage Model - Part 2," *Journal of Applied Mechanics*, ASME, Vol. 45, June 1978, pp 251-257.

40. Bogdanoff, J., "A New Cumulative Damage Model - Part 3," *Journal of Applied Mechanics*, ASME, Vol. 45, Dec. 1978, pp 733-739.

41. Bogdanoff, J., "A New Cumulative Damage Model - Part 4," *Journal of Applied Mechanics*, ASME, Vol. 47, March 1980, pp 40-44.

42. Kozin, F., and J. Bogdanoff, "A Critical Analysis of Some Probabilistic Models of Fatigue Crack Growth," *Journal of Engineering Fracture Mechanics*, Vol. 14, 1981, pp 59-89.

43. Pook, L. P., "Basic Statistics of Fatigue Crack Growth," NEL Report No. 595, National Engineering Laboratory, 1975.

44. Clark, W. G., Jr., and S. J. Hudak, Jr., "Variability in Fatigue Crack Growth Rate Testing," ASTM, E24.04.01 Task Group Report, Westinghouse Research Laboratories, 1974.

45. Frank, K. H., and J. W. Fisher, "Analysis of Error in Determining Fatigue Crack Growth Rates," Fritz Engineering Laboratory Report No. 358.10 Lehigh University, Bethlehem, Pa., Mar. 1971.

46. Hahn, G. J., and S. S. Shapiro, *Statistical Models in Engineering*, John Wiley & Sons, Inc., New York, 1967.